Cranial bone histology of *Metoposaurus krasiejowensis* (Amphibia, Temnospondyli) from the Late Triassic of Poland (#10008)

First submission

Please read the **Important notes** below, and the **Review guidance** on the next page.
When ready **submit online**. The manuscript starts on page 3.

Important notes

Editor and deadline

Andrew Farke / 28 Apr 2016

Files	7 Figure file(s) 1 Table file(s) 1 Other file(s) Please visit the overview page to **download and review** the files not included in this review pdf.
Declarations	No notable declarations are present

Review guidelines

Please in full read before you begin

How to review

When ready **submit your review online**. The review form is divided into 5 sections. Please consider these when composing your review:

1. **BASIC REPORTING**
2. **EXPERIMENTAL DESIGN**
3. **VALIDITY OF THE FINDINGS**
4. General comments
5. Confidential notes to the editor

You can also annotate this **pdf** and upload it as part of your review

To finish, enter your editorial recommendation (accept, revise or reject) and submit.

BASIC REPORTING

- Clear, unambiguous, professional English language used throughout.
- Intro & background to show context. Literature well referenced & relevant.
- Structure conforms to **PeerJ standard**, discipline norm, or improved for clarity.
- Figures are relevant, high quality, well labelled & described.
- Raw data supplied (See **PeerJ policy**).

EXPERIMENTAL DESIGN

- Original primary research within **Scope of the journal**.
- Research question well defined, relevant & meaningful. It is stated how research fills an identified knowledge gap.
- Rigorous investigation performed to a high technical & ethical standard.
- Methods described with sufficient detail & information to replicate.

VALIDITY OF THE FINDINGS

- Impact and novelty not assessed. Negative/inconclusive results accepted. *Meaningful* replication encouraged where rationale & benefit to literature is clearly stated.
- Data is robust, statistically sound, & controlled.
- Conclusion well stated, linked to original research question & limited to supporting results.
- Speculation is welcome, but should be identified as such.

The above is the editorial criteria summary. To view in full visit **https://peerj.com/about/editorial-criteria/**

Cranial bone histology of *Metoposaurus krasiejowensis* (Amphibia, Temnospondyli) from the Late Triassic of Poland

Kamil Gruntmejer, Dorota Konietzko-Meier, Adam Bodzioch

In this study a detailed description of the 21 skull bones of *Metoposaurus krasiejowensis* from the Late Triassic of Poland is presented. All dermal bones show a diploë structure, with the ornamented external surface. The ridges consist of well vascularized parallel-fibered bone; the valleys are built of an avascular layer of lamellar bone. The dense clumps of thin, well mineralized Sharpey's fibers are preserved. The growth marks are manifested in four ways: a sequence of resting lines; layers of lamellar bone alternated with layers with Interwoven Structural Fibers (ISF); thick, avascular annuli and high vascularized zones; and the alternations of valleys and ridges. The thick middle region consists of cancellous bone, with varying porosity. The thin and less vascularized internal cortex consists of parallel-fibered bone. Calcified cartilage is observed in the quadrate and the exoccipital. The skull bones show strong variability within the microanatomical and histological levels. The histological framework is not bone-limited, but varies even in one single bone; this seems to be related to the specific position of the bone and depends on the local biomechanical loading of the particular part of the skull. The large accumulation of Sharpey's fibers in the occipital condyles indicates the presence of strong muscles and ligaments connecting the skull to the vertebral column. The dynamic processes during the ornamentation deposition are observed indicate that the position of the ridges and grooves change during ~~the~~ growth and could be the specific adaptation to biomechanical conditions and stress distribution during the bone development. In the supratemporal the cementing lines indicated the remodeling process could be involved into the creations of sculpture.

Cranial bone histology of *Metoposaurus krasiejowensis* (Amphibia, Temnospondyli) from the Late Triassic of Poland

Kamil Gruntmejer[1,2,*], Dorota Konietzko-Meier[1,2,3], Adam Bodzioch[1]

[1] Opole University, Department of Biosystematics, Laboratory of Palaeobiology, Oleska 22, 45-052 Opole, Poland

[2] Opole University, European Centre of Palaeontology, Oleska 48, 45-052 Opole, Poland

[3] University of Bonn, Steinmann Institute, Nussallee 8, 53115 Bonn, Germany

[*]gruntmejerkamil@gmail.com

* - corresponding author

ABSTRACT

In this study a detailed description of the 21 skull bones of *Metoposaurus krasiejowensis* from the Late Triassic of Poland is presented. All dermal bones show a diploë structure, with the ornamented external surface. The ridges consist of well vascularized parallel-fibered bone; the valleys are built of an avascular layer of lamellar bone. The dense clumps of thin, well mineralized Sharpey's fibers are preserved. The growth marks are manifested in four ways: a sequence of resting lines; layers of lamellar bone alternated with layers with Interwoven Structural Fibers (ISF); thick, avascular annuli and high vascularized zones; and the alternations of valleys and ridges. The thick middle region consists of cancellous bone, with varying porosity. The thin and less vascularized internal cortex consists of parallel-fibered bone. Calcified cartilage is observed in the quadrate and the exoccipital. The skull bones show strong variability within the microanatomical and histological levels. The histological framework is not bone-limited, but varies even in one single bone; this seems to be related to the specific position of the bone and depends on the local biomechanical loading of the particular part of the skull. The large accumulation of Sharpey's fibers in the occipital condyles indicates the presence of strong muscles and ligaments connecting the skull to the vertebral column. The dynamic processes during the ornamentation deposition are observed indicate that the position of the ridges and grooves change during the growth and could be the specific adaptation to biomechanical conditions and stress distribution during the bone development. In the supratemporal the

cementing lines indicated the remodeling process could be involved into the creations of sculpture.

Keywords:
dermal bones, skull, microanatomy, growth pattern

INTRODUCTION

Metoposaurids were large, up to 3 meters long, late Triassic Temnospondyli with a strongly dorso-ventrally flattened body, and ~~well~~ adapted to aquatic life. The most characteristic and best known part of the *Metoposaurus* skeleton is the extremely flat parabolic skull with anteriorly located orbits (*e.g*. Schoch & Milner, 2000).

The flat bones of the skull develop via direct transformation of preexisting connective tissue (Francillion-Vieillot et al., 1990). The external surface of the dermal bones is characteristically ornamented. A network of raised, reticulate ridges that enclose approximately flat-bottomed, interlocking, polygonal cells is the most common type. The vast majority of these cells are four-, five-, or six-sided, creating a honeycomb- or waffle iron-like texture. In some temnospondyls, this is essentially the only texture present. The second texture type comprises raised, parallel to sub-parallel ridges separated by round-bottomed grooves (Rinehart & Lucas, 2013). The function of the ornamentation is still unclear. The best supported hypotheses suggest the increase the surface area for skin supports, increasing the strength of the bone or the protection of blood vessels (summarized in Coldiron, 1974; Witzmann, 2009; Rinehart & Lucas, 2013).

The histology of temnospondyl dermal bones was first described by Gross (1934), who provided a short description of the skull bones of *Mastodonsaurus*, *Metoposaurus* and *Plagiosternum*, and recognized that the dermal bones exhibit a diploë structure. Later, histological studies on the dermal bones in Temnospondyli have focused mainly on morphology, vascular network and collagen fibres organization (Bystrow, 1947; Enlow & Brown, 1956; Coldiron, 1974; de Ricqlès, 1981; Castanet *et al*, 2003; Scheyer, 2007) and were limited only to the few taxa. The systematic studies of dermal bones within numerous tetrapod taxa were provided by Witzmann (2009) and de Buffrénil et al. (2016).

Recent the histological studies of metoposaurids have focused mainly on the long bones, ribs and vertebrae (Steyer et al., 2004; Gądek, 2012; Konietzko-Meier & Klein, 2013; Konietzko-Meier & Sander, 2013; Konietzko-Meier et al., 2013; Koniezko-Meier et al., 2014). Up until now the dermal bones of *Metoposaurus* have not been studied in detail histologically. The only record of the histological description of *Metoposaurus diagnosticus* dermal bone was given by Gross (1934) and later re-described by Witzmann (2009). However, it is unclear if the illustrated section was derived from the skull or the pectoral girdle, or even if the tested bone-fragment belongs to *Metoposaurus* at all.

The main goal of this study is to present the detailed description of the histology of almost all bones from one skull and determine, if possible, the tendencies and variability of the histological framework from the one *Metoposaurus krasiejowensis* (Sulej, 2002) skull. The temnospondyl skull functionally represents one skeletal element, however, anatomically, it is a conglomerate of numerous bones various in shape and thickness, having various functions and biomechanical loading (i.e. Fortuny et al., 2011, Fortuny et al., 2012). Another question that arises is if the various functions of the single bones are also reflected in the histology, and if the

histological data may be useful for interpretations the skull mechanics. The results of this question, however, will be published as a separate paper.

MATERIAL AND METHODS

Material – The skull (UOPB 01029; 40 cm in length) of *Metoposaurus krasiejowensis* was studied histologically (Figs. 1 and 2). The roof side of the skull was almost completely preserved, whereas on the palatal side only the fragments of the vomer, parasphenoid, pterygoids, quadrates and exoccipitals were preserved. The species discovered in Poland was originally described as *Metoposaurus diagnosticus krasiejowensis* Sulej, 2002, the subspecies of an older *Metoposaurus diagnosticus* (Meyer, 1842). Brusatte *et al*. (2015) resigned using the subspecies for the German *M. diagnosticus diagnosticus* (von Meyer, 1842) and the Polish *M. diagnosticus krasiejowensis* and suggested to refer both taxa on the separate species level as *M. diagnosticus* and *M. krasiejowensis* instead. This taxonomy is followed in this study.

Locality – The examined material comes from the famous locality in Krasiejów where a large number of disarticulated skeletons have been discovered in the Upper Triassic (Keuper), fine-grained, continental sediments. The bones can be found in two main bone-bearing horizons referred to as the lower and the upper horizon (Dzik & Sulej, 2007). The lower horizon has been deposited on an alluvial plain during a catastrophic mud-flow event (Bodzioch & Kowal-Linka, 2012). The skull presented here, has been excavated from the less than 1 m thick lower bone-bearing layer, which is very rich in *Metoposaurus krasiejowensis* remains accompanied by relatively ~~a~~ high diversified fossil assemblage. Vertebrates are represented by a second temnospondyl, *Cyclotosaurus intermedius* (Sulej & Majer, 2005), a phytosaur (*Palaeorhinus*; see Dzik, 2001), a typical terrestrial tetrapod aetosaur *Stagonolepis olenkae* (Sulej, 2010), pterosaurs

(Dzik & Sulej, 2007), ~~until recently undefined till now~~ sphaenodonts and other small tetrapods (Dzik & Sulej, 2007), and fishes (dipnoans described recently by Skrzycki 2014, as well as various actinopterygian and chondrichthyan species). Invertebrates, such as unionid bivalves (Dzik et al., 2000; Dzik & Skawina, 2011; Skawina 2013), cycloids (Dzik, 2008) spinicaudatan crustaceans (Olempska, 2004), fresh-water ostracods (Olempska, 2004, 2011) and some gastropods, are also very common. The upper horizon is restricted to lenses cemented with calcium carbonate, interpreted as a meander deposit (e.g. Gruszka and Zieliński, 2009). It is dominated by strictly terrestrial animals including *Stagonolepis* and the primitive dinosauromorph *Silesaurus opolensis* (Dzik, 2003). Aquatic vertebrates such as amphibians and phytosaurs are less common compared to the lower horizon. Apart from that, one fragmentary specimen of the rauisuchian *Polonosuchus silesiacus* (Brusatte et al., 2010) was excavated between the upper and lower horizons.

According to complex stratigraphic studies of the Upper Silesian Keuper, the bone-bearing beds have been deposited in the early Norian times (Racki & Szulc, 2014; Szulc et al., 2015a, b), however, biochronological speculations uphold the Late Carnian age (e.g. Dzik & Sulej 2007; Lucas et al. 2007; Lucas, 2015).

Methods – The skull was sectioned in 20 planes (Fig. 2) and the thin sections were prepared according to standard petrographic procedures (Lamm, 2014). The thin sections were ground and polished to a thickness of about 60-80 µm using wet SiC grinding powders (SiC 600, 800). Subsequently, the thin sections were studied under a LEICA DMLP light microscope in plane and cross polarized light.

The histological nomenclature follows Francillion-Vieillot et al. (1990) and Witzmann (2009). According to Francillion-Vieillot et al. (1990) the annual growth cycle consists of a

thick, fast growing zone, a thin, slow growing annulus, and a Line of Arrested Growth (LAG). In this study, the term zone is used as in its traditional meaning, for the highly vascularized layer, with lower organization of collagen fibers. The term annulus refers to the layer without vascular canals and higher organization of collagen fibers, but usually similar in thickness as a zone. In the studied material, no clear LAGs can be observed, instead adjacent to the annuli, numerous lines are present. To avoid nomenclature problems, all lines representing the cessation of growth are referred in this study as resting lines, without determination if they occur annually or not (Konietzko-Meier & Sander, 2013) – also see discussion.

In the thin sections, the average thickness of the entire bone and of each layer was estimated, expressed as an arithmetical average from three measurements of the thickness of the entire bone/layer. The thickness of the external layer was measured three times on the distance between the border line with middle region and the bottom of valleys and three times as the distance between the border line with middle region and the top of ridges. The mathematical average was calculated from these measurements. The minimum and maximum thicknesses represent the lowest and largest measurement, respectively, for each described layer. As the borders between external cortex/middle region/internal cortex were taken the line where the clearly visible increasing of the remodeling degree of the middle region is visible (the number of the erosion cavities, independent of their size, is visible higher). For the estimation of the ratio between the three components (E – external cortex, M – middle region, I – internal cortex; E:M:I), the average thickness of the external cortex was taken as one and then proportionally the value for middle region and internal cortex were calculated. Note that the internal cortex of dermal bone is oriented to the visceral surface of the body, thus in parasphenoid, pterygoid and vomer the external cortex is then oriented ventrally.

A detailed description of each bone is presented in the Supplementary Material.

RESULTS

Microanatomy of dermal bones

Most dermal bones of the skull are flat plates. Only the premaxillas and maxillas possess a more complicated shape (Fig. 3). The premaxilla is built up of three branches: the dental shelf, the alary process (Schoch, 1999) which connects the skull roof to its margin, and the vomeral process, which connects the dental shelf to the vomer (Fig. 3A). The maxilla is built up from two branches, the dorsal branch with an ornamented external cortex, and the ventral branch with the dental shelf (Fig. 3B).

The dermal bones show the clear diploë structure (Fig. 4). The external cortex of the skull-roof bones created variably ornamentations build from a combination of grooves or tubercles and ridges (Table 1, Fig. 1), respectively visible in the cross-section as valleys and ridges (Fig. 4A). The thickness of the flat bones varies from under 0.2 to over 10 millimeters (Table 1), with different proportions between the particular layers. No relation can be observed between the thickness of the external cortex and the thickness of the entire bone, i.e. the external cortex of the tabular and postorbital/jugal about one mm thick, and the average thickness of the skull bones is, respectively, almost ten and six mm (Table 1). The relatively thin squamosum 2 with an average thickness of only about three mm, developed an external cortex which takes up almost half of the bone thickness (Table 1). The largest part of the bone almost always consists of the middle region (which is two to eleven times thicker as the external cortex), with the exception of squamosum 2, where the middle region is the thinnest (Table 1). The internal cortex

183 is the thinnest of the three layers and composes usually only 20% to 80% of the thickness of
184 external cortex, with the exception of the parasphenoid (Table 1).
185
186 **General histology of dermal bones**
187 **External cortex** – In all sections the external cortex is consists of parallel-fibred bone,
188 whereas in the valleys lamellar bone often occurs (Fig. 4B and C). The elongated osteocyte
189 lacunae with branched canaliculi in the bone matrix are numerous (Fig. 5A). Vascular canals are
190 mostly longitudinally oriented (Fig. 5A, B). The degree of vascularization varies from relatively
191 low in the premaxilla and frontal, moderate in the maxilla and prefrontal, to highly vascularized
192 in the jugal, postorbital, parietal, squamosum, quadratojugal, vomer and parasphenoid. In the
193 nasal, postparietal, postfrontal, tabular and supratemporal, numerous vascular canals within the
194 ridges are visible, which are arranged in rows parallel to the bony surface, whereas the valleys
195 are avascular. The external cortex is dominated by simple vascular canals and primary osteons.
196 In some bones (nasal, lacrimal, prefrontal, tabular, squamosum, vomer and parasphenoid), the
197 secondary osteons and single erosion cavities are visible in the transition region to the middle
198 layer (for details see the Supplementary Material).
199 Typical for the external cortex are distinct collagen fibers (Fig. 5C, E). In some bones (jugal,
200 postorbital, postfronat, postparietal, tabular) they create a thick Intervowen Structural Fibres
201 (ISF) (Fig. 5E). In the premaxilla, maxilla, nasal, lacrimal, jugal, postorbital, postparietal, and
202 quadratojugal, well-mineralized Sharpey's fibers can be observed which are relatively short but
203 numerous, and sometimes packed densely in bundles. In the prefrontal, frontal, postfrontal,
204 parietal, supratemporal, squamosum, tabular and vomer, Sharpey's fibers are rare and occur

mostly in the deeper parts of the sculptural ridges (Fig. 5C). In the parasphenoid and pterygoid, Sharpey's fibers cannot be observed.

Growth marks are expressed in various ways. In the ridges of the lacrimal, frontal, jugal, postfrontal, tabular, quadratojugal and squamosum 2, they are manifested as a sequence of thin resting lines (Fig. 5D). In the postparietal, a sequence of lamellar bone layers and layers consisting of ISF are visible (Fig. 5E). In the quadratojugal, two thick annuli built up of lamellar bone alternate with two highly vascularized zones (Fig. 5F). In the postfronal, squamosum 1, supratemporal, tabular, jugal and quadratojugal, the alternations of valleys and ridges are preserved. The remains of older valleys are filled with the highly vascularized tissue which then constructed the ridges of the next generation (Fig. 5G). In the supratemporal the cementing lines indicated the remodeling process involved into the creations of sculpture is visible (Fig. 5H).

Middle region – The external cortex transits gradually into the cancellous middle region. The simple vascular canals and primary osteons, of various shapes, are mostly located next to the border between the middle and external regions. A significant part of the middle region is strongly remodeled. The few large erosion cavities (up to 2000 µm in diameter) are present in the premaxilla, nasal, lacrimal, jugal, prefrontal, postparietal, squamosum 1, quadratojugal and all studied bones from the palatal side of the skull. The most highly remodeled middle region occurs in the vomer, where erosion cavities in some areas exceed 3000 µm in length (Fig. 6A). In the lacrimal and prefrontal, erosion cavities reach up to the external cortex. The maxilla is dominated by numerous, but medium-sized erosion cavities. In the postfrontal, parietal and supratemporal, erosion cavities are small (less than 500 µm in diameter). In the postfrontal they appear sporadically, whereas occur numerous in parietal and supratemporal (Fig. 6B). The middle region in the tabular and squamosum 2 does not show the typical trabecular structure. The

intensive remodeling is visible; however, the tissue is relatively compact, almost without erosion cavities (Fig. 6C).

Internal cortex – The internal cortex consists of parallel-fibered to lamellar bone. The degree of vascularization varies from very low, almost avascular, in the parietal, postfrontal, supratemporal and squamosum, low in the premaxilla, prefrontal, nasal, and postparietal, moderate in the maxilla, frontal, vomer and parasphenoid, to high in the lacrimal, jugal, postorbital and quadratojugal (Fig. 6D-F). Osteocyte lacunae, showing slightly elongated shapes, are very frequent. Growth marks are visible in form of resting lines. The amount of lines varies from four in the postfrontal and parietal, three in the postparietal, supratemporal and jugal, to two in the nasale (Fig. 6D). In the parasphenoid, well developed zones and annuli can be observed (Fig. 6G). Zones are built of thick, well vascularized layers, while annuli are represented by thinner, avascular layers. The numerous Sharpey's fibers packed in bundles are visible in the tabular and vomer.

Endochondral bones

Quadrate – The partially preserved and well-vascularized cortex consists of parallel-fibered and lamellar bone (Fig. 7A, B). The simple vascular canals occur sporadically, and secondary osteons are more common (Fig. 7A, B). The Sharpey's fibers are very short and occur only in the subsurface parts of the cortex. The elongated osteocyte lacunae are present mainly within the lamellar bone, which outlines the osteons. They do not possess canaliculi. Growth marks cannot be observed.

The central region consists is of spongiosa and is characterized by large pore spaces and irregular trabeculae (Fig. 7C), which contain clumps of calcified cartilage (see also the Supplementary Material).

Exoccipital – The cortex consists of parallel-fibered bone and is relatively well-vascularized (Fig. 7D). The simple vascular are few in number (Fig. 7E, F) and located only in the outermost part of the cortex. The secondary osteons are more frequent (Fig. 7D). Well-mineralized, densely packed bundles of Sharpey's fibers are common and can be seen throughout the entire cortex (Fig. 7D, E). In the exoccipital, the Sharpey´s fibers are most abundant and pronounced among all examined bones. Rounded osteocyte lacunae are numerous. Growth marks are absent.

The central region consists of an irregular network of bony trabeculae, with large pore spaces between them (Fig. 7G). In the medial parts of the bone tissue, where trabeculae are poorly developed, accumulations of calcified cartilage are quite common (Fig. 7H).

DISCUSSION

The histological variability – Witzmann (2009) investigated fragments of dermal bones from 20 taxa and concluded that for every taxon, the bone microanatomy and histology were consistent. Intraspecific variability of the histology of dermal bones was only observed in *Mastodonsaurus giganteus* and *Plagiosternum granulosum* and only affects the degree of vascularization and remodeling of the bone (Witzmann, 2009).

Nevertheless, in the *Metoposaurus krasiejowensis* skull, the observed variability is very high and despite bones diploë structure typical for all dermal bones, can be seen in both,

microanatomical and histological levels. The bones show various thicknesses, different proportions between the layers, variations in the vascularization systems, tissue organizations, the presence and organization of Sharpey's fibers, degree of remodeling, and growth pattern (see also the Supplementary Material for the detailed description). The combination of these characters concludes that each sectioning-plane in the skull represents a unique framework. The histological properties are not related to the bone, but strictly depend on the particular sectioning-plane. The transition between the „histological types" is fluent. The jugal and postorbital, sectioned in the suture region, represent the same microanatomical and histological framework (Figs. 2 j and po, 3F; Table 1), whereas the squamosum sectioned in the frontal part of the bone (Fig. 2, sq1) and next to the otic notch (Fig. 2, sq2), showed different architecture on both microanatomical and histological levels (Figs. 3K, L). This suggests that the histological framework is not specifically bone-limited, but seems to be related to the specific area of the skull and i.e. depended on the growth of the entire skull and each bone separately, or to the local biomechanical loading on the particular part of the skull. Fortuny et al. (2012), based on the Finite Elements Analysis, showed that the hypothetical biomechanical stress along the skull is different for each skull-morphotype and depend directly on the shape of the skull and position of the orbits. If the bone framework is related to the biomechanical loading, the high variability of temnospondyls skulls results that each taxon might has a unique histological architecture of homologous bones.

Skeletochronological information – In the external cortex of the *Metoposaurus* skull, four types of growth alternation can be observed: numerous resting lines, the sequence of lamellar layers combined with the high-fibrous tissue (ISF), thick zones and annuli and the alternation of ridges and valleys (Fig. 5D-G).

In the lacrimal, frontal, jugal, postfrontal, postparietal, tabular and quadratojugal, the distinct growth marks are manifested as a sequence of numerous thin lines (Fig. 5D). Similar growth marks, present in the external and internal cortices of the dermal bone, have been observed in several temnospondyl taxa (Scheyer, 2007; Witzmann, 2009). In fast-growing amniotes, the presence of several growth lines (Line of Arrested Growth –LAG) next to the surface of bone is known as the External Fundamental System (EFS), and indicates a slowing down of growth, suggesting that the maximum size has been reached (Sander, 2000; Chinsamy-Turan, 2005; Erickson, 2005; Turvey et al., 2005; Sander et al., 2011). In *Metoposaurus* long bones, similar structures are present in the inner and outer part of the cortex, suggesting that accumulation of external resting lines does not mean the cessation of growth at all, but only the oscillation in growth rate during one season (Konietzko-Meier & Klein, 2013; Konietzko-Meier & Sander, 2013). Then, the complex with accumulation of resting lines is interpreted as the one annulus deposited during one, dry season (Konietzko-Meier & Sander, 2013; Konietzko-Meier & Klein, 2013). As in the long bones, the two highly vascularized parts of the external cortex represent the fast growing zones, and the avascular layers annuli, and the entire external cortex two growth seasons. The sequences of lamellar bone and layers with accumulation of ISF visible in the postprietal (Fig. 5E) can be interpreted as three years of growth. Specific growth marks also represent the alternation of valleys and ridges preserved in the postfronal, squamosum, supratemporal, trabeculare, jugal, and quadratojugal. In these bones, two generations of valleys/ridges are visible (Fig. 5G). However, for all types of growth marks, it is not known how many growth indicators have already been remodeled. In the internal cortex, two to four resting lines are visible; the only exception is the parasphenoid (Fig. 6D). The structure of the internal cortex in the parasphenoid (Fig. 6G) mostly resembles the growth sequence seen in the

318 *Metoposaurus* long bones (Konietzko-Meier & Klein, 2013; Konietzko-Meier & Sander, 2013).
319 The two thick avascular layers represent the annuli, and combined with the two high
320 vascularized zones indicate two growth seasons.

321 Due to the different number of preserved cycles in one skull the estimation of individual
322 age based on the skeletochronological information is very difficult. Without testing the whole
323 growth series, it is not possible to estimate the amount of remodeled tissue and the growth
324 pattern of each bone and thus, no direct conclusion about the individual age of sectioned skull
325 can be provided.

326 Cranial sutures were not visible on the skull surface (Gruntmejer, 2012). The
327 disappearance of all traces of sutures on the skull surface during ontogeny is a phenomena often
328 encountered in adult individuals (Moazen et al., 2008). In the completely preserved skeletons of
329 *Dutuitosaurus ouazzoui* (Dutuit, 1976), a skull of similar length (about 400 mm) as the here
330 described, corresponds with about 142 mm long femur (Dutuit, 1976: pl XXXI; personal
331 observation DKM). Steyer et al. (2004) calculated the individual age of the adult *Dutuitosaurus*
332 femur, comparable in length, for eight to nine years. For the *Metoposaurus* from Poland, large
333 femora are not known; the largest one which was studied histologically is about 90 mm long and
334 is estimated at four years of age (Konietzko-Meier & Klein, 2013). However, comparing
335 skeletochronological data of *Metoposaurus* with that of *Dutuitosaurus* revealed that the femora
336 of overlapping sizes show a similar age in both taxa, whereas the larger femora of *Dutuitosaurus*
337 are older compared to the smaller *Metoposaurus* femora (Konietzko-Meier & Klein, 2013).
338 Thus, on the basis of skeletochronology, a strong developmental plasticity can be excluded for
339 both taxa. The individual age of the Krasiejów skull, based on the comparison with
340 *Dutuitosaurus,* can be estimated at about eight to ten years. With the preservation of maximum

three growth layers in the external cortex and two in the internal one, the amount of remodeled growth marks could reach up to six to seven. This indicates a relatively fast remodeling rate of the dermal bones of the skull compared to the long bones.

Remodelling degree – Among the sections from the *Metoposaurus* skull, four main remodeling degrees could be observed in the middle region. The relatively lowest remodeled samples are from the postfrontal, parietal and supratemporal. A few large erosion cavities are present in the premaxilla, nasal, lacrimal, jugal, prefrontal, postparietal, squamosum, quadratojugal and all studied bones from the palatal side of the skull. The maxilla is dominated by numerous, but medium sized erosion cavities. In the middle region of the tabular and squamosum 2, the bone deposition exceeds the bone resorption and it does not represent the typical spongious structure.

The increase in remodeling degree is known as ~~a~~ one of the developmental characters. Witzmann (2009) published the detailed histology of dermal bones from a young adult and adult *Mastodonsaurus,* and observed an increase in remodeling (expressed as an increase of the erosion cavities sizes) in the older specimen. In the *Metoposaurus* skull, different histological stages can be observed among different bones in the skull. The low (postfrontal, parietal and supratemporal) and highly (premaxilla, nasal, lacrimal, jugal, prefrontal, postparietal, squamosum, quadratojugal) remodeled bones seem to represent two stages of the same process, resulting in the increase in porosity of the middle region. This may indicate the sequence of the skull ossification during ontogeny, with the latest ossification of bones occurring on the central part of the skull roof. However, less remodeled samples originate from the groves-ridges regions, whereas the other sections come from the reticulate areas. This confirms the hypothesis presented first by Bystrow (1935) that the polygonal reticulate structures are the center of

ossification and ridges-grooves areas show the direction and extent of growth from theses ossification centers. In this case, different remodeling degrees, which resemble the ontogenetic change, is the result of longitudinal growth of the bone.

Dynamic of the sculpture pattern – Although dermal sculpture was early recognized as a characteristic for basal tetrapods (e.g. von Meyer, 1858; Fraas, 1889; Fritsch, 1889; Zittel, 1911), the morphogenesis of the sculptures is still questionable (summarized by Witzmann et al., 2010, de Buffrénil et al., 2016). Among extant tetrapods, growth of dermal bony tubercles and ridges has been studied in osteoderms of squamates and in dermal skull bones and osteoderms of crocodiles. In squamates, the presence of pits and ridges on the external surface of osteoderms follows from both local resorption and growth of bone (Zylberberg and Castanet, 1985; Levrat-Calviac & Zylberberg, 1986), whereas in crocodile dermal bones, de Buffrénil (1982) stated that sculpture is mainly the result of local resorption. In contrast, Vickaryous and Hall (2008) found no evidence for morphogenesis of bone sculpture by resorption in *Alligator mississippiensis* and presumed that sculptural ridges develop by preferential bone growth. Concerning basal tetrapods, Bystrow (1935, 1947) showed that the development of bone sculpture in the temnospondyls *Benthosuchus*, *Platyoposaurus* and *Dvinosaurus* took place solely by growth of the bony ridges and tubercles, and resorptive processes were not involved. The thin sections of the dermal bones of skull and pectoral girdle in the basal tetrapods investigated by Witzmann (2009), corroborate Bystrow's findings and show that the dermal sculpture did not develop by local resorption of the bone surface, comparable to the pattern in basal tetrapod osteoderms (Witzmann & Soler-Gijón 2008). According to the last study (de Buffrénil et al., 2016) the involvement of several complex remodeling processes, with the local succession of resorption and reconstruction cycles, is frequent and occurs in all major gnathostome clades. All temnospondyl sections share an

important common feature: the lack of superficial remodeling (resorption and reconstruction cycles). The supratemporal of *Metoposaurus* however show ~~the clearly~~ remodeling process involved in~~to~~ the sculpture creation (Fig. 5H). Because of it is the only one sample it is difficult to generalize the observation, but it proofs that the osteogenic mechanisms involved in the creation and growth are still not clear.

The latest study of de Buffrénil et al. (2016) confirmed, however, that the distinct dynamic processes are involved in the creation and growth of pits and ridges. ~~Authors (de~~ Buffrénil et al., 2016) observed six main patterns of modification of ornamentation image during growth. The simplest one is repetition of the width or position of pits and ridges from one growth stage to the following one. The ridges can drift diverge symmetrically in two opposite directions or the ridges around a given pit may migrate in the same direction. Also the change of size of the ridges is possible providing to the gradual narrowing of pit diameter (convergent ridge drift) or opposite process may occur when the reduction of ridge width is observed. In most drastic case the pits can be entirely filled, and disappear to be replaced in situ by ridges.

The sections from the *Metoposaurus* skull show that the new bone deposition mostly repeats the pattern of sculptures present in the younger stages (Fig. 5D-F); but an ridges drift and valley/ridges alternation my also occur (Fig. 5G). In the last case in such places, where valleys occurred, ridges are being deposited during the next bone generation stage. However, the distance between newly created tops of the ridges is not distinctively different than of the previous generation.

It indicates that the metric pattern of the sculpture is relatively stable, but the position of the ridges and grooves is dynamic during growth as a specific adaptation to different biomechanical loading on the new, larger bone.

Sharpey's fibers – The well-mineralized Sharpey's fibers are present in the cortex of all bones of the *Metoposaurus krasiejowensis* skull. In dermal bones, they are most likely the remains of soft tissue and small muscle attachments (Francillion-Vieillot et al., 1990). In the occipital condyles, Sharpey's fibers are densely packed in bundles and they are much thicker and longer (Fig. 7D) than in the other bones. The Sharpey's fibers occur here in similar amounts like in vertebrae (Konietzko-Meier et al., 2013). Large concentrations of Sharpey's fibers indicate that the exoccipital creates an attachment point for well developed, strong muscles and ligaments which connects the skull to the vertebral column.

Quadrate bone and exoccipital – These bones clearly differ from all other bones of the skull. Their internal structure is very similar to vertebral intercentra. In the case of *Metoposaurus krasiejowensis*, the histology and ossification process of the vertebrae have been detailed described (Konietzko-Meier et al., 2013). The quadrate and exoccipital consists of a trabecular middle region, surrounded by a thin layer of well-vascularized cortex. The presence of cartilage (Fig. 7H) indicates that ossification follows a pattern known for vertebrae with relatively slow ossification of the trabecular part and late development of the periosteal cortex (Konietzko-Meier et al., 2013).

ACKNOWLEDGEMENST

The authors acknowledge Olaf Dülfer (University of Bonn, Steinman Institute) for preparing some of the thin-sections. We are grateful to Kayleigh Wiersma (University of Bonn, Steinmann

Institute) for improving the English. Aurore Canoville and Martin Sander are acknowledged for fruitful discussion. We thank both reviewers (…..) and editors for all comments.

Author Contributions

Conceived and designed the experiments: KG DKM AB. Analyzed the data: DKM KG AB. Contributed reagents/materials/analysis tools: DKM KG AB. Wrote the paper: DKM KG AB.

REFERENCES

1. Bodzioch A, Kowal-Linka M. 2012. Unraveling the origin of the Late Triassic multitaxic bone accumulation at Krasiejow (S Poland) by diagenetic analysis. *Palaeogeography, Palaeoclimatology, Palaeoecology* 346/347:25-36.
2. Brusatte SL, Nesbitt SJ, Irmis RB, Butler RJ, Benton MJ, Norell MA. 2010. The origin and early radiation of dinosaurs. *Earth-Science Reviews* 101:68-100.
3. Brusatte SL, Butler MJ, Mateus O, Steyer JS. 2015. A new species of *Metoposaurus* from the Late Triassic of Portugal and comments on the systematics and biogeography of Metoposaurid Temnospondyls. *Journal of Vertebrate Paleontology*, 35(3): e912988, DOI: 10.1080/02724634.2014.912988.
4. Buffrénil de V. 1982. Morphogenesis of bone ornamentation in extant and extinct crocodilians. *Zoomorphology* 99(2):155-166.

5. Buffrénil de V, Clarac F, Canoville A, Laurin M. 2016. Comparative data on the differentiation and growth of bone ornamentation in Gnathostomes (Chordata: Vertebrata). *Journal of Morphology* (in press.).
6. Bystrow AP, 1935. Morphologische Untersuchungen der deckknochen Schädels der Stegocephalen. *Acta Zoologica* 16:65-141.
7. Bystrow AP. 1947. Hydrophilous and zenophilous labyrinthodonts. *Acta Zoologica* 28:137-164.
8. Castanet J, Francillon-Vieillot H, de Ricqlès A. 2003. The skeletal histology of the Amphibia. In H. Heatwole and M. Davies (eds.), Amphibian Biology, Volume 5, Osteology. Surrey Beatty and Sons, Chipping Norton, New South Wales, Australia, 1598-1683.
9. Chinsamy-Turan A. 2005. The Microstructure of Dinosaur Bone: Deciphering Biology with Fine-scale Techniques. Johns Hopkins University Press, Baltimore. 1-195.
10. Coldiron RW. 1974. Possible functions of ornament in labyrinthodont amphibians. *Occasional Papers of the Museum of Natural History of the University of Kansas*, Lawrence, 33:1-19.
11. Dutuit JM. 1976. Introduction à l'etude paleontologique du Trias continental marocain. Description des premiers Stegocephales recueillis dans le couloir d'Argana (Atlas occidental). *Memoires du Museum National d'Histoire Naturelle Paris Ser. C* 36:1-253.
12. Dzik J, Sulej T, Kaim A, Niedźwiedzki R. 2000. Późnotriasowe cmentarzysko kręgowców lądowych w Krasiejowie na Śląsku Opolskim. *Przegląd Geologiczny* 48:226-35.

13. Dzik J. 2001. A new *Paleorhinus* fauna in the early Late Triassic of Poland. *Journal of Vertebrate Paleontology* 21:625-627.

14. Dzik J. 2003. A beaked herbivorous archosaur with dinosaur affinities from the early Late Triassic of Poland. *Journal of Vertebrate Paleontology* 23:556-574.

15. Dzik J, Sulej T. 2007. A review of the early Late Triassic Krasiejów biota from Silesia, Poland. *Palaeontologia Polonica* 64:3-27.

16. Dzik J. 2008. Gill structure and relationships of the Triassic cycloid crustaceans. *Journal of Morphology* 269:1501-1519.

17. Enlow DH, Brown SO. 1956. A comparative histological study of fossil and recent bone tissues. *I. Texas Journal of Science* 8:405-43.

18. Erickson GM. 2005. Assessing dinosaur growth patterns: a microscopic revolution. *Trends in Ecology and Evolution* 20(12):677-84.

19. Fortuny J, Marcé-Nogué J, de Esteban-Trivigno S, Gil L, Galobart Á. 2011. Temnospondyli bite club: ecomorphological patterns of the most diverse group of early tetrapods. *Journal of Evolutionary Biology* 24:2040-2054.

20. Fortuny J, Marce´-Nogue´ J, Gil L, Galobart A`. 2012. Skull mechanics and the evolutionary patterns of the otic notch closure in Capitosaurs (Amphibia: Temnospondyli). *The Anatomical Record* 295:1134-1146.

21. Fraas E. 1889. Die Labyrinthodonten der Schwäbischen Trias. *Palaeontographica* 36:1-158.

22. Francillon-Vieillot H, de Buffrénil V, Castanet J, Géraudie J, Meunier F-J, Sire J-Y, Zylberberg L, de Ricqlès A. 1990. Microstructure and mineralization of vertebrate

497 skeletal tissues. In: Carter JG [ed.]: Skeletal Biomineralization: Patterns, Processes and
498 Evolutionary Trends, Vol. I. Van Nostrand Reinhold, New York. 471-530.
499 23. Fritsch A. 1889. Fauna der Gaskohle und der Kalksteine der Permformation Böhmens,
500 Vol. 2. Prag: Selbstverlag. 1-132.
501 24. Gądek K. 2012. Palaeohistology of ribs and clavicle of *Metoposaurus diagnosticus* from
502 Krasiejów (Upper Silesia, Poland). *Opole Scientific Society Nature Journal* 45:39-42.
503 25. Gross W. 1934. Die Typen des mikroskopischen Knochenbaues bei fossilen
504 Stegocephalen und Reptilien. *Zeitschrift für Anatomie und Entwicklungsgeschichte*
505 203:731-64.
506 26. Gruntmejer K. 2012. Morphology and function of cranial sutures of the Triassic
507 amphibian *Metoposaurus diagnosticus* (Temnospondyli) from southwest Poland. In: Jagt-
508 Yazykova E, Jagt J, Bodzioch A, & Konietzko-Meier D. [eds] Krasiejów –
509 palaeontological inspirations. *ZPW Plik*, Bytom. 34-54.
510 27. Gruszka B, Zieliński T. 2008. Evidence for a very low-energy fluvial system: a case
511 study from the dinosaur-bearing Upper Triassic rocks of Southern Poland. *Geological*
512 *Quarterly* 52:239-252.
513 28. Konietzko-Meier D, Sander PM. 2013 Longe bone histology of Metoposaurus
514 diagnosticus (Temnospondyli) from the Late Triassic of Krasiejów (Poland) and its
515 paleobiological implications. *Journal of Vertebrate Paleontology* 35(5):1-16.
516 29. Konietzko-Meier D, Klein N. 2013. Unique growth pattern of *Metoposaurus diagnosticus*
517 *krasiejowensis* (Amphibia, Temnospondyli) from the Upper Triassic of Krasiejów,
518 Poland. *Palaeogeography Palaeoclimatology Palaeoecology* 370:145-157.

519 30. Konietzko-Meier D, Bodzioch A, Sander PM, 2013. Histological characteristics of the
520 vertebral intercentra of *Metoposaurus diagnosticus* (Temnospondyli) from the Upper
521 Triassic of Krasiejów (Upper Silesia, Poland). *Earth and Environmental Science*
522 *Transactions of the Royal Society of Edinburgh* 103:1-14.
523 31. Konietzko-Meier D, Danto M, Gądek K, 2014. The microstructural variability of the
524 intercentra among temnospondyl amphibians. *Biological Journal of the Linnean Society*
525 112:747-764.
526 32. Levrat-Calviac V, Zylberberg L. 1986. The structure of the osteoderms in the gekko:
527 *Tarentola mauritanica*. *American Journal of Anatomy* 176:437-446.
528 33. Lucas SG. 2015. Age and correlation of Late Triassic tetrapods from southern Poland.
529 *Annales Societatis Geologorum Poloniae* 85(4):627-635.
530 34. Lucas SG, Spielmann JA, Hunt AP. 2007. Bio-chronological significance of Late Triassic
531 tetrapods from Krasiejów, Poland. *New Mexico Museum of Natural History and Science*
532 *Bulletin* 41:248-258.
533 35. Meyer E. 1842. Labyrinthodonten—Genera. Neues Jahrbuch für Mineralogie,
534 *Geographie, Geologie, Palaeontologie* 1842:301-304.
535 36. Meyer H von. 1858. Reptilien aus der Steinkohlenformation in Deutschland.
536 *Palaeontographica* 6:59-219.
537 37. Moazen M, Curtis N, Evans SE, O'Higgins P, Fagan M.J. 2008. Rigid-body analysis of a
538 lizard skull: Modelling the skull of *Uromastyx hardwickii*. *Journal Biomechanics*
539 41:1274-1280.

38. Mukherjee D, Ray S, Sengupta DP. 2010. Preliminary observations of the bone microstructure, growth patterns, and life habits of some Triassic Temnospondyls from India. *Journal of Vertebrate Paleontology* 30(1):78-93.

39. Olempska E. 2004. Late Triassic spinicaudatan crustaceans from southwestern Poland. *Acta Palaeontologica Polonica* 49(3):429-442.

40. Olempska E. 2011. Fresh-water ostracods from the Late Triassic of Poland. *Joannea Geologie und Paläontologie* 11:154-155.

41. Lamm ET. 2014. Preparation and sectioning of specimens. In: Padian K, Lamm ET, (eds.), Bone histology of fossil tetrapods, advancing methods, analysis, and interpretation. University of California Press. Barkley, Los Angeles, London. 35-54.

42. Racki G, Szulc J. 2014. Formacja grabowska – podstawowa jednostka litostratygraficzna kajpru Górnego Śląska. *Przegląd Geologiczny* 63(2):103-113.

43. Ricqlès A. de 1981. Recherches paléohistologiques sur les os longs des tétrapodes. VI.- Stégocéphales. *Annales de Paléontologie* 67:141-160.

44. Rienhart LF, Lucas SG, 2013. The functional morphology of dermal bone ornamentation in temnospondyl amphibian. In: Tanner LH, Spielmann JA & Lucas SG [eds] The Triassic System. New Mexico Museum of Natural History and Science, Bulletin 61. 524-532.

45. Sanchez S, Germain D, de Ricqlès, Abourachid A, Goussard F, Tafforeau P, 2010. Limb-bone histology of temnospondyls: implications for understanding the diversification of palaeoecologies and patterns of locomotion of Permo-Triassic tetrapods. *Journal of Evolutionary Biology* 1-15.

562 46. Sander PM. 2000. Long bone histology of the Tendaguru sauropods: implications for
563 growth and biology. *Paleobiology* 26:466-488.
564 47. Sander PM, Klein N, Stein K, Wings O. 2011. Sauropod bone histology and its
565 implications for sauropod biology. In Klein N, K. Remes K, Gee C T & Sander PM [eds]
566 Biology of the Sauropod Dinosaurs: Understanding the Life of Giants. Life of the Past
567 (series ed. J. Farlow). Indiana University Press, Bloomington. 276-302
568 48. Scheyer TM. 2007: Skeletal histology of the dermal armor of Placodontia: the occurrence
569 of 'postcranial fibro-cartilaginous bone' and its developmental implications. *Journal of*
570 *Anatomy* 211:737-753.
571 49. Schoch RR. 1999. Comparative osteology of *Mastodonsaurus giganteus* (Jaeger, 1828)
572 from the Middle Triassic (Lettenkeuper: Longobardian) of Germany (Baden-
573 Württemberg, Bayern, Thüringen). *Stuttgarter Beiträge zur Naturkunde Serie B*
574 *(Geologie und Paläontologie)* 278:1-170.
575 50. Schoch RR, Milner AR. 2000. Stereospondyli. *Handbuch der Palaeoherpetologie* 3B.
576 Munich: Verlag Dr. Friedrich Pfeil 1-230.
577 51. Skawina A, Dzik J. 2011. Umbonal musculature and relationships of the Late Triassic
578 filibranch unionoid bivalves. *Zoological Journal of the Linnean Society* 163:863-883.
579 52. Skawina A. 2013. Population dynamics and taphonomy of the Late Triassic (Carnian)
580 freshwater bivalves from Krasiejów (Poland). *Palaeogeography, Palaeoclimatology,*
581 *Palaeoecology* 379:68-80.
582 53. Skrzycki P. 2015. New species of lungfish (Sarcopterygii, Dipnoi) from the Late Triassic
583 Krasiejów site in Poland, with remarks on the ontogeny of Triassic dipnoan tooth plates.
584 *Journal of Vertebrate Paleontology* 35(5):e964357.

585 54. Steyer JS, Laurin M, Castanet J, de Ricqle`s A. 2004. First histological and
586 skeletochronological data on temnospondyl growth: palaeoecological and
587 palaeoclimatological implications. *Palaeogeography, Palaeoclimatology, Palaeoecology*
588 206:193-201.
589 55. Sulej T, 2002. Species discrimination of the Late Triassic temnospondyl amphibian
590 Metoposaurus diagnosticus. *Acta Paleontologia Polonica* 47(3):535-546.
591 56. Sulej T. 2005. A new rauisuchian reptile (Diapsida: Archosauria) from the Late Triassic
592 of Poland. *Journal of Vertebrate Paleontology* 25(1):78-86.
593 57. Sulej T, Majer D. 2005. The temnospondyl amphibian *Cyclotosaurus* from the Upper
594 Triassic of Poland. *Palaeontology* 48:157-170.
595 58. Sulej T. 2007: Osteology, variability, and evolution of *Metoposaurus*, a temnospondyl
596 from the Late Triassic of Poland. *Paleontologia Polonica* 64:29-139.
597 59. Sulej T. 2010. The skull of an early Late Triassic aetosaur and the evolution of the
598 stagonolepidid archosaurian reptiles. *Zoological Journal of the Linnean Society* 158:860-
599 881.
600 60. Szulc J, Racki G, Jewuła K. 2015a. Key aspects of the stratigraphy of the Upper Silesian
601 middle Keuper, southern Poland. *Annales Societatis Geologorum Poloniae* 85(4):557-
602 586.
603 61. Szulc J, Racki G, Jewuła K, Środoń J. 2015b. How many Upper Triassic bone–bearing
604 levels are there in Upper Silesia (southern Poland)? A critical overview of stratigraphy
605 and facies. *Annales Societatis Geologorum Poloniae* 85(4):587-626.
606 62. Turvey SP, Green OR, Holdaway RN. 2005. Cortical growth marks reveal extended
607 juvenile development in New Zealand moa. *Nature* 435:940-943.

608 63. Vickaryous MK, Hall BK. 2008. Development of the dermal skeleton in *Alligator*
609 *mississippiensis* (Archosauria, Crocodylia) with comments on the homology of
610 osteoderms. *Journal of Morphology* 269:398-422.
611 64. Witzmann F, Soler-Gijón R. 2008. The bone histology of osteoderms in temnospondyl
612 amphibians and in the chroniosuchian *Bystrowiella*. *Acta Zoologica* (Stockholm) 91: 96-
613 114. DOI 10.1463–6395.1111/j2008.00385.x
614 65. Witzmann F. 2009. Comparative histology of sculptured dermal bones in basal tetrapods,
615 and the implications for the soft tissue dermis. *Palaeodiversity* 2:233-270.
616 66. Witzmann F, Scholz H, Müller J, Kardjilov N. 2010. Sculpture and vascularization of
617 dermal bones, and the implications for the physiology of basal tetrapods. *Zoological*
618 *Journal of the Linnean Society* 160:302-340.
619 67. Zittel KA. 1911. Grundzüge der Paläontologie (Paläozoologie). II. Abteilung. Vertebrata.
620 Verlag von R. Oldenbourg, München and Berlin. 1-589.
621 68. Zylberberg L, Castanet J. 1985. New data on the structure and the growth of the
622 osteoderms in the reptile *Anguis fragilis* L. (Anguidae, Squamata). *Journal of*
623 *Morphology* 186:327-342.
624
625
626
627
628
629
630

631

632

633 **Fig. 1.** The skull of *Metoposaurus krasiejowensis* (UOPB 01029) from Late Triassic of Poland.
634 **(A)** Dorsal view of skull; **(B)** Ventral view of the skull. Scale bar equals 10 cm.

635

636 **Fig. 2.** The sectioning planes of the *Metoposaurus krasiejowensis* skull (UOPB 01029) from
637 Late Triassic of Poland. **(A)** The skull roof; **(B)** The palatal side of the skull. The sectioning
638 planes are marked by red lines. Dark grey color indicates preserved parts of the skull; the
639 destroyed or sediment-covered regions are indicated by the light grey color. Scale bar equals 10
640 cm. Abbreviations: pm = premaxilla, m = maxilla, n = nasal, l = lacrimal, prf = prefrontal, j =
641 jugal, po = postorbital, pf = postfrontal, f = frontal, p = parietal, st = supratemporal, sq1 =
642 squamosum 1, sq2 = squamosum 2, pp = postparietal, t = tabular, qj = quadratojugal, v = vomer,
643 ps = parasphenoid, pt = pterygoid, q = quadrate bone, ex = exoccipital.

644

645 **Fig. 3.** General microanatomy of the skull bones of *Metoposaurus krasiejowensis* (UOPB 01029)
646 from Late Triassic of Poland. **(A)** premaxilla; **(B)** maxilla; **(C)** nasal; **(D)** lacrimal; **(E)**
647 prefrontal; **(F)** jugal/ postorbital; **(G)** postfrontal; **(H)** frontal; **(I)** parietal; **(J)** supratemporal; **(K)**
648 squamosum 1; **(L)** squamosum 2; **(M)** postparietal; **(N)** tabular; **(O)** quadratojugal; **(P)**
649 parasphenoid; **(Q)** vomer; **(R)** pterygoid; **(S)** quadrate bone; **(T)** exoccipital. Scale bar equals 10
650 mm. Abbreviations: ap = alary process, ds = dental shelf, vp = vomeral process.

651

652 **Fig. 4.** Detailed microanatomy of the skull bones of *Metoposaurus krasiejowensis (*UOPB
653 01029) from Late Triassic of Poland, based on the frontal. **(A)** A valley and two ridges; **(B)**

654 Enlargement of (A); the external and internal cortex, and trabecular middle region with
655 numerous and large erosion cavities are visible; image in cross-polarized light; **(C)** The same as
656 (B), but in plane-polarized light. Dashed lines mark the approximately border between the
657 external cortex/middle region/internal cortex. Scale bars equal 10 mm for (A), and 500 µm for
658 (B-C). Abbreviations: g = groove, v = valley, EC = external cortex, MR = middle region, IC =
659 internal cortex, ER = erosion cavities, LB = lamellar bone, PFB = parallel-fibred bone.
660

661 **Fig. 5.** Histology of the external cortex of the skull bones of *Metoposaurus krasiejowensis*
662 (UOPB 01029) from Late Triassic of Poland. **(A)** Fragment of external cortex of the frontal,
663 image in plane-polarized light; **(B)** Same as (A), but in cross-polarized light; **(C)** External cortex
664 of the tabular with distinct Sharpey's fibers in the area of the sculptural ridges, image in cross-
665 polarized light; **(D)** The resting lines (black arrows) in the cortex of squamosum2, image in
666 plane-polarized light; **(E)** The resting lines expressed as an alternation of lamellar layers and
667 layers with distinct Interwoven Structural Fibers (ISF) in the external cortex of the postparietal,
668 image in cross-polarized light; **(F)** Zones and annuli present in the external cortex of the
669 quadratojugal, image in cross-polarized light; **(G)** Alternation of valleys and ridges in the
670 postfrontal, image in cross-polarized light; note that remains of lamellar bone in the deep part of
671 cortex are present, representing the bottom of a valley from an older generation. **(H)** The
672 cementing lines (black arrows) visible in the superficial part of the external cortex of the
673 supratemporal. Dashed lines mark the approximate border between the external cortex/middle
674 region/internal cortex. Scale bars equal for (A-E) and (H) 100 µm and for (F)-(G) 500 µm.
675 Abbreviations: OL = osteocyte lacunae, FLB = fibro-lamellar bone, PO = primary osteons, SF =

676 Sharpey's fibers, LB = lamellar bone, ISF = Interwoven Structural Fibers, A = annulus, Z =
677 zone, r = ridge, v = valley.
678
679 **Fig. 6.** The details of the histology of the middle region and internal cortex of the skull (UOPB
680 01029) bones of *Metoposaurus krasiejowensis* from Late Triassic of Poland. **(A)** Large erosion
681 cavities present in the middle region of the vomer; image in plane-polarized light; **(B)** Poorly
682 remodeled, well vascularized middle region of the parietal; image in plane-polarized light; **(C)**
683 Poorly vascularized fragment of the middle region of the squamosum2; image in plane-polarized
684 light; **(D)** Avascular internal cortex with resting lines (black arrows) visible in the parietal; image
685 in plane-polarized light; **(E)** Moderately vascularized internal cortex of the premaxilla; image in
686 plane-polarized light; **(F)** Highly vascularized internal cortex of the jugal; image in plane-
687 polarized light; **(G)** Alternation of thick annuli and zones visible in the internal cortex of the
688 parasphenoid; image in cross-polarized light. Dashed lines mark the approximately border
689 between the external cortex/middle region/internal cortex. Scale bars equal 100 μm for (D) and
690 (G) and 500 μm for other photographs. Abbreviations: IC = internal cortex, MR = middle region,
691 EC = external cortex, VC = vascular canals, A = annulus, Z = zone.
692
693 **Fig. 7.** Histological details of the quadratum (A-C) and exoccipitale (D-H) of *Metoposaurus*
694 *krasiejowensis* skull (UOPB 01029) from Late Triassic of Poland. **(A)** Fragment of cortex of the
695 quadratum; image in plane-polarized light; **(B)** The same as (A), but in cross-polarized light; **(C)**
696 Trabecular bone of the quadrate bone; image in plane-polarized; **(D)** Fragment of cortex of the
697 exoccipitale with distinct Sharpey's fibers; image in cross-polarized light; **(E)** Close-up of (D),
698 note that the Sharpey's fibers are also visible in plane-polarized light; **(F)** The same as (E) but in

699 cross-polarized light; **(G)** Trabeculae visible in the central part of the exoeccipitale, image in
700 plane-polarized light; **(H)** Remains of calcified cartilage preserved in the trabeculae part of
701 exoccipital, image in cross-polarized light. Scale bars equal 500 µm for (C), (D) and (G), and
702 100 µm for other photographs. Abbreviations: C = cortex, TR= trabecular region, OL = osteocyte
703 lacunae, PO = primary osteons, PFL = parallel-fibred bone, VC = vascular canals, ER = erosion
704 cavities, SO = secondary osteons, SF = Sharpey's fibers, CC = calcified cartilage.
705

Table 1(on next page)

Microanatomy of the sampled bones of Metoposaurus krasiejowensis[i] skull (UOPB 01029).

1 Microanatomy of the sampled bones of *Metoposaurus krasiejowensis* skull (UOPB 01029).

bone	ornamentation	min-max thickness (µm)	average thickness (µm)[1]	E:M:I[2]	thickness of the external cortex (µm)
premaxilla (pm)	not preserved	3000 - 5000	4081.2	1:5.4:0.6	583.0
maxilla (m)	not preserved	4000-12000	10720.0	1:11.8:0.6	800.0
nasal (n)	relatively high ridges (about 1000 µm)	1000-8000	1404.0	1:3.6:0.6	270.0
lacrimal (l)	medium high (500 µm), steep ridges and wide grooves	2250-8000	2790.0	1:7.5:0.8	300.0
prefrontal (prf)	medium high (500 µm) and steep ridges	4000-6000	5022.0	1:3.7:0.7	930.0
jugal (j)	high ridges (about 1000 µm) and wide grooves	4000-6500	5900	1:4.2:0.7	1000.0
postorbital (po)	high ridges (about 1000 µm) and wide grooves	4000-6500	5900	1:4.2:0.7	1000.0
postfrontal (pf)	low ridges (about 300 µm) and shallow grooves	3000-5000	3212.0	1:5.7:0.6	440.0
frontal (f)	high ridges (about 1000 µm) and wide grooves	4000-5000	4686.0	1:5.5:0.6	660.0
parietal (p)	high ridges (about 1000 µm) and narrow pits	1000-4000	1960.0	1:3.5:0.4	400.0
supratemporal (st)	high ridges (about 1500 µm) and wide grooves	3000-5000	5130.0	1:4.4:0.3	900.0
squamosum 1 (sq1)	very high ridges (up to 2000 µm) and wide grooves	3000-7000	4700.0	1:2.2:0.2	1100.0
squamosum 2 (sq2)	high ridges (about 1000 µm) and wide grooves	1200-3900	3050.0	1:0.3:0.5	1750.0
postparietal (pp)	steep, high ridges (about 1500 µm) and polygonal pits	7500-10500	6020.0	1:3.1:0.2	1400.0
tabular (t)	high ridges (about	10000-	9760.0	1:6.5:0.8	1000.0

	1000 μm) and wide pits	12000			
quadratojugal (qj)	high ridges (about 1000 μm) and wide grooves	5000-7000	5100.0	1:2.9:0.6	900.0
vomer (v)	no clear sculpture	3000-6000	3379.0	1:2.8:0.7	650.0
parasphenoid (ps)	no clear sculpture	2000-5000	3750.0	1:5:1.5	900.0
pterygoid (pt)	no clear sculpture	5500-8000	5750.0	1:5.4:1	550.0
quadrate bone (q)*	-	diameter 20 mm			
exoccipital (ex)*	-	diameter 20 mm			

[1]The average thickness of entire bone was estimated in thin sections, expressed as an arithmetical average from three measurements of the thickness of a bone taken on the bottom of valleys and the top of ridges[; 2] For the estimation of ratio between external cortex (E), medial region (M) and internal cortex (I): E:M:I, the thickness of external cortex was taken as one and then proportionally the value for medial region and internal cortex were calculated;

*Non-dermal bone

Figure 1(on next page)

The skull of Metoposaurus krasiejowensis [i](UOPB 01029) from Late Triassic of Poland.

(A) **Dorsal view of skull; (B)** Ventral view of the skull. Scale bar equals 10 cm.

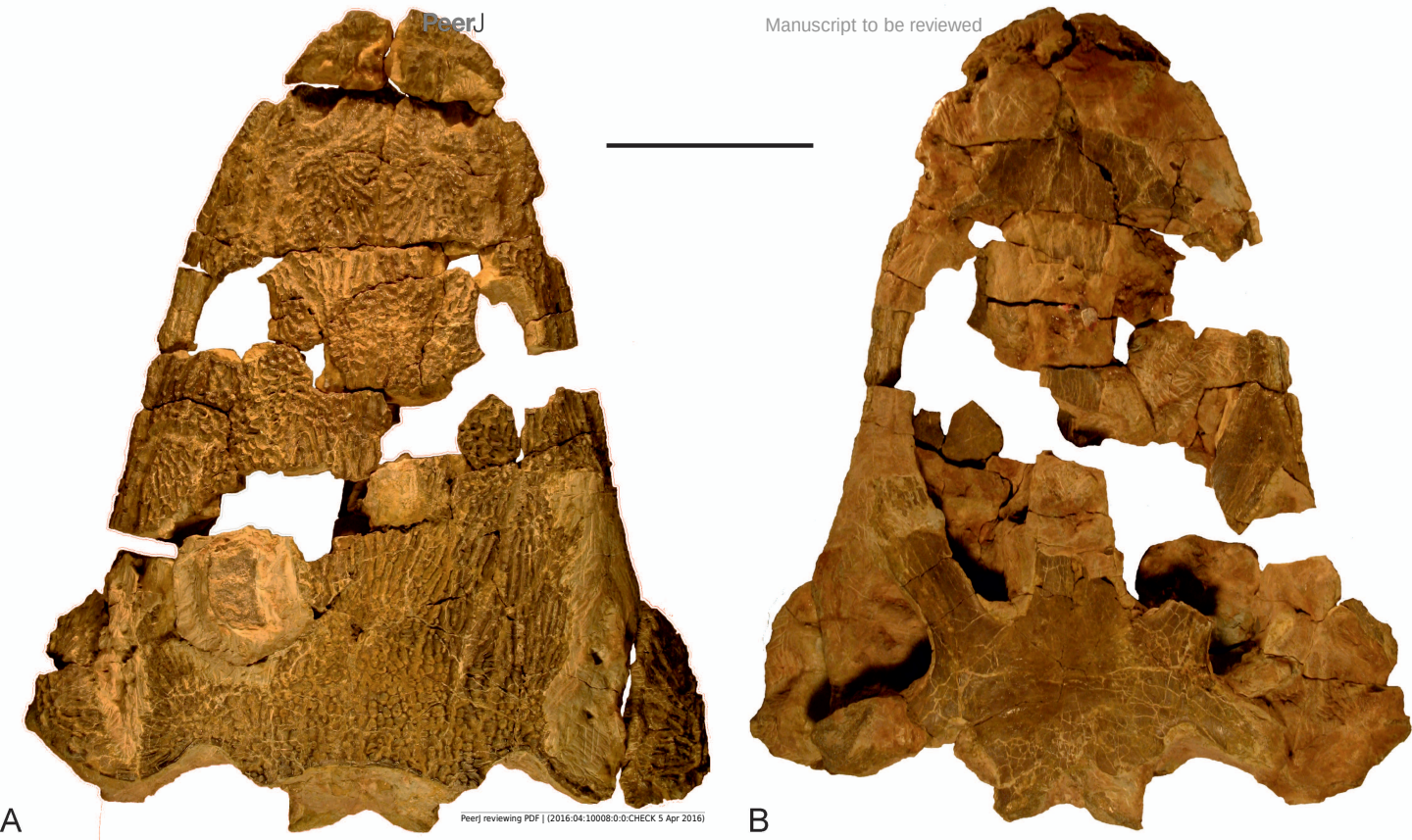

A

B

Figure 2(on next page)

The sectioning planes of the Metoposaurus krasiejowensis[i] skull (UOPB 01029) from Late Triassic of Poland.

(A) **The skull roof; (B)** The palatal side of the skull. [b]The sectioning planes are marked by red lines. Dark grey color indicates preserved parts of the skull; the destroyed or sediment-covered regions are indicated by the light grey color. Scale bar equals 10 cm. Abbreviations: pm = premaxilla, m = maxilla, n = nasal, l = lacrimal, prf = prefrontal, j = jugal, po = postorbital, pf = postfrontal, f = frontal, p = parietal, st = supratemporal, sq1 = squamosum 1, sq2 = squamosum 2, pp = postparietal, t = tabular, qj = quadratojugal, v = vomer, ps = parasphenoid, pt = pterygoid, q = quadrate bone, ex = exoccipital.

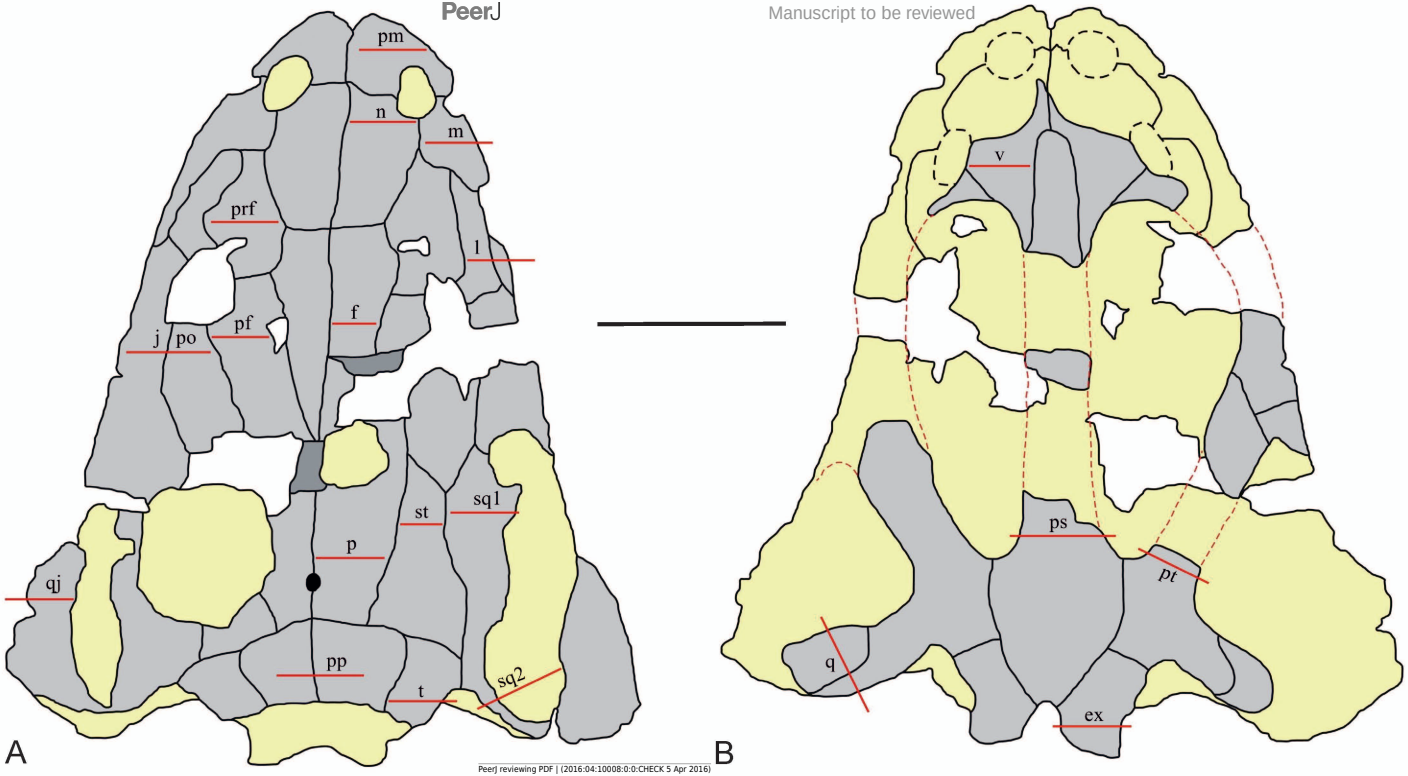
pm
n
m
prf
l
f
j
po
pf
st
sq1
p
qj
pp
t
sq2
A
v
ps
pt
q
ex
B

Figure 3(on next page)

General microanatomy of the skull bones of Metoposaurus krasiejowensis[i] (UOPB 01029) from Late Triassic of Poland.

(A) **premaxilla; (B)** maxilla; (C) **nasal; (D)** lacrimal; (E) **prefrontal; (F)** jugal/ postorbital; (G) **postfrontal; (H)** frontal; (I) **parietal; (J)** supratemporal; (K) **squamosum 1; (L)** squamosum 2; (M) **postparietal; (N)** tabular; (O) **quadratojugal; (P)** parasphenoid; (Q) **vomer; (R)** pterygoid; (S) **quadrate bone; (T)** exoccipital. Scale bar equals 10 mm. Abbreviations: ap = alary process, ds = dental shelf, vp = vomeral process.

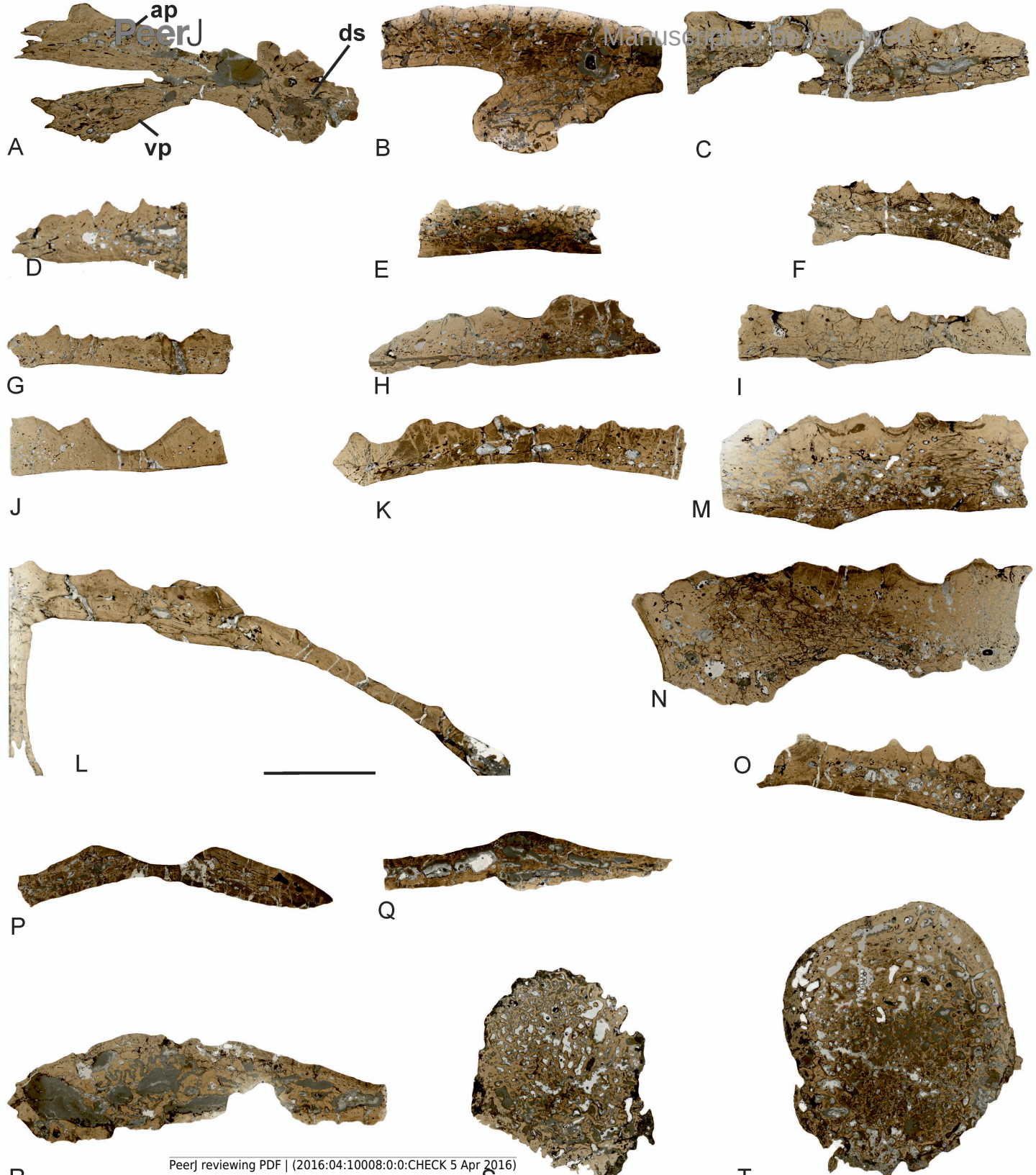

Figure 4(on next page)

Detailed microanatomy of the skull bones of Metoposaurus krasiejowensis ([i]UOPB 01029) from Late Triassic of Poland, based on the frontal.

(A) **A valley and two ridges; (B)** Enlargement of (A); the external and internal cortex, and trabecular middle region with numerous and large erosion cavities are visible; image in cross-polarized light; (C)[b] The same as (B), but in plane-polarized light. Dashed lines mark the approximately border between the external cortex/middle region/internal cortex. Scale bars equal 10 mm for (A), and 500 µm for (B-C). Abbreviations: g = groove, v = valley, EC = external cortex, MR = middle region, IC = internal cortex, ER = erosion cavities, LB = lamellar bone, PFB = parallel-fibred bone.

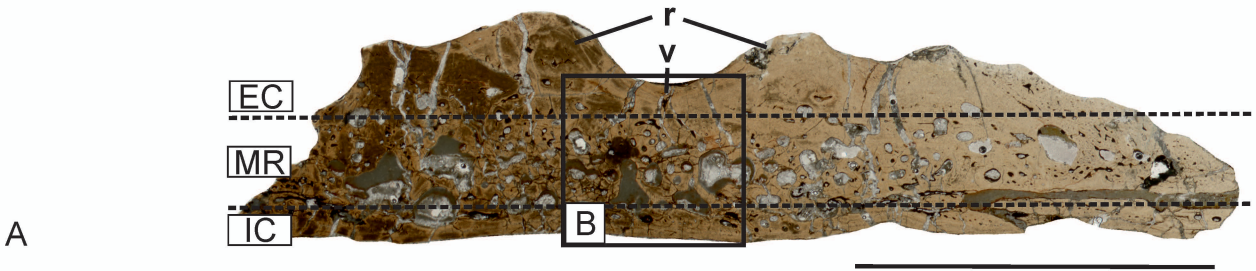
r
v
EC
MR
IC
B
A

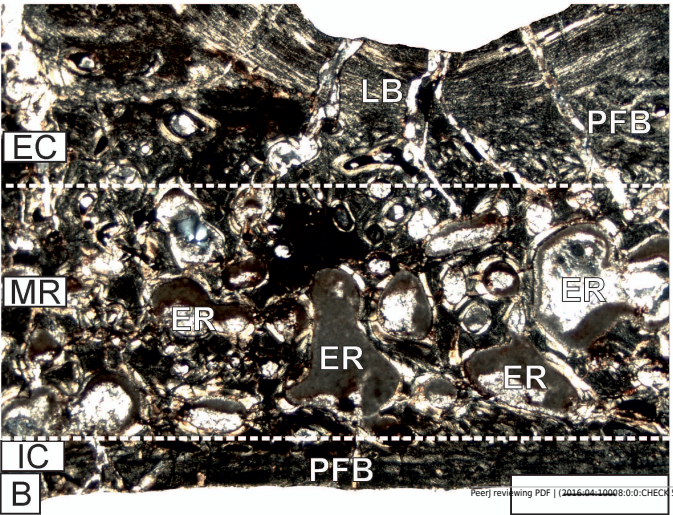
LB
PFB
EC
MR
ER
ER
ER
ER
IC
PFB
B

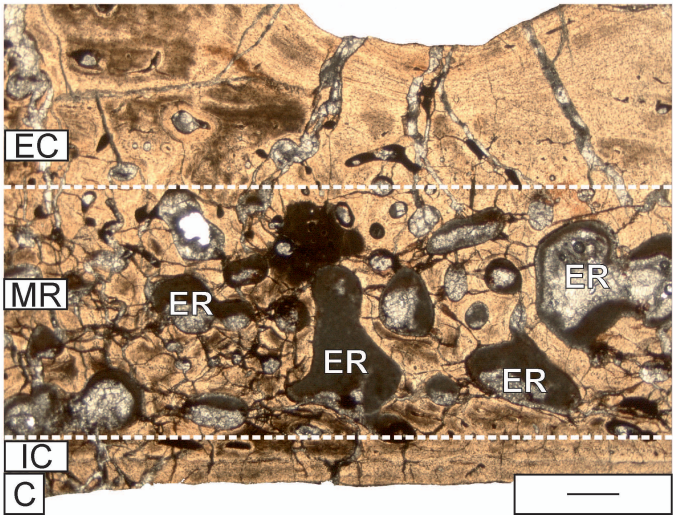
EC
MR
ER
ER
ER
ER
IC
C

Figure 5(on next page)

Histology of the external cortex of the skull bones of Metoposaurus krasiejowensis [i](UOPB 01029) from Late Triassic of Poland.

(A) **Fragment of external cortex of the frontal, image in plane-polarized light; (B)** Same as (A), but in cross-polarized light; (C) **External cortex of the tabular with distinct Sharpey's fibers in the area of the sculptural ridges, image in cross-polarized light; (D)** The resting lines (black arrows) in the cortex of squamosum2, image in plane-polarized light; (E) **The resting lines expressed as an alternation of lamellar layers and layers with distinct Interwoven Structural Fibers (ISF) in the external cortex of the postparietal, image in cross-polarized light; (F)** Zones and annuli present in the external cortex of the quadratojugal, image in cross-polarized light; (G) **Alternation of valleys and ridges in the postfrontal, image in cross-polarized light; note that remains of lamellar bone in the deep part of cortex are present, representing the bottom of a valley from an older generation. (H)** The cementing lines (black arrows) visible in the superficial part of the external cortex of the supratemporal. Dashed lines mark the approximate border between the external cortex/middle region/internal cortex. Scale bars equal for (A-E) and (H) 100 µm and for (F)-(G) 500 µm. Abbreviations: OL = osteocyte lacunae, FLB = fibro-lamellar bone, PO = primary osteons, SF = Sharpey's fibers, LB = lamellar bone, ISF = Interwoven Structural Fibers, A = annulus, Z = zone, r = ridge, v = valley.

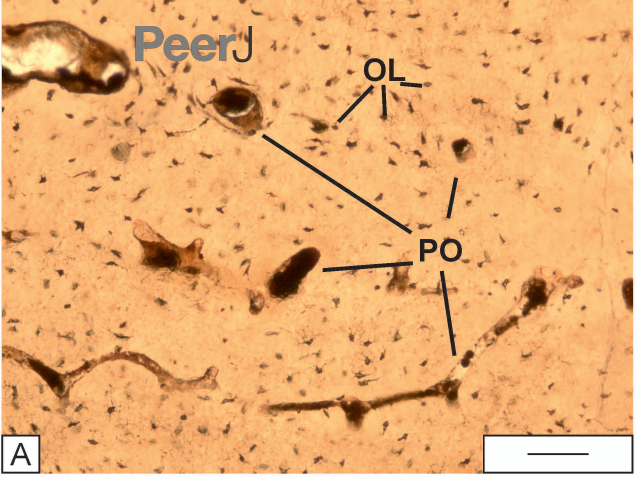

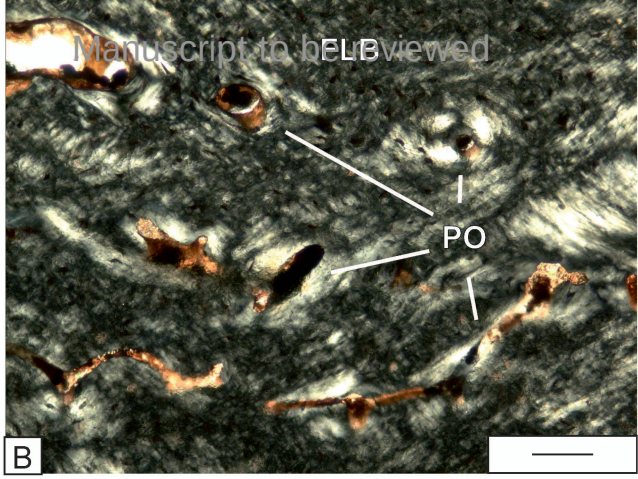

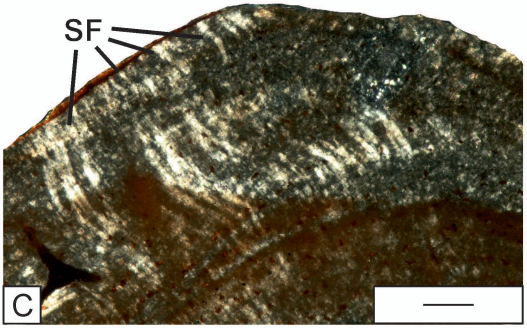

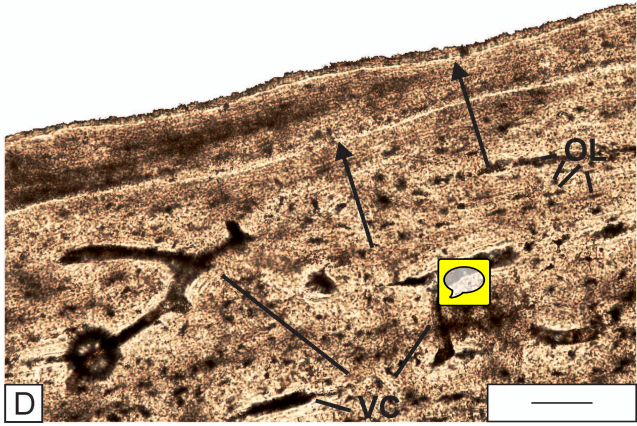

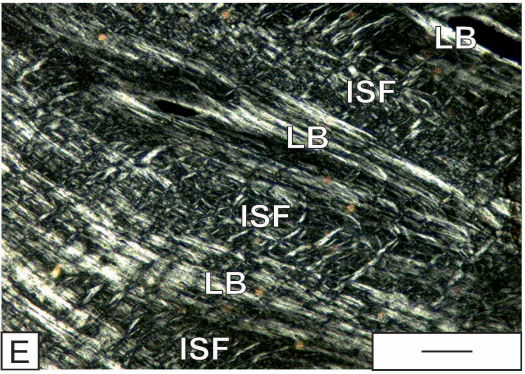

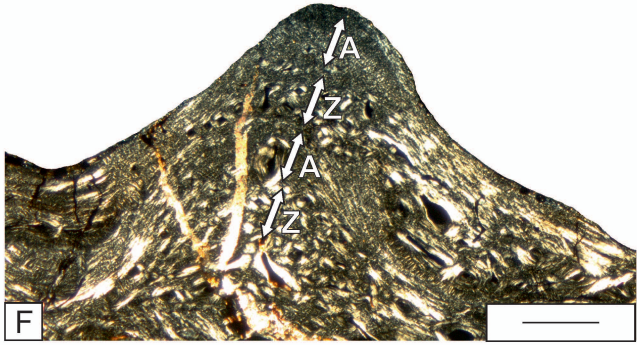

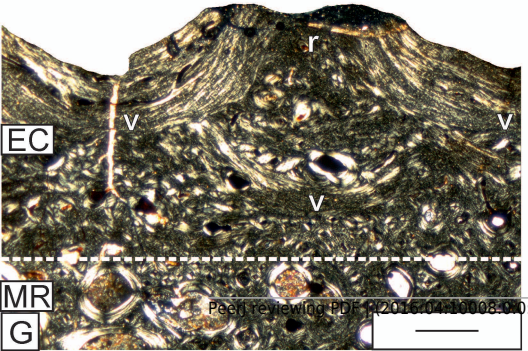

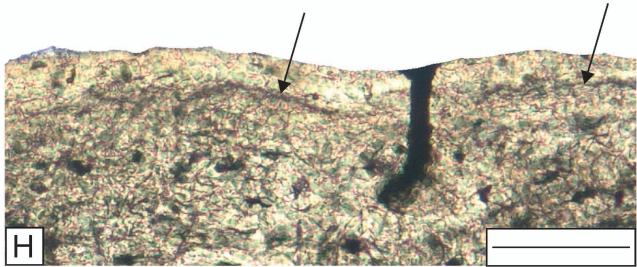

Figure 6(on next page)

The details of the histology of the middle region and internal cortex of the skull (UOPB 01029) bones of Metoposaurus krasiejowensis[i] from Late Triassic of Poland.

(A) **Large erosion cavities present in the middle region of the vomer; image in plane-polarized light; (B)** Poorly remodeled, well vascularized middle region of the parietal; image in plane-polarized light; (C) **Poorly vascularized fragment of the middle region of the squamosum2; image in plane-polarized light; (D)** Avascular internal cortex with resting lines (black arrows) visible in the parietal; image in plane-polarized light; (E) **Moderately vascularized internal cortex of the premaxilla; image in plane-polarized light; (F)** Highly vascularized internal cortex of the jugal; image in plane-polarized light; (G)[b] Alternation of thick annuli and zones visible in the internal cortex of the parasphenoid; image in cross-polarized light. Dashed lines mark the approximately border between the external cortex/middle region/internal cortex. Scale bars equal 100 µm for (D) and (G) and 500 µm for other photographs. Abbreviations: IC = internal cortex, MR = middle region, EC = external cortex, VC = vascular canals, A = annulus, Z = zone.

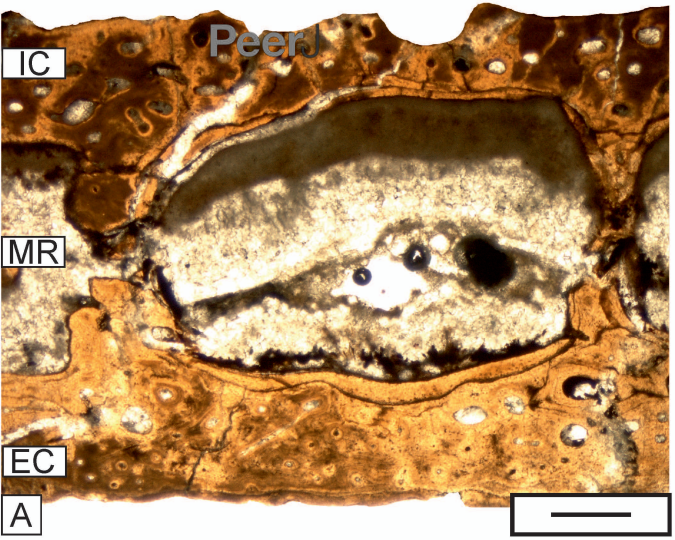

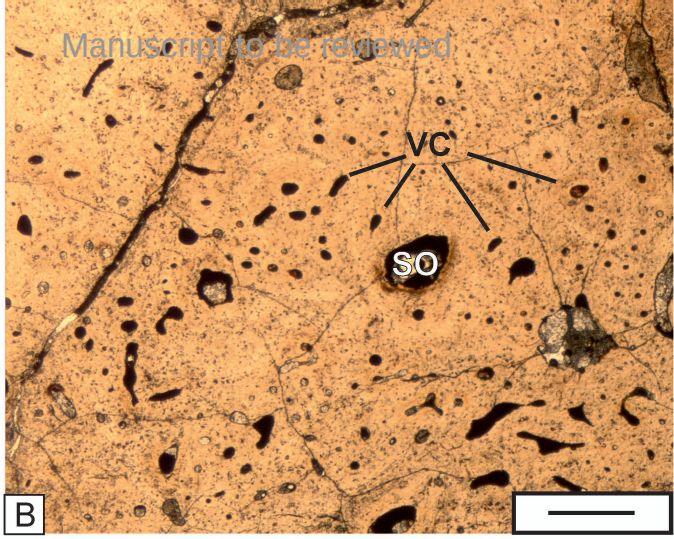

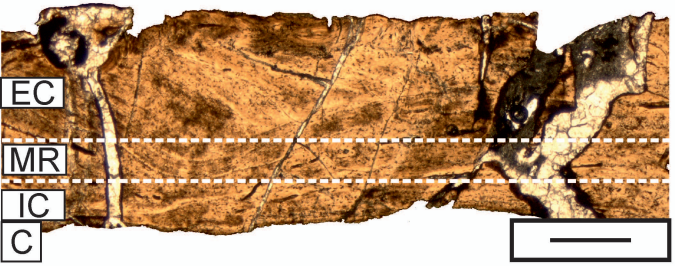

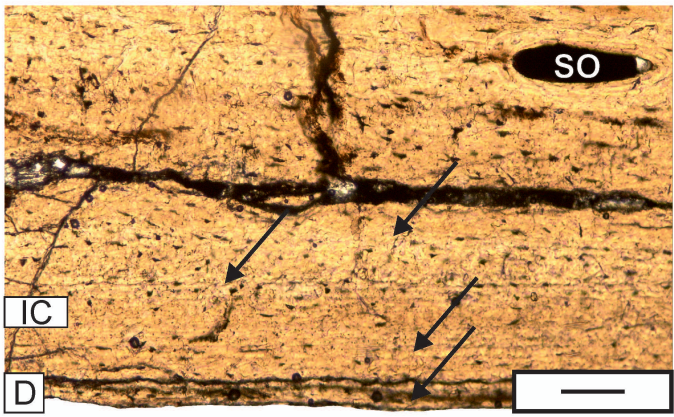

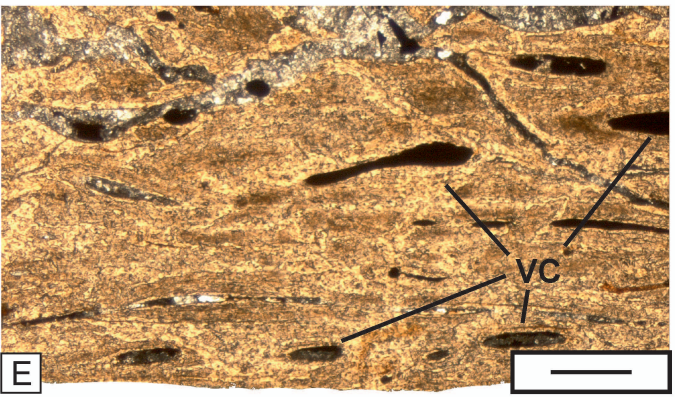

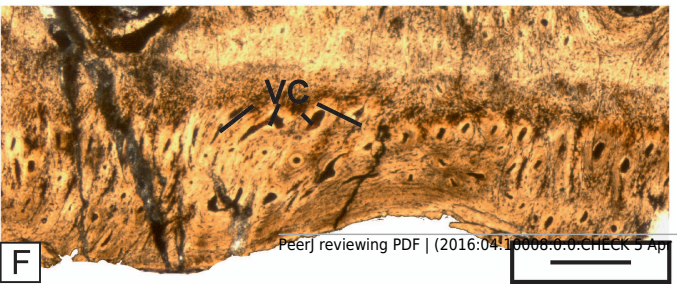

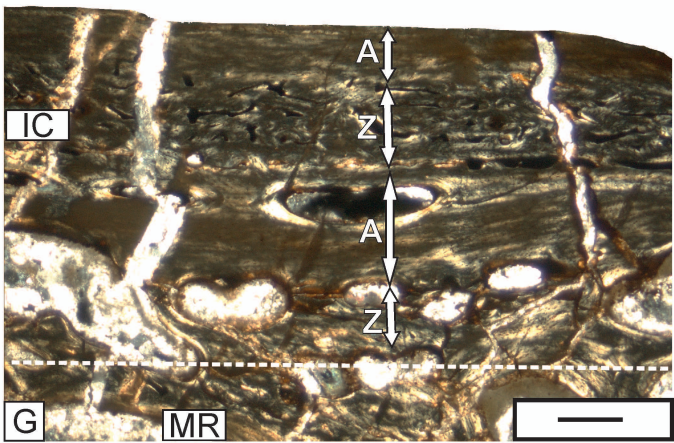

Figure 7 (on next page)

Histological details of the quadratum (A-C) and exooccipitale (D-H) of Metoposaurus krasiejowensis [i]skull (UOPB 01029) from Late Triassic of Poland.

(A) **Fragment of cortex of the quadratum; image in plane-polarized light; (B)** The same as (A), but in cross-polarized light; (C) **Trabecular bone of the quadrate bone; image in plane-polarized; (D)** Fragment of cortex of the exooccipitale with distinct Sharpey's fibers; image in cross-polarized light; (E) **Close-up of (D), note that the Sharpey's fibers are also visible in plane-polarized light; (F)** The same as (E) but in cross-polarized light; (G) **Trabeculae visible in the central part of the exooccipitale, image in plane-polarized light; (H)** Remains of calcified cartilage preserved in the trabeculae part of exoccipital, image in cross-polarized light. Scale bars equal 500 µm for (C), (D) and (G), and 100 µm for other photographs. Abbreviations: C = cortex, TR= trabecular region, OL = osteocyte lacunae, PO = primary osteons, PFL = parallel-fibred bone, VC = vascular canals, ER = erosion cavities, SO = secondary osteons, SF = Sharpey's fibers, CC = calcified cartilage.

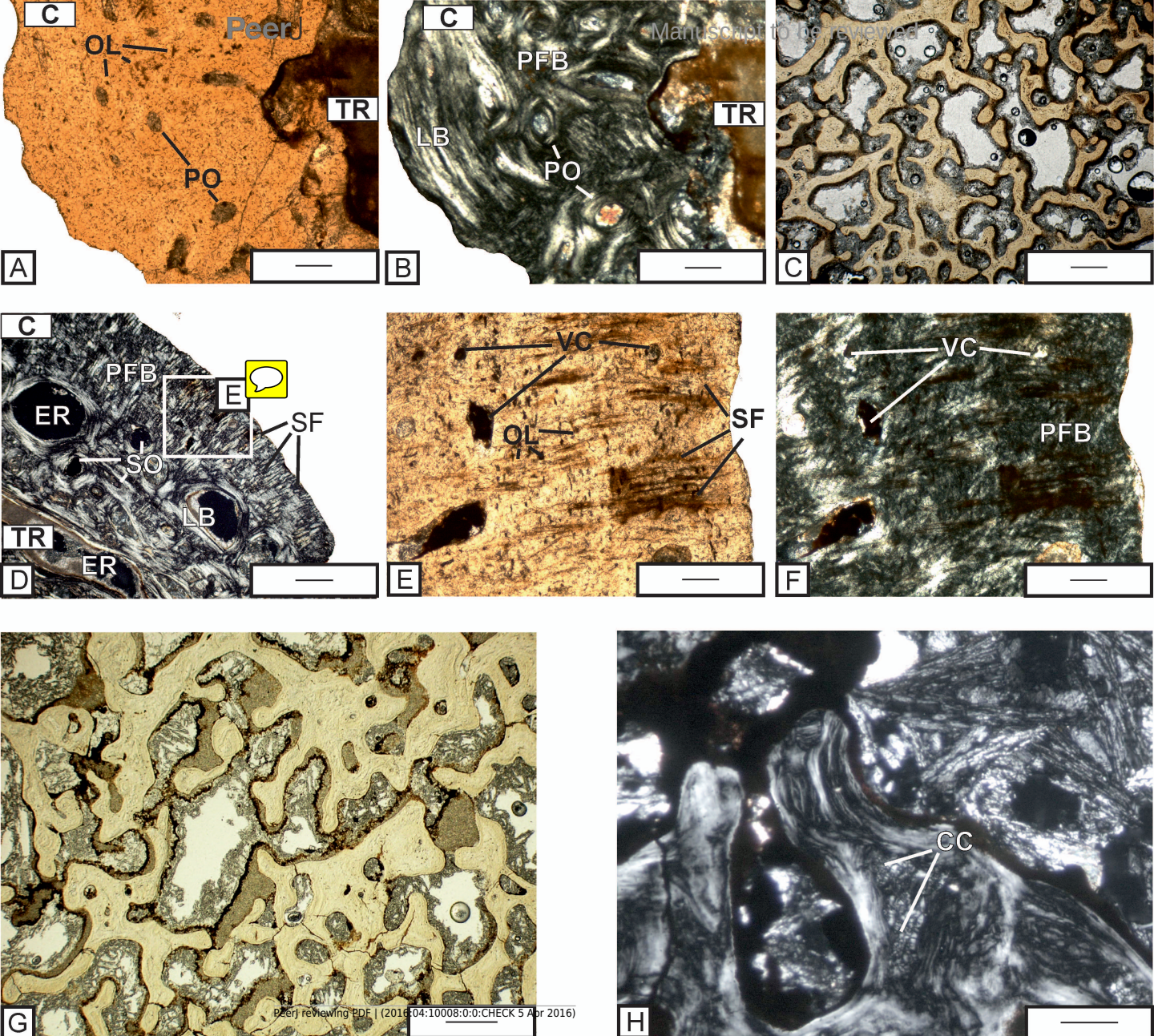

The detailed histological description of the skull bones of *Metoposaurus* from the Late Triassic of Poland

Supplementary material to:

Cranial bone histology of *Metoposaurus krasiejowensis* (Amphibia, Temnospondyli) from the Late Triassic of Poland

Kamil Gruntmejer[1,2,*], Dorota Konietzko-Meier[1,2,3], Adam Bodzioch[1,2]

[1] Opole University, Department of Biosystematics, Laboratory of Palaeobiology, Oleska 22, 45-052 Opole, Poland

[2] Opole University, European Centre of Palaeontology, Oleska 48, 45-052 Opole, Poland

[3] University of Bonn, Steinmann Institute, Nussallee 8, 53115 Bonn, Germany

*gruntmejerkamil@gmail.com

Table of contents:

Histology of dermal bones of skull roof

Premaxilla

The sample of the right premaxilla was analyzed histologically (Fig. 1). The thickness of the alary branch is from 3 mm to 5 mm, and the ratio between E:M:I is 1:5.4:0.6.

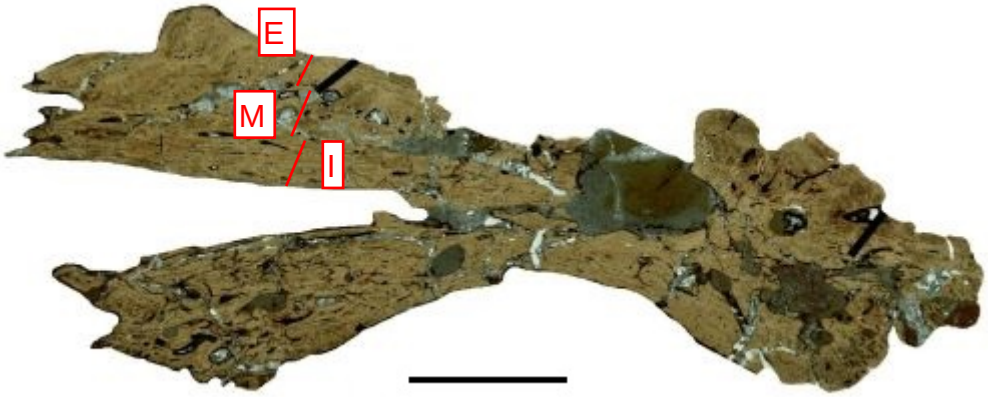

Fig. 1. Histological section of the right premaxilla. Scale bar equals 5 mm.

External cortex - The parallel-fibred bone is poorly vascularized. Well mineralized Sharpey's fibers are relatively short but very numerous and occur only in the outermost part of the bone (Fig. 2A). The growth marks are not visible.

Middle region - The external cortex transits to cancellous middle region characterized by relatively large erosion cavities, up to 2000 µm in diameter (Fig. 2B, C). Middle region is well vascularized (Fig. 2D). In some parts of the middle region the relatively high concentration of secondary osteons is visible (Fig. 2E).

The **internal cortex** is poorly vascularized and consists of parallel-fibred bone. The Sharpey's fibers are not numerous (Fig. 2F).

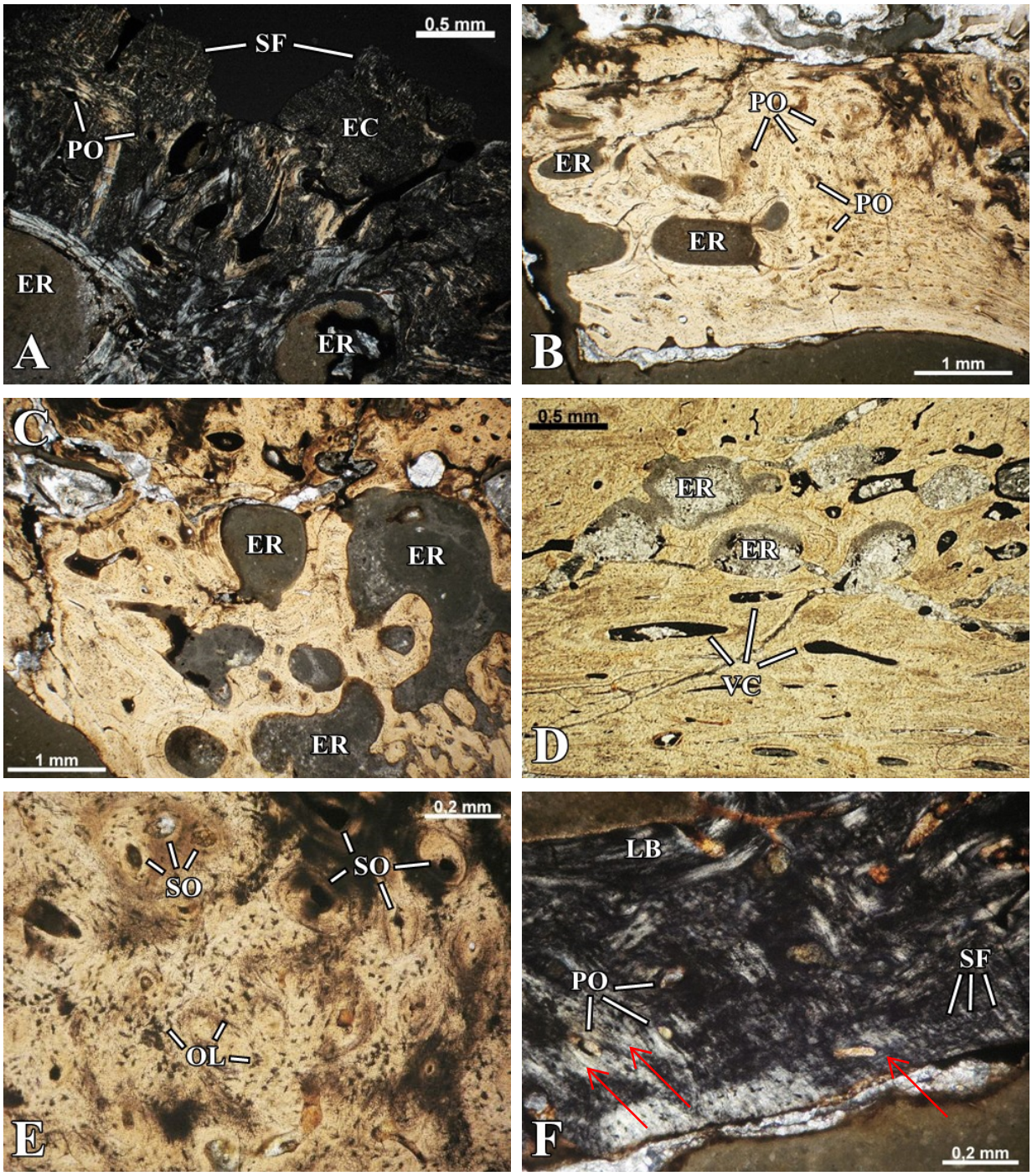

Fig. 2. The histological details of the premaxilla of *Metoposaurus krasiejowensis*. **(A)** External cortex with distinct Sharpey's fibers in the area of sculptural ridges; image in CPL; **(B-C)** Middle region with numerous and large erosion cavities; image in PPL; **(D)** Vascular canals in the upper parts of middle region; image in PPL; **(E)** The primary and secondary osteons visible in the middle region; image in PPL; **(F)** Middle region and internal cortex; image in CPL. Abbreviations: SF = Sharpey's fibers, EC = External cortex, PO = Primary osteons, SO = secondary osteons, ER = Erosion cavities, VC = Vascular canals, OL = Osteocyte lacunae, LB = Lamellar bone, PPL = plane polarized light, CPL = cross polarized light.

Maxilla

The maxilla is built up from two branches, the dorsal one with ornamented external cortex and ventro-lateral with dental shelf. The external surface of the tested bone is destroyed and the details of the ornamentation are not preserved (Fig. 3). Bone thickness of the dorsal branch varies from 4 mm to 12 mm, and the ratio E:M:I is 1:11.8:0.6.

Fig. 3. Histological section of the right maxilla. Scale bar equals 5 mm.

External cortex - The remnant of the cortex consists of relatively well vascularized parallel-fibred bone (Fig. 4A). The primary osteons are less numerous than the simple vascular canals (Fig. 4B, C). The growth marks are not visible. Sharpey's fibers are relatively short but very numerous.

Middle region - The middle region is heavily cracked, however, the remains of well vascularized, cancellous bone are visible. The numerous primary osteons, about 100 µm in diameter, and much larger secondary osteons, about 150 µm in diameter are present (Fig. 4D). The simple vascular canals, various in shapes are mostly located next to the borders between the middle region with the external and internal cortexes. A significant part of the middle region is strongly eroded. The irregular erosion cavities are numerous, various in sizes, from about 370 µm to over 2000 µm in diameter. Inside the erosion cavities the secondary

deposited lamellar bone is present. The elliptically elongated osteocyte lacunae can be observed.

Internal cortex - The internal cortex about 440 µm thick, consists of parallel-fibred bone, is much thinner than the external cortex (Fig. 4E). The degree of vascularization is relatively moderate. In some areas, the cortex is avascular, while in other areas numerous accumulations of simple vascular canals and primary/secondary osteons can be observed. The vascular canals are mostly oriented parallel to the bone surface (Fig. 4F). They are usually about 200 µm long. The osteocyte lacunae are very numerous and slightly elongated. The Sharpey's fibers are not present.

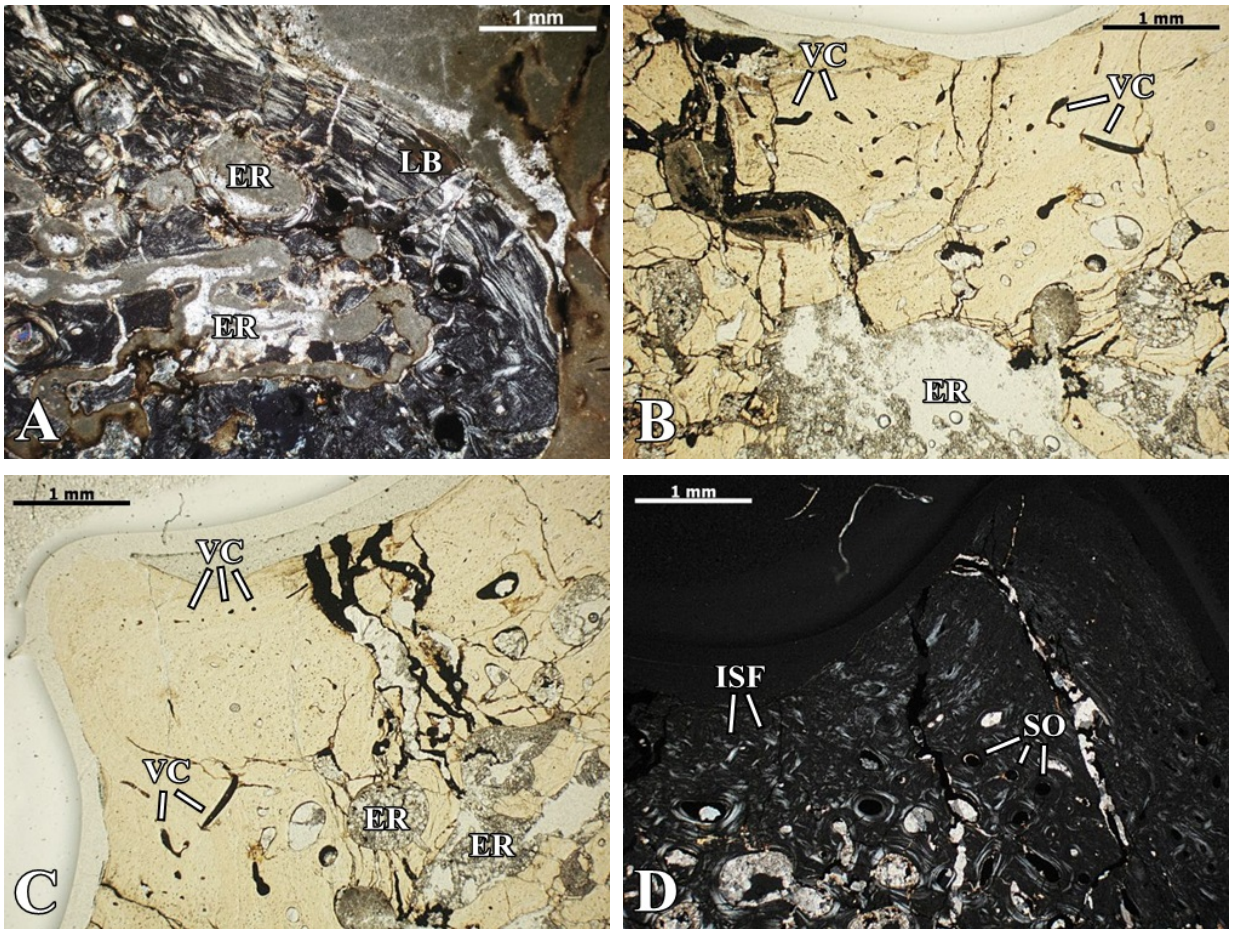

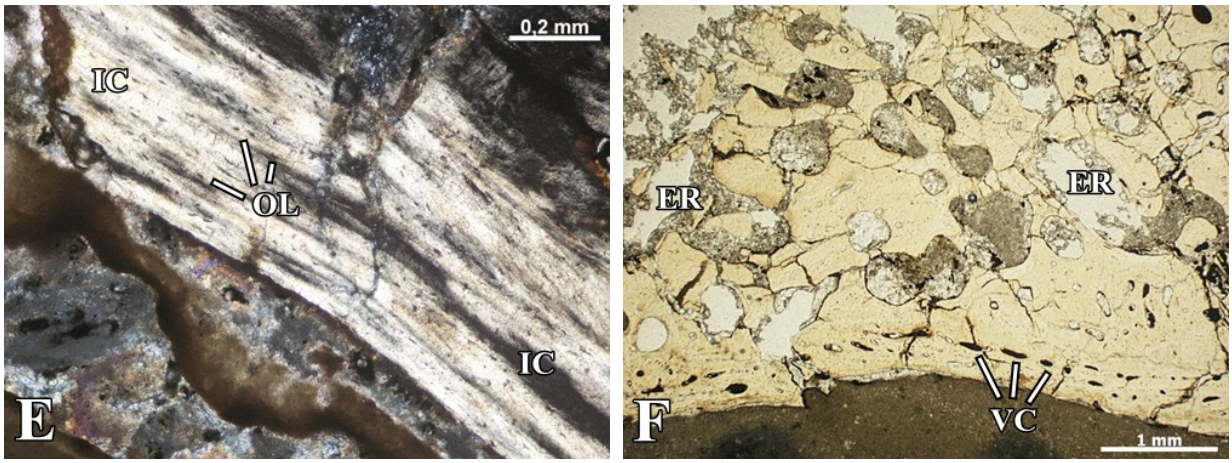

Fig. 4. The histological details of the maxilla of *Metoposaurus krasiejowensis*. **(A)** Distinct parallel-fibred bone, which create the external cortex; image in CPL; **(B-C)** Vascular canals in the area of sculptural ridges and valleys; image in PPL; **(D)** External cortex and middle region, with distinct, numerous secondary osteons; image in CPL; **(E)** Avascular internal cortex with visible, numerous cell lacunae; image in CPL; **(F)** Porous middle region and well vascularized internal cortex; image in PPL. Abbreviations: PFB = Parallel-fibred bone, SO = secondary osteons, ER = Erosion cavities, VC = Vascular canals, ISF = Interwoven Structural Fiber bundles, IC = Internal cortex, OL = Osteocyte lacunae, PPL = plane polarized light, CPL = cross polarized light.

Nasal

The thin section was prepared from the frontal part of the right nasal. Its external surface possesses distinct ornamentation. In cross section, the sculptured ridges are moderate high (Fig. 5). Bone thickness ranges from 1 mm to about 8 mm, and the E:M:I ratio is 1:3.6:0.6.

Fig. 5. Histological section of the right nasal. Scale bar equals 5 mm.

External cortex - The external cortex consists of parallel-fibred bone, with an average thickness about 270 µm. Only in the area of the ridges the cortex becomes significantly thicker, to nearly 1900 µm. The external cortex is relatively well vascularized. The simply vascular canals are present in its deeper part, and some of them may fragmentary penetrate into the middle region. Within the shallow and wide grooves, the elongated, simple vascular canals (500 µm in length) are arranged in regular rows, parallel to the bone surface. The ridges are practically avascular. Sporadically, the primary and slightly larger secondary osteons can be observed also in the deeper parts of external cortex. The numerous, short Sharpey's fibers are visible mainly in the sculptural ridges. The rounded osteocyte lacunae are very numerous. The growth marks are nor visible.

Middle region - The middle region is very vast and spongy area with well-developed vascular network (Fig. 6A). The relatively large, approximately 400 µm in length and irregularly arranged simple vascular canals are present next the borders with external and internal cortexes. They can partially penetrate into the internal cortex. In the central part of the middle region, the simple vascular canals are almost absent, whereas very numerous secondary osteons with diameters ranging from 90 µm to 170 µm can be observed (Fig. 6B). The thickness of the lamellar bone inside the secondary osteons is 140 µm approximately. In the central part of the middle region, large and irregular erosion cavities occur, with length ranging from 300 µm to over 2500 µm (Fig. 6C). On the edges of erosion cavities, the lamellar bone of variable thickness is present. The elongate osteocyte lacunae with branching canaliculi often appear.

Internal cortex - The internal cortex consists of parallel-fibred bone, with a maximum thickness of about 490 µm. It is almost avascular, except for few simple vascular canals which partially penetrate from the middle region (Fig. 6D). The Sharpey's fibers are not visible in the internal cortex. The elliptical osteocyte lacunae (about 20 µm in length) with

branched canaliculi are numerous. They typically extend in ordered rows, oriented parallel to the collagen fibers. The growth marks are visible as an alternation of lamellar layers and two resting lines.

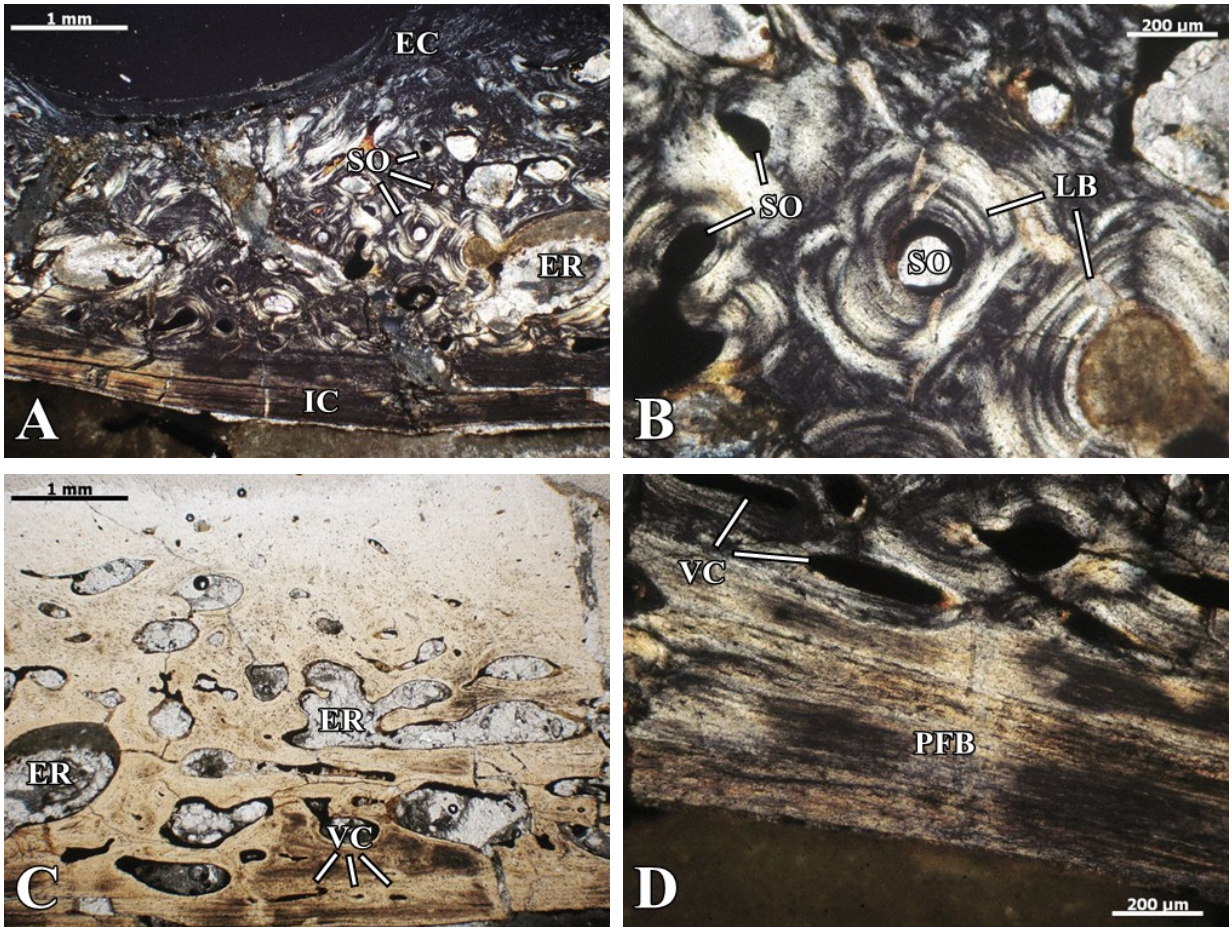

Fig. 6. The histological details of the nasal of *Metoposaurus krasiejowensis*. **(A)** Diploë structure of nasal; image in CPL; **(B)** Dense accumulation of secondary osteons in the middle region; image in CPL; **(C)** Highly eroded middle region; image in PPL; **(D)** Avascular internal cortex; image in CPL. Abbreviations: EC = External cortex, SO = secondary osteons, ER = Erosion cavities, LB = Lamellar bone, VC = Vascular canals, IC = Internal cortex, PFB = Parallel-fibred bone, PPL = plane polarized light, CPL = cross polarized light.

Lacrimal

The histological thin section was prepared from the middle part of the right lacrimal, above the edge of the orbit (Fig. 7). The external surface of the lacrimal bears the irregular

sculpture of medium high (0.5 mm), steep ridges and wide grooves. The average bone thickness in cross-section is 2.7 mm, and the ratio E:M:I is 1:7.5:0.8.

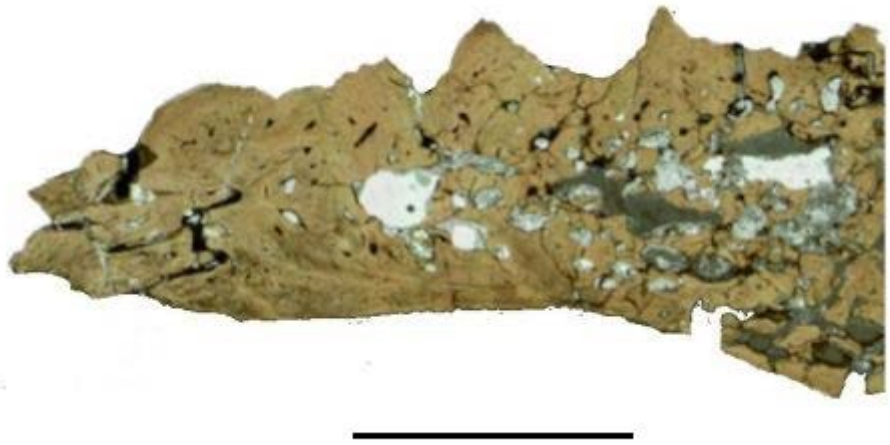

Fig. 7. Histological section of the right lacrimal. Scale bar equals 5 mm.

External cortex - The variable in thickness external cortex consists of parallel-fibred bone (Fig. 8A). The cortex is the thickest within the ridges, up to 430 µm, while in the sculptural grooves the bone thickness is approximately 130 µm. The external cortex is well vascularized with numerous, anastomosing simple vascular canals. These canals are more numerous in ridges then in grooves (Fig. 8B & 8C). The thin (about 10 µm in diameter), well mineralized Sharpey's fibers are packed in bundles. They occur within sculptural ridges and on sutural edges. In the upper parts of ridges, the distinct growth marks manifested as a sequence of thin resting lines and layers of parallel-fibred bone are present. The irregularly arranged osteocyte lacunae possess branched canaliculi.

Middle region - In its central parts large, ranging from 320 µm to almost 2500 µm in diameter, erosion cavities are present (Fig. 8D). The edges of the erosion cavities are partially surrounding by the thin layer of lamellar bone. The degree of vascularization of the middle region is relatively high, the irregularly arranged simple vascular canals and secondary

osteons, about 110 µm in diameter, are very numerous (Fig. 8E). In some parts of the middle region, the small secondary osteons occur in dense clusters (Fig. 8F). The elliptically elongated osteocyte lacunae, approximately 20 µm in length, are numerous.

Internal cortex - The internal cortex, of variable, up to 1000 µm thickness, consists of parallel-fibred bone. It is relatively well vascularized. The simple vascular canals are arranged in several rows, orientated with its long axis at an angle of about 45^0 with respect to the cortex. The secondary osteons appear very rarely. Elliptical osteocyte lacunae are very numerous and irregularly arranged in the bone matrix.

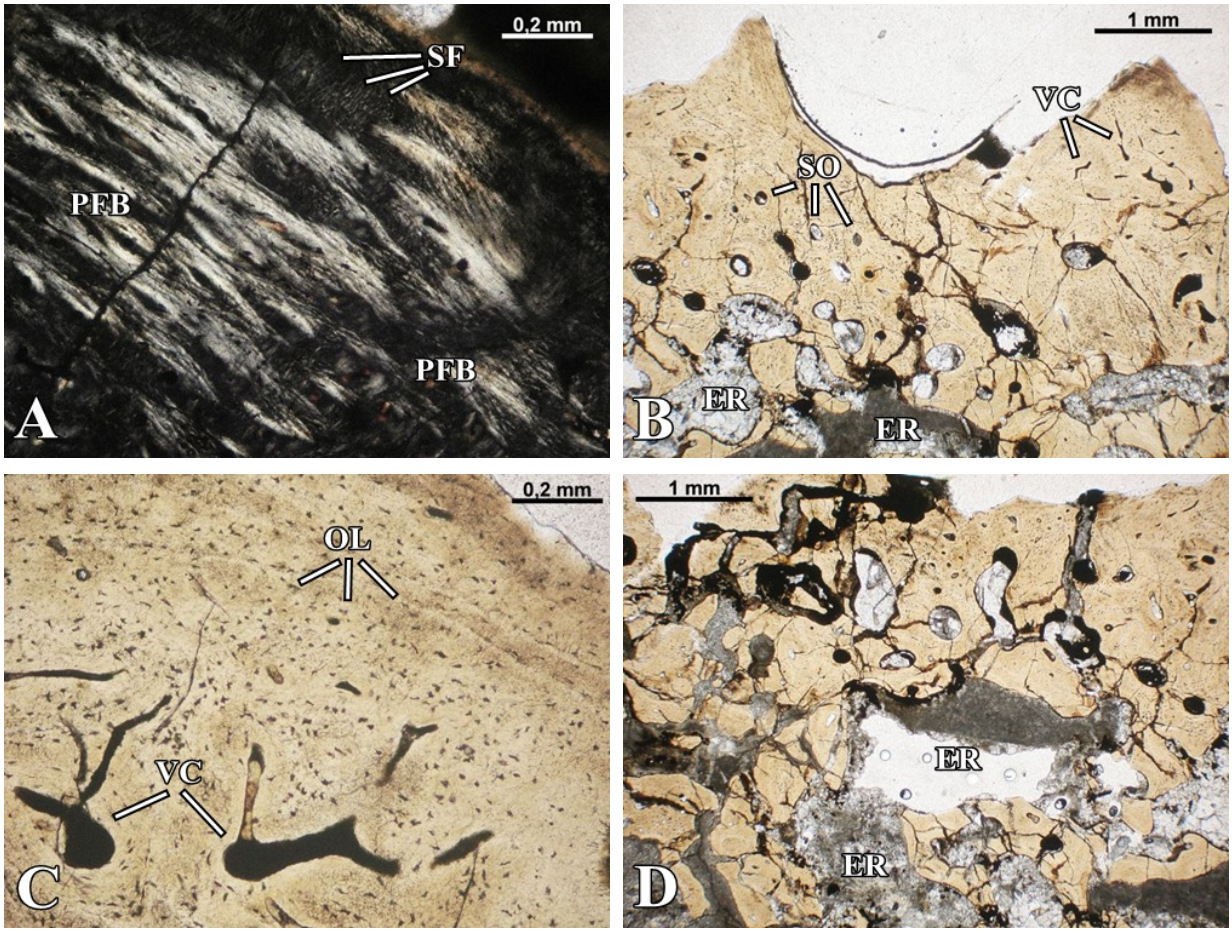

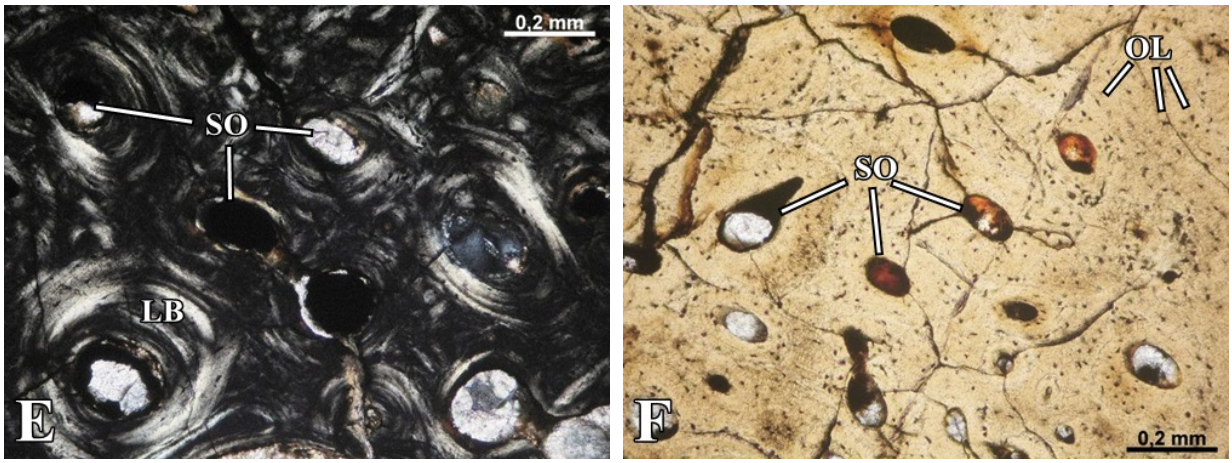

Fig. 8. The histological details of the lacrimal of *Metoposaurus krasiejowensis*. **(A)** Parallel-fibred bone and short bundles of Sharpey's fibers in external cortex; image in CPL; **(B)** Ornamented and well vascularized external surface of lacrimal; image in PPL; **(C)** Vascular canals in external cortex; image in PPL; **(D)** Middle region with large erosion cavities; image in PPL; **(E-F)** Dense accumulation of secondary osteons in the middle region; images in CPL (E) and PPL (F). Abbreviations: PFB = Parallel-fibred bone, SF = Sharpey's fibers, EC = External cortex, SO = secondary osteons, ER = Erosion cavities, VC = Vascular canals, LB = Lamellar bone, OL = Osteocyte lacunae, PPL = plane polarized light, CPL = cross polarized light.

Prefrontal

The investigated section of the left prefrontal was prepared from the middle part of this bone (Fig. 9). The external surface of the bone possesses distinct ornamentation – high and steep ridges and deep grooves. Sectional bone thickness is about 5 mm, and the ratio E:M:I is 1:3.7:0.7.

Fig. 9. Histological section of the left prefrontal. Scale bar equals 5 mm.

External cortex - The fragmentarily preserved external cortex consists of parallel-fibred bone. The irregular simple vascular canals appear within the sculptural grooves. The primary osteons are less numerous than simple vascular canals. The Sharpey's fibers occasional appear, especially in areas where the sculptural grooves are shallower. The elongated osteocyte lacunae with branched canaliculi are very numerous in the bone matrix. The growth marks are not present.

Middle region - The vast middle region consists of partially eroded cancellous bone. The erosion cavities are various in sizes, ranging from 280 µm to about 2000 µm (Fig. 10A, B). They are relatively small in upper parts of middle region, while in the deeper part they are significantly larger. The lamellar bone surrounds partially their edges. The simple vascular canals are not numerous. The primary and secondary osteons, with a diameter about 100 µm, are more numerous (Fig. 10C). The round osteocyte lacunae are as numerous as in the external cortex.

Internal cortex - The internal cortex consists of parallel-fibred bone, with variable thickness up to 650 µm. The entire internal cortex is poorly vascularized (Fig. 10D). The simple vascular canals are not visible and the primary osteons, with diameters about 130 µm, are rarely. The Sharpey's fibers are not present. The elliptically elongated osteocyte lacunae with branched canaliculi are not as numerous as in external cortex and middle region.

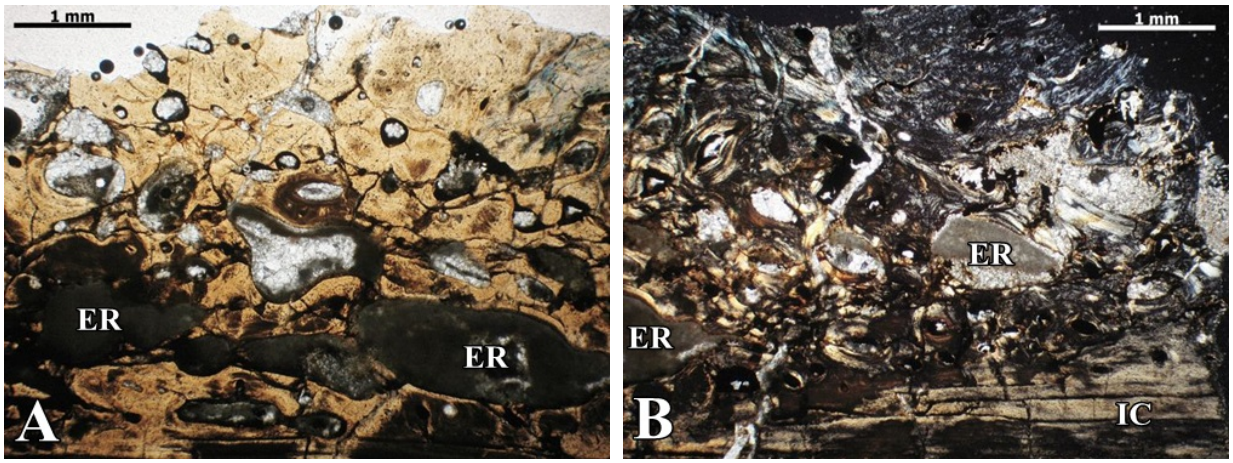

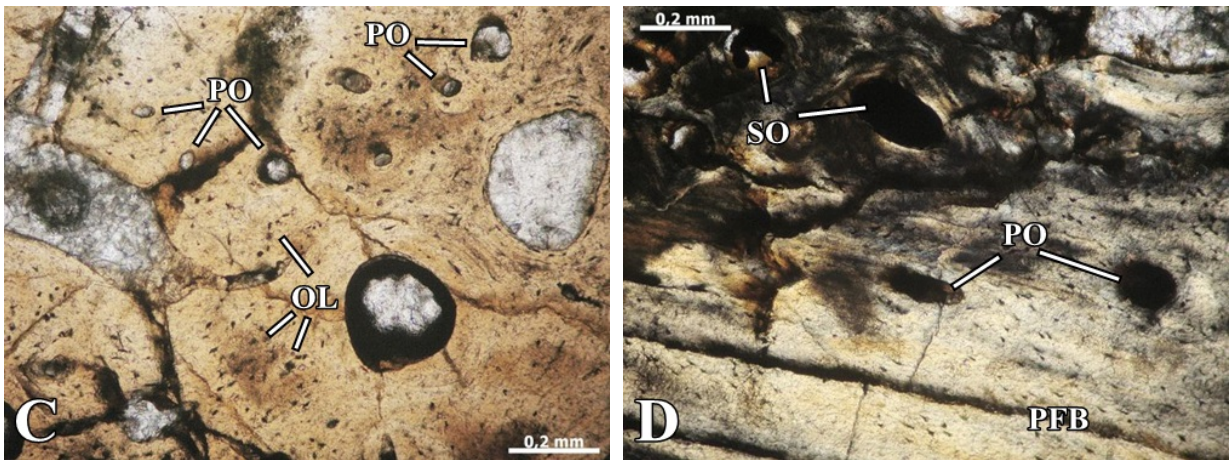

Fig. 10. The histological details of the prefrontal of *Metoposaurus krasiejowensis*. **(A-B)** Middle region with large erosion cavities; images in CPP (A) and PPL (B); **(C)** Small primary osteons and numerous osteocyte lacunae; image in PPL; **(D)** Part of internal cortex with visible secondary and primary osteons; image in CPL. Abbreviations: ER = Erosion cavities, PO = Primary osteons; SO = secondary osteons, PFB = Parallel-fibred bone, IC = Internal cortex, OL = Osteocyte lacunae, PPL = plane polarized light, CPL = cross polarized light.

Jugal & Postorbital

The histological sample was made from the left part of the skull. The external surface of jugal and postorbital is sculptured by high (of about 1 mm) ridges and deep, wide grooves (Fig. 11). The average thickness of the sectioned bones is 5.9 mm and the ratio E:M:I is 1:4.2:0.7.

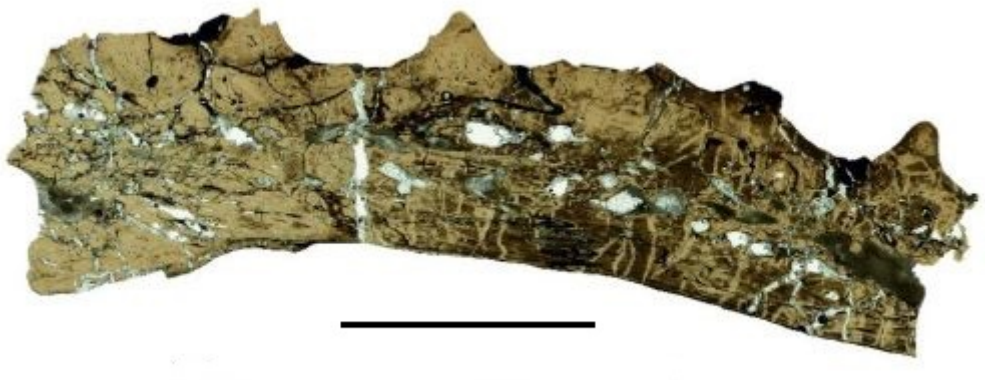

Fig. 11. Histological section of the left jugal and the postorbital. Scale bar equals 5 mm.

External cortex - The well vascularized external cortex of relatively high thickness consists of parallel-fibred bone. The very numerous, irregularly arranged simple vascular canals are grouped in some fragments of cortex. In the central parts of the ridges, the simple vascular canals are elongated and relatively small (about 80 µm), while deeper they are almost double in length (Fig. 12A, D). The round simple vascular canals are arranged in several regular rows in the ridges (Fig. 12B). In the outermost row the simple canals are very small, about 60 µm in diameter, while deeper they become more elongated to about 150 µm in length. The not numerous small primary osteons occur mainly in the deeper parts of the external cortex. A short, well mineralized and packed in bundles Sharpey's fibers, with diameter about 10 µm, are observed next to the surface and on the sutural edges (Fig. 12C). Within the sculptural ridges of jugal, the growth marks, manifested as a sequence of thin resting lines and the layers of parallel-fibred bone, can be observed (Fig. 12E, F). In some places the alternation of valleys and ridges is preserved. The rounded and elongated osteocyte lacunae with branched canaliculi are very numerous in the entire external cortex.

Middle region - The extensive, highly eroded and well vascularized middle region consists of cancellous bone. The elongated, simple vascular canals are less numerous than in the external cortex. The large secondary osteons of about 150 µm in diameter are common. The large erosion cavities, with lengths up to 1800 µm occur in the deeper parts of the middle region (Fig. 12G). The thickness of irregularly arranged trabeculae varies from 160 µm to over 450 µm. The interiors of the erosion cavities are partially lined by discontinuous layer of the lamellar bone. The middle region is heavily cracked (Fig. 12H). The slightly elongated osteocyte lacunae are very numerous.

Internal cortex - The internal cortex of a relatively constant thickness consists of parallel-fibred bone. Only in jugal, the cortex becomes slightly thicker. The vascular network is poorly developed, but in some places the simple vascular canals can be observed. The long

axes of the numerous and extending radially simple vascular canals (100 μm in length) are orientated an angle of about 80^0 relative to the middle region (Fig. 12I). The secondary osteons are not numerous. The Sharpey's fibers are not visible. The elongated osteocyte lacunae are very numerous. They are oriented parallel to the collagen fibers and possess branched canaliculi (Fig. 12J). The growth marks are visible in jugal as an alternation of lamellar layers and three resting lines.

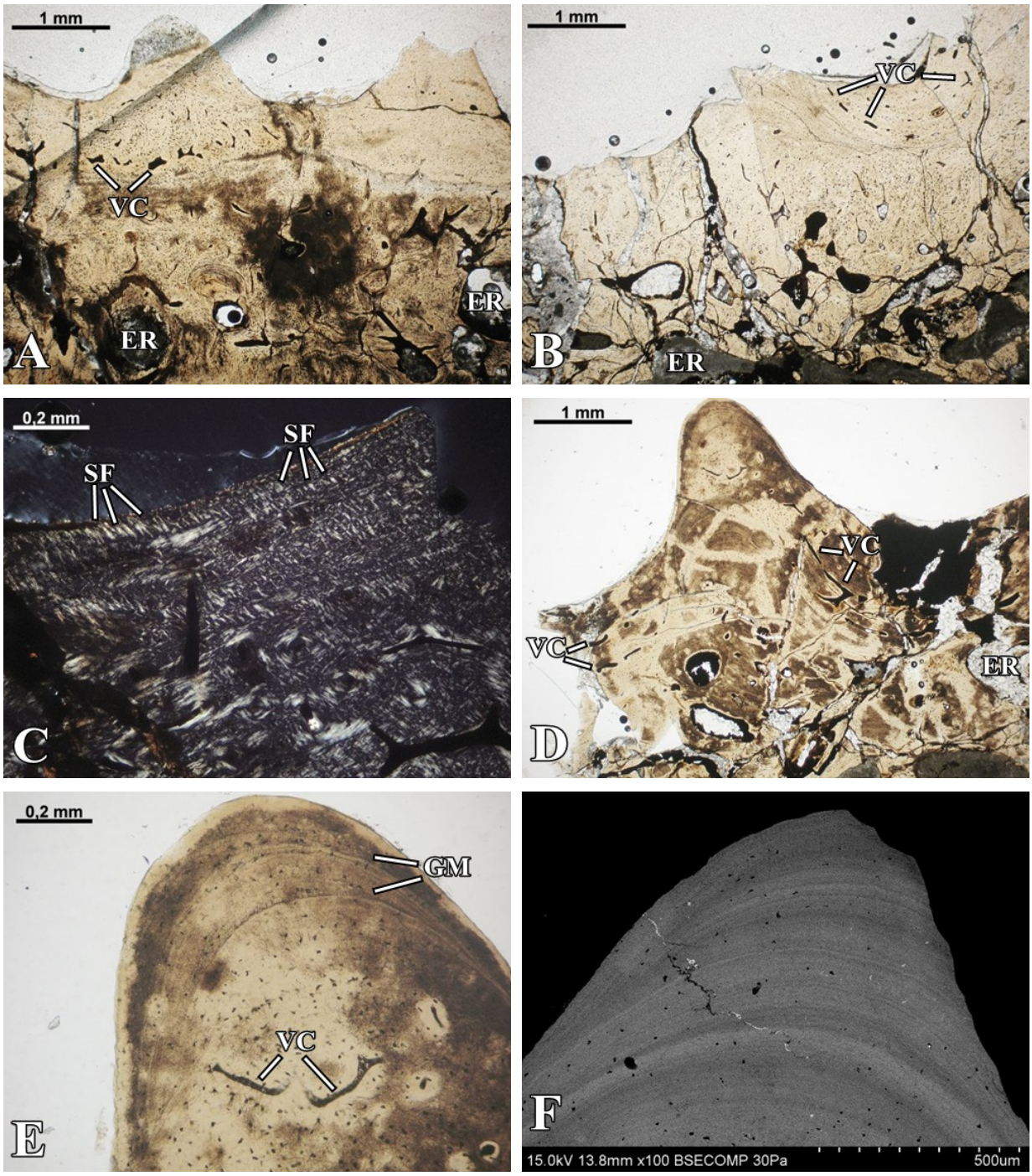

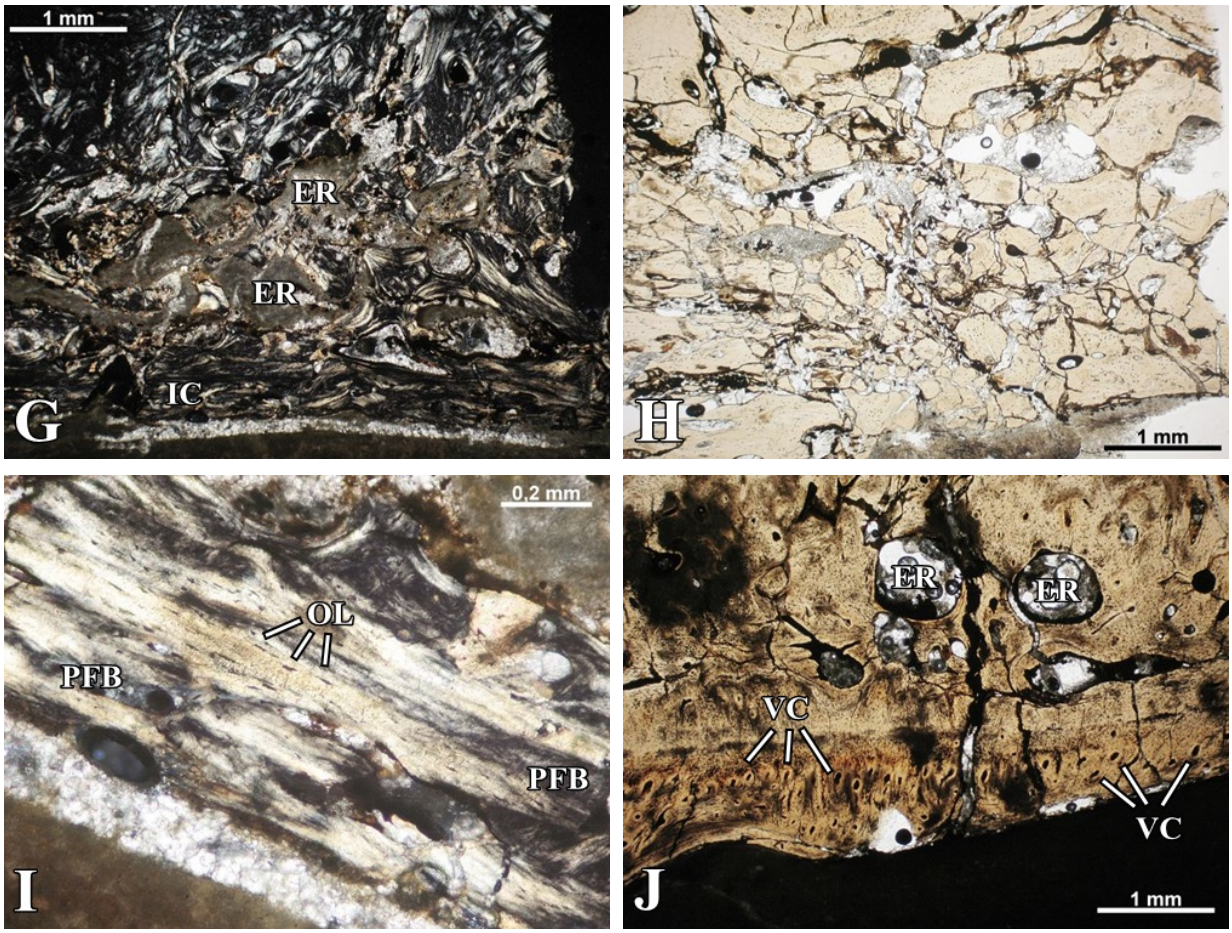

Fig. 12. The histological details of the jugal and the postorbital of *Metoposaurus krasiejowensis*. **(A-B, D)** Well vascularized external surface in the jugal and the postorbital; image in PPL; **(C)** Dense bundles of well mineralized Sharpey's fibers in the external cortex; image in CPL; **(E-F)** Numerous growth marks structure in the area of sculptural ridges; images in PPL (E) and in scanning electron microscope (F); **(G-H)** Heavily eroded and cracked middle region; image in CPL (G) and PPL (H); **(I)** Parallel-fibred bone with distinct, numerous osteocyte lacunae; image in CPL; **(J)** Well vascularized part of internal cortex; image in PPL. Abbreviations: VC = Vascular canals, ER = Erosion cavities, SF = Sharpey's fibers, GM = Growth marks structure, PFB = Parallel-fibred bone, OL = Osteocyte lacunae, PPL = plane polarized light, CPL = cross polarized light.

Postfrontal

The histological sample was prepared from the left postfrontal, behind the posterior edge of the orbit (Fig. 13). The clear ornamentation of external surface consists of about 0.3 mm high ridges and shallow grooves. The bone thickness ranges from 3 mm to 5 mm and the ratio E:M:I is 1:5.7:0.6.

Fig. 13. Histological section of the left postfrontal. Scale bar equals 5 mm.

External cortex - The well vascularized external cortex, with a thickness of about 440 µm, consists of parallel-fibred bone. The irregularly arranged simple vascular canals are very numerous. Within the sculptural grooves, the simple vascular canals are strongly elongated to even 400 µm in length. The small and rare primary osteons occur especially in the deeper parts of the external cortex. The preserved fragments of the sculptural ridges possess the cyclical growth marks, manifested as a sequence of thin resting lines and layers of parallel-fibred bone, which follow the shape of the ridges. In some areas the alternation of valleys and ridges is preserved. The rounded osteocyte lacunae are very numerous in the entire cortex. The Sharpey's fibers are rare. The distinct collagen fibers create a thick Interwoven Structural Fibers (IFS).

Middle region - The middle region consists of cancellous bone, but the erosion cavities are small, up to 450 µm, and appear sporadically (Fig. 14A, B). Their irregular edges are partially lined by layers of lamellar bone. The elongated simple vascular canals can be observed next to the border with the external cortex. The small primary osteons, with a diameter of about 70 µm, and larger, about 120 µm secondary osteons are very numerous (Fig. 14C). The thickness of the layer of lamellar bone inside secondary osteons is 70 µm. In some parts of the bone, the small secondary osteons form Haversian tissue. The elongated osteocyte lacunae with diameter about 10 µm are randomly arranged in the bone matrix.

Internal cortex - The thin, almost avascular internal cortex consists of parallel-fibred bone (Fig. 14D). Its average thickness is 240 µm. The osteocyte lacunae are less numerous then in the external and middle regions. They are elongated and directed parallel to the long axis of the internal cortex. The Sharpey's fibers are not present. The growth marks are visible as the alternation of lamellar layers and four resting lines.

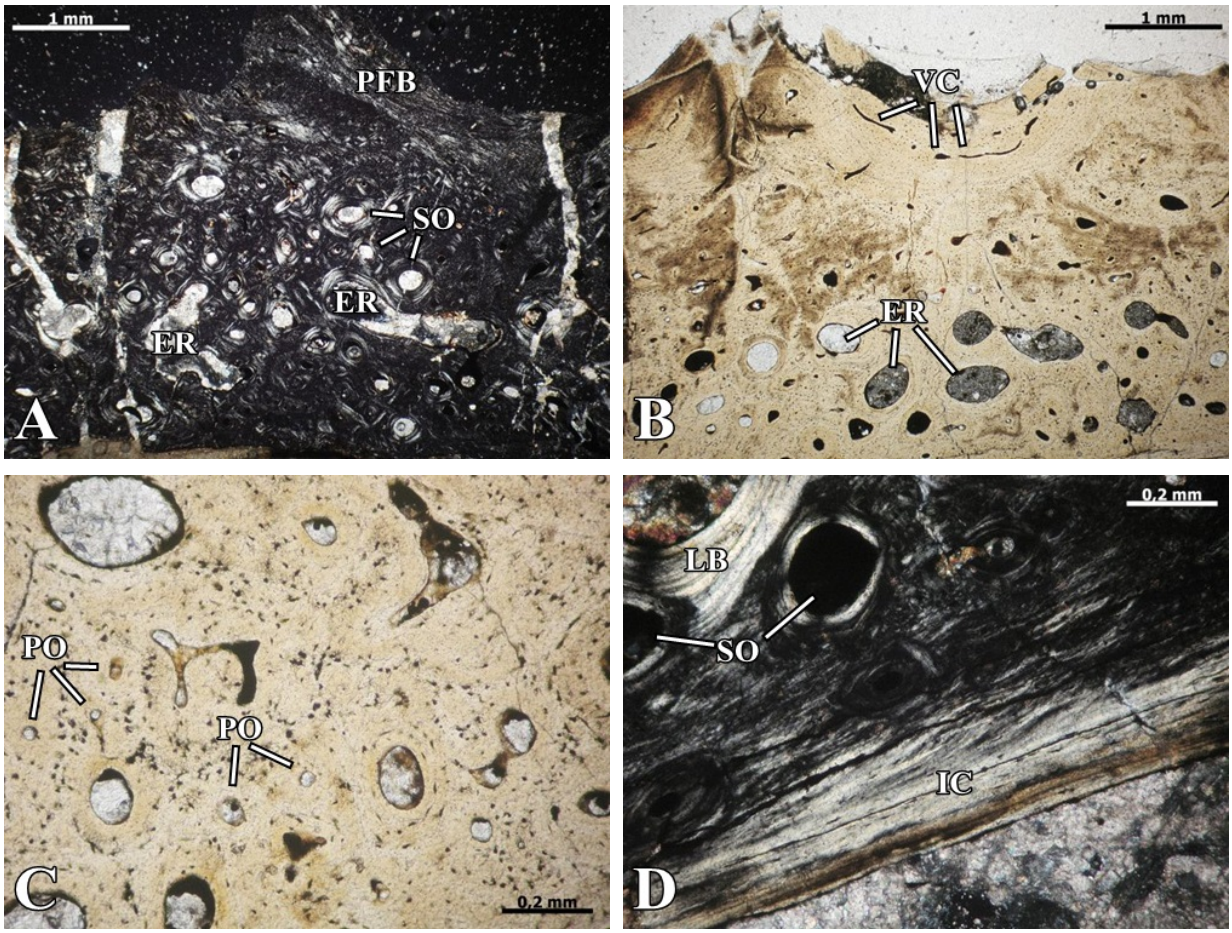

Fig. 14. The histological details of the postfrontal of *Metoposaurus krasiejowensis*. **(A-B)** External cortex and middle region in CPL (A) and PPL (B); **(C)** Small and numerous primary osteons in middle region; image in PPL; **(D)** Thin, avascular internal cortex; image in CPL. Abbreviations: PFB = Parallel-fibred bone, SO = secondary osteons, PO = Primary osteons, ER = Erosion cavities, VC = Vascular canals, LB = Lamellar bone, IC = Internal cortex, PPL = plane polarized light, CPL = cross polarized light.

Frontal

The histological sample was prepared from the middle part of the right frontal (Fig. 15). The dermal sculpture of frontal is composed of high ridges and wide grooves. The average bone thickness is about 4.7 mm, and the ratio E:M:I is 1:5.5:0.6.

Fig. 15. Histological section of the right frontal. Scale bar equals 5 mm.

External cortex - The external cortex consists of parallel-fibred bone with a thickness approximately 660 µm. The cortex is relatively poor vascularized (Fig. 16A). The small and irregular simple vascular canals are present in deeper areas of external cortex, next to the border with the middle region. The primary and secondary osteons are not visible. The Sharpey's fibers are short and rare. They appear occasionally in the cortex only as very short bundles and are more numerous on the edges of cranial suture. The growth marks, manifested as a sequence of thin resting lines and the layers of parallel-fibred bone, occur in the apexes of the sculptural ridges and in the ridges. They follow the shape of the ridges and grooves (Fig. 16B). The rounded osteocyte lacunae of about 10 µm in diameter and with branched canaliculi are numerous in the entire cortex.

Middle region - Well vascularized and highly eroded middle region consists of cancellous bone. The irregular in shape and different in size simple vascular canals are very numerous. In upper part of middle region the amount of simple vascular canals increases. The numerous secondary osteons, about 180 µm in diameter, do not form a Haversian tissue. The

erosion cavities, from 360 µm to over 1350 µm in length, are present in the large amount in the middle region (Fig. 16C). The rounded bone cell lacunae with preserved canaliculi are more numerous in the middle region than in the external cortex.

Internal cortex - The thin internal cortex consists of parallel-fibred bone (Fig. 16D). The average thickness of cortex is 420 µm. The vascularization of the internal cortex is moderate. The longitudinal, simple vascular canals appear more frequently than the secondary osteons. The Sharpey's fibers cannot be observed. The elliptically elongated osteocyte lacunae with a diameter about 20 µm are as numerous as in external cortex. They are oriented in regular rows parallel to the cortex fibers.

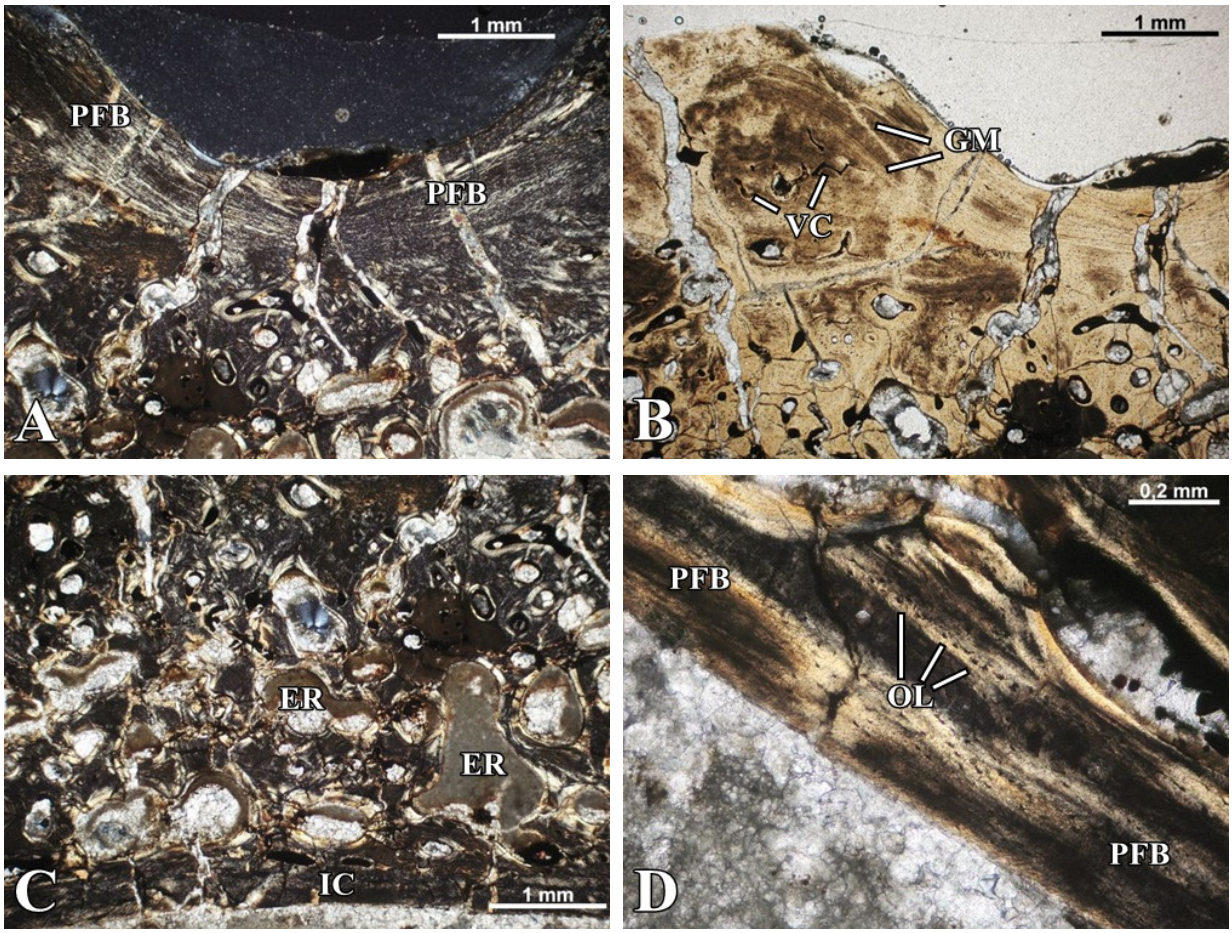

Fig. 16. The histological details of the frontal of *Metoposaurus krasiejowensis*. **(A)** Thick layer of parallel-fibred bone within the sculptural ridges; image in CPL; **(B)** Well vascularized, sculptural ridges with distinct growth marks structures; image in PPL; **(C)** Highly porous and remodeled middle region; image in CPL; **(D)** Avascular

internal cortex with numerous osteocyte lacunae; image in CPL. Abbreviations: PFB = Parallel-fibred bone, VC = Vascular canals, GM = Growth marks structure, ER = Erosion cavities, IC = Internal cortex, OL = Osteocyte lacunae, PPL = plane polarized light, CPL = cross polarized light.

Parietal

The investigated section of the right parietal was prepared from the middle part of this bone, approximately 1.5 cm above the pineal foramen. The external surface of the parietal bears a polygonal sculpture builds from ridges about 1 mm high, and narrow pits (Fig. 17). The thickness of the bone is about 5 mm, and the ratio E:M:I is 1:3.5:0.4.

Fig. 17. Histological section of the right parietal. Scale bar equals 5 mm.

External cortex - The external cortex consists of variable in thickness parallel-fibred bone (Fig. 18A). In the grooves, the average thickness of cortex is 240 µm, while in the sculptural ridges are much thicker to over 650 µm. The simple vascular canals are very numerous, mostly in the deeper parts of the external cortex. They are strongly elongate to about 180 µm (Fig. 18B & 18C). The primary osteons are small, with diameters of about 30 µm, and they appear in much lower amounts. The few Sharpey's fibers occur occasionally in the sculptural ridges in the form of short bundles. The rounded osteocyte lacunae, with diameters of 10 µm, are numerous within the entire bone matrix. The growth marks are not visible.

Middle region - The well vascularized middle region create a vast area consists of cancellous bone. The erosion cavities are small, about 270 µm in diameter (Fig. 18D). The simple vascular canals, irregular in shape and variable in sizes, primary and secondary osteons are numerous (Fig. 18E). The secondary osteon are large, about 90 µm in diameter. The rounded and elongated osteocyte lacunae, with a diameter about 10 µm, occur in similar quantities as in the external cortex. The branched canaliculi cannot be observed.

Internal cortex - The thin internal cortex consists of parallel-fibred bone. Its thickness is usually less than 150 µm, but in some areas may be up to 250 µm. The internal cortex is avascular in the entire width (Fig. 18F). The Sharpey's fibers are not visible. The number of the elongated osteocyte lacunae (about 20 µm in length) is considerably lower. The growth marks are visible as an alternation of lamellar layers and three resting lines.

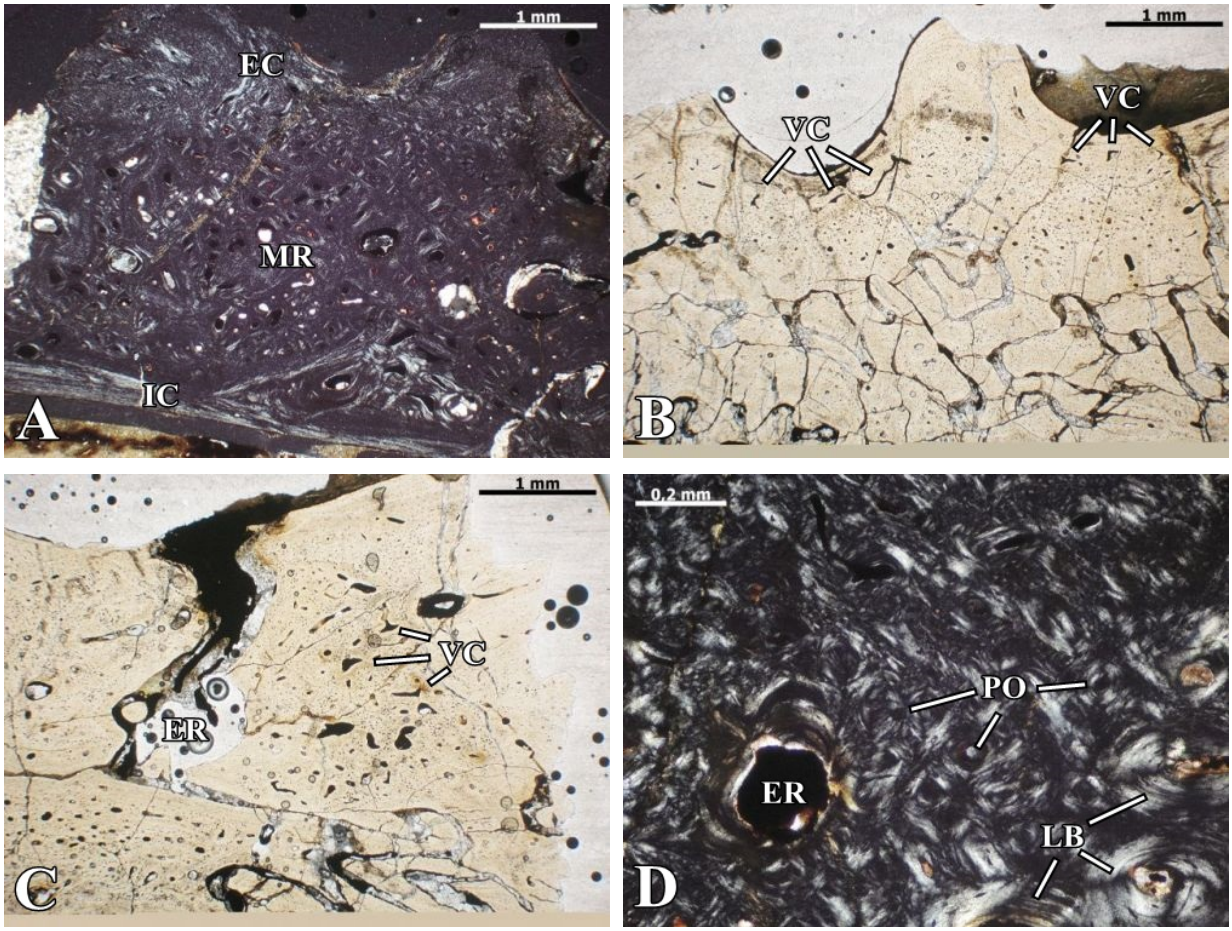

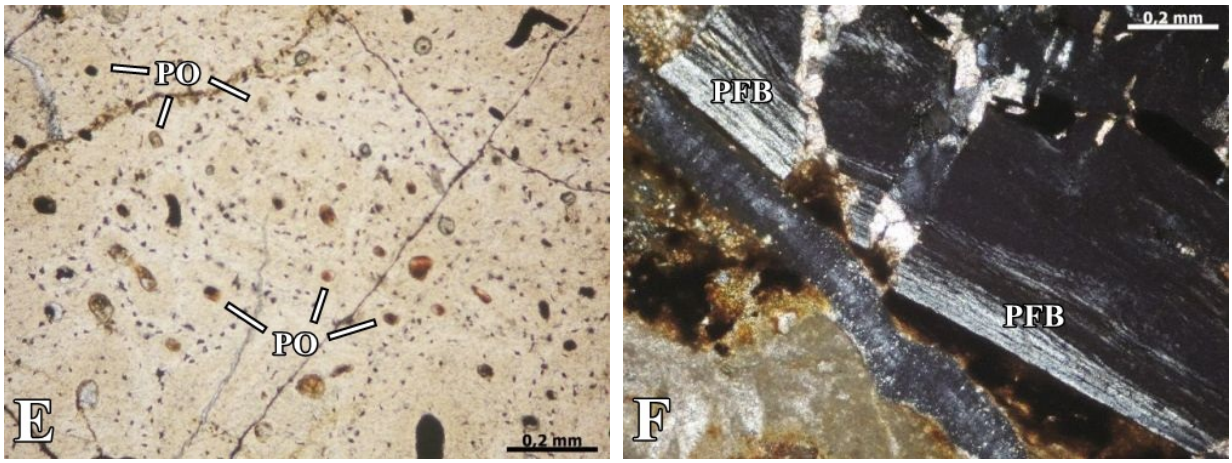

Fig. 18. The histological details of the parietal of *Metoposaurus krasiejowensis*. **(A)** Cross section of parietal, with distinct external cortex, middle region and internal cortex; image in CPL; **(B-C)** Well develop vascular network in the upper and deeper parts of external cortex; images in PPL; **(D-E)** Dense accumulation of small primary osteons in the middle region; images in CPL (D) and PPL (E); **(F)** Thin and avascular internal cortex; image in CPL. Abbreviations: EC = External cortex, MR = Middle region, IC = Internal cortex, VC = Simple vascular canals, ER = Erosion cavities, PO = Primary osteons, LB = Lamellar bone, PFB = Parallel-fibred bone, PPL = plane polarized light, CPL = cross polarized light.

Supratemporal

The thin section was prepared from the anterior part of the right supratemporal (Fig. 19). The external surface of this dermal bone possesses the polygonal sculpture with high, about 1.5 mm ridges and deep grooves. The sectional bone thickness is from 3 mm to 5 mm, and the ratio E:M:I is 1:4.4:0.3.

Fig. 19. Histological section of the right supratemporal. Scale bar equals 5 mm.

External cortex - The external cortex with a thickness approximately 900 µm, consists of parallel-fibred bone. The simple vascular canals, variable in size, from 50 µm to over 400 µm in length, form a dense vascular network (Fig. 20A). They are present in larger amounts within the sculptural ridges, while in the grooves they are much smaller and arranged in orderly rows (Fig. 20B & 20C). The small primary osteons appears very rarely. The short Sharpey's fibers are visible mainly in the deeper parts of the external cortex. The rounded osteocyte lacunae with branched canaliculi are numerous. In some places the alternation of valleys and ridges is preserved.

Middle region - The external cortex transits to cancellous and well vascularized middle region. The erosion cavities, about 340 µm in diameter, are dense concentrated in some areas of the central parts of the middle region, whereas in other areas their amount is limited. The simple vascular canals and secondary osteons, ranging from 50 µm to 250 µm in diameter, are numerous (Fig. 20D). The small secondary osteons occur in densely packed clusters in some places forming the Haversian tissue (Fig. 20E). The elongated osteocyte lacunae are numerous and possess branching canaliculi.

Internal cortex - The thin, about 200 µm, internal cortex consists of parallel-fibred bone. The internal cortex is practically avascular on the entire length (Fig. 20F). The secondary osteons are small and appear very rare. The Sharpey's fibers are not visible. The elongate osteocyte lacunae of about 20 µm in length are not numerous. Their longer axes are oriented parallel to the cortex fibers. The growth marks are visible as an alternation of lamellar layers and three resting lines.

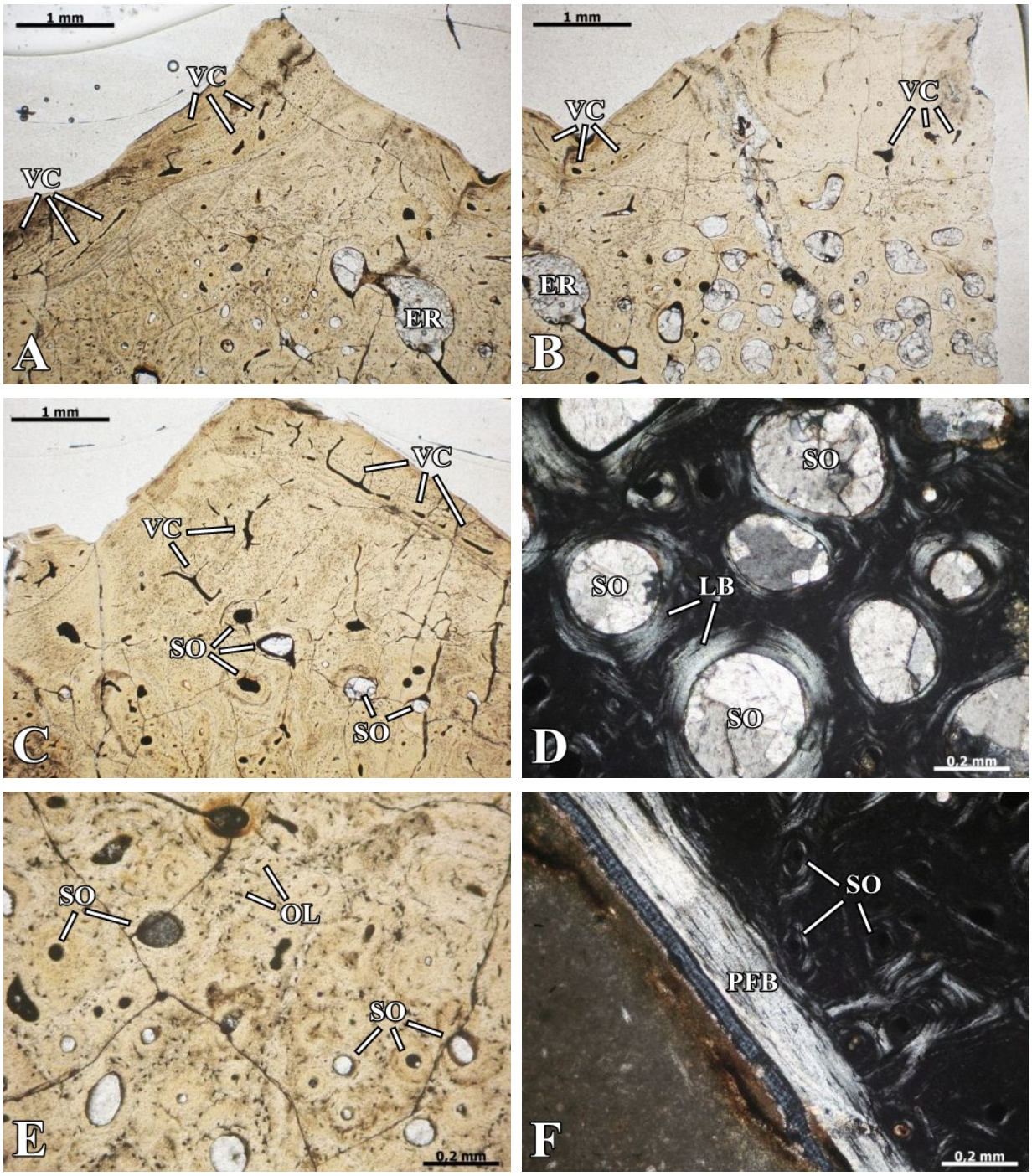

Fig. 20. The histological details of the supratemporal of *Metoposaurus krasiejowensis*. **(A-C)** Well developed vascular network in the external cortex (vascular canals) and in the middle region (secondary osteons); images in PPL; **(D)** Large and numerous secondary osteons; image in CPL; **(E)** Beginning of Haversian tissue visible in the middle region; image in PPL; **(F)** Thin and avascular internal cortex; image in CPL. Abbreviations: VC = Simple vascular canals, ER = Erosion cavities, SO = Secondary osteons, LB = Lamellar bone, PFB = Parallel-fibred bone, OL = Osteocyte lacunae, PPL = plane polarized light, CPL = cross polarized light.

Squamosum 1

The histological thin section was prepared from the front part of the right squamosum (Fig. 21). The external surface of the squamosum is characterized by a clear developed sculpture, consists of the high for 2 mm ridges and of the wide grooves. The bone thickness is about 5 mm, and the ratio E:M:I is 1:2.2:0.2.

Fig. 21. Histological section of the right squamosum 1. Scale bar equals 5 mm.

External cortex - The external cortex with a maximum thickness of about 1100 µm, consists of parallel-fibred bone. The external cortex is well vascularized, mainly by the simple vascular canals irregular in shape and of variable size. The small secondary osteons, with a diameter about 30 µm, occur sporadically, mainly in the central parts of the external cortex. The thin Sharpey's fibers occur in the deeper parts of the sculptural ridges (Fig. 22A). The rounded osteocyte lacunae with branched canaliculi appear in the moderate numbers. In some places the alternation of valleys and ridges is preserved.

Middle region - The middle region is created by the well vascularized bone. The huge erosion cavities, in excess of 900 µm in diameter, are partially surrounded by the layers of the lamellar bone (Fig. 22B, C). The very numerous simple vascular canals are irregularly arranged in the bone matrix (Fig. 22D). The most numerous are, variable in size, secondary osteons. The largest, reaching up to 200 µm in diameter, are located in the central part of the middle region (Fig. 22E). In some areas, next the border with the internal cortex, the

arrangement of the osteons is more orderly. The rounded osteocyte lacunae with branched canaliculi are very numerous.

Internal cortex - The internal cortex consists of parallel-fibred bone and it is much thinner than the external cortex. Its average thickness is 250 μm. The internal cortex is avascular on the entire width (Fig. 22F). The Sharpey's fibers are not visible. The osteocyte lacunae occur sporadically. Their shape is elliptically elongated to about 20 μm, and they are arranged in the several, cyclic rows.

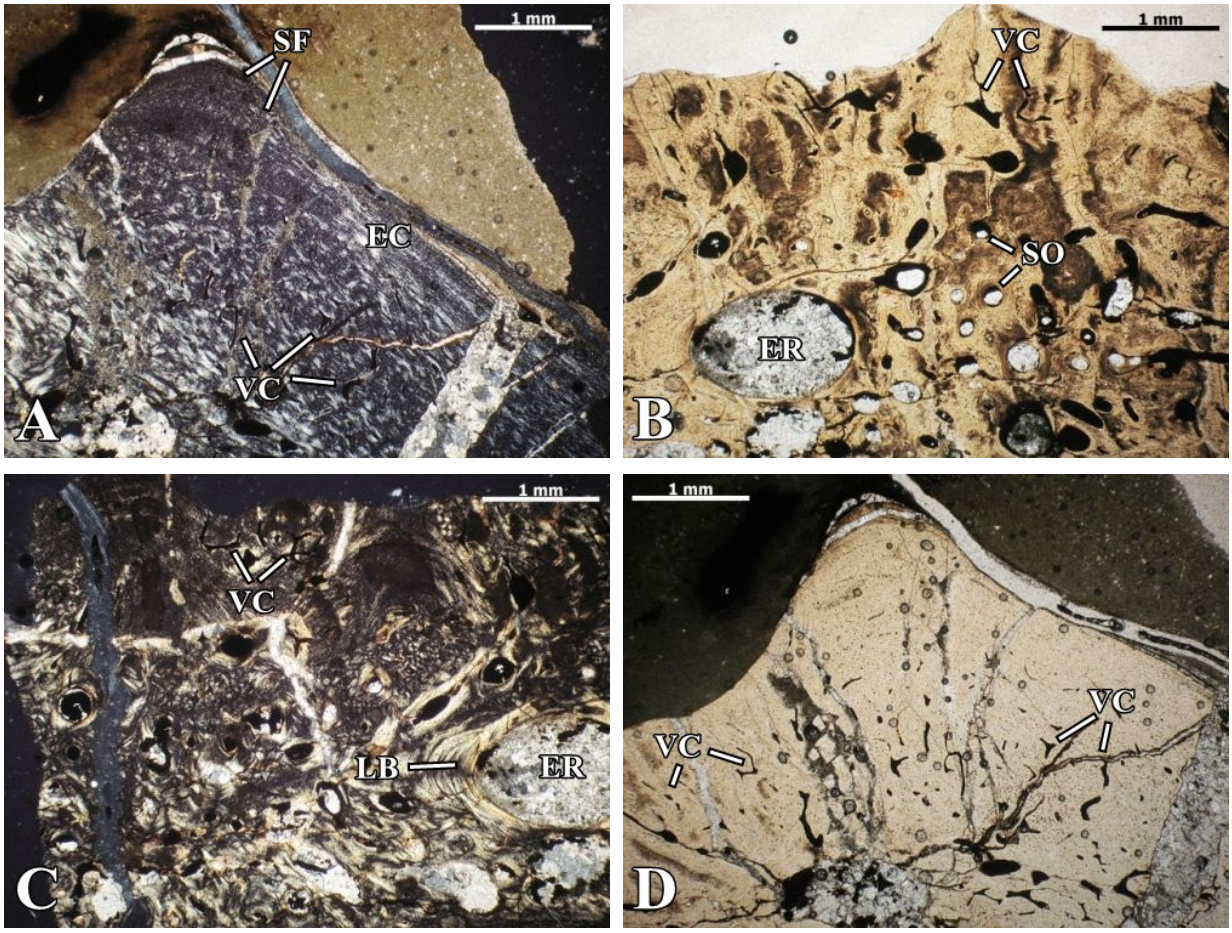

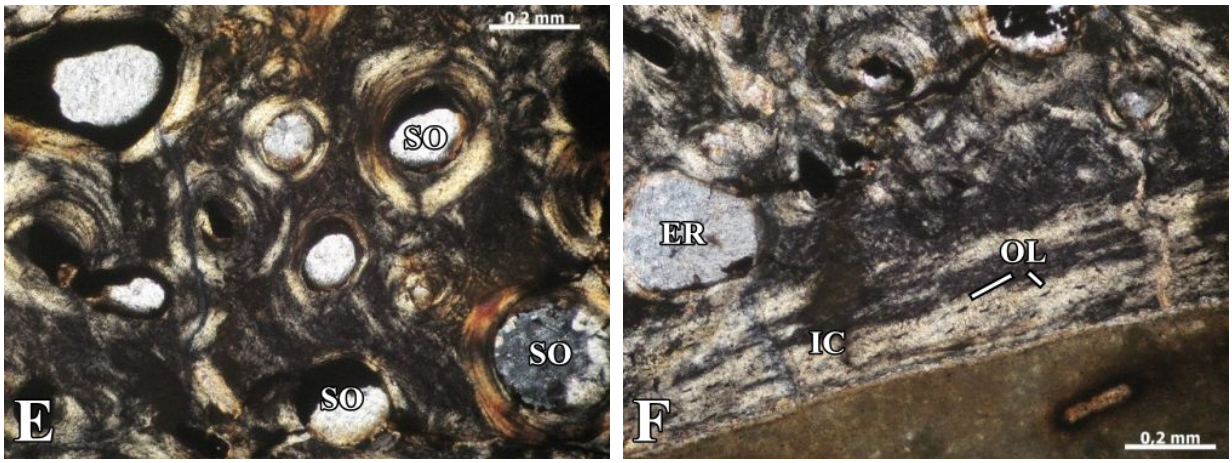

Fig. 22. The histological details of the squamosum 1 of *Metoposaurus krasiejowensis*. **(A)** Thick external cortex in the area of sculptural ridges with distinct Sharpey's fibers; image in CPL; **(B-D)** Well vascularized external cortex (vascular canals) and middle region (secondary osteons); images in PPL (B, D) and CPL (C); **(E)** Dense accumulation of large secondary osteons; image in CPL; **(F)** Avascular internal cortex with distinct osteocyte lacunae; image in CPL. Abbreviations: EC = External cortex, SF = Sharpey's fibers, VC = Vascular canals, ER = Erosion cavities, SO = secondary osteons, LB = Lamellar bone, IC = Internal cortex, OL = Osteocyte lacunae, PPL = plane polarized light, CPL = cross polarized light.

Squamosum 2

The histological thin section was prepared from the posterior (near the otic notch) part of the right squamosum. The external surface of squamosum 2 is characterized by a shallow sculpture (Fig. 23). The bone thickness is about 3 mm, and the ratio E:M:I is 1:0.3:0.5. It is the only bone in which the middle region is the thinnest part of the bone.

Fig. 23. Histological section of the right squamosum 2. Scale bar equals 10 mm.

External cortex - The external cortex with an average thickness of about 1100 µm, consists of parallel-fibred bone (Fig. 24A). Next to the surface the thin, avascular layer with thick collagen fibers is visible. Deeper part of the cortex is poor vascularized, mainly by the irregularly in shape vascular canals. The thin Sharpey's fibers occur in the deeper parts of the sculptural ridges (Fig. 24B). The rounded osteocyte lacunae with branched canaliculi appear in the moderate numbers (Fig. 24C). The degree of vascularization increases in the posterior part of section.

Middle region - The external cortex transfers gradually to the middle region. The middle region is poorly porous (Fig. 24D, E). Only the few erosion cavities with thick layer of lamellar bone are preserved. The entire part of middle region is highly remodeled and filled by the relatively compact secondary bone (Fig. 24F).

Internal cortex - The avascular on the entire width internal cortex consists of parallel-fibred bone. The Sharpey's fibers are not visible. The osteocyte lacunae are present in very low amounts.

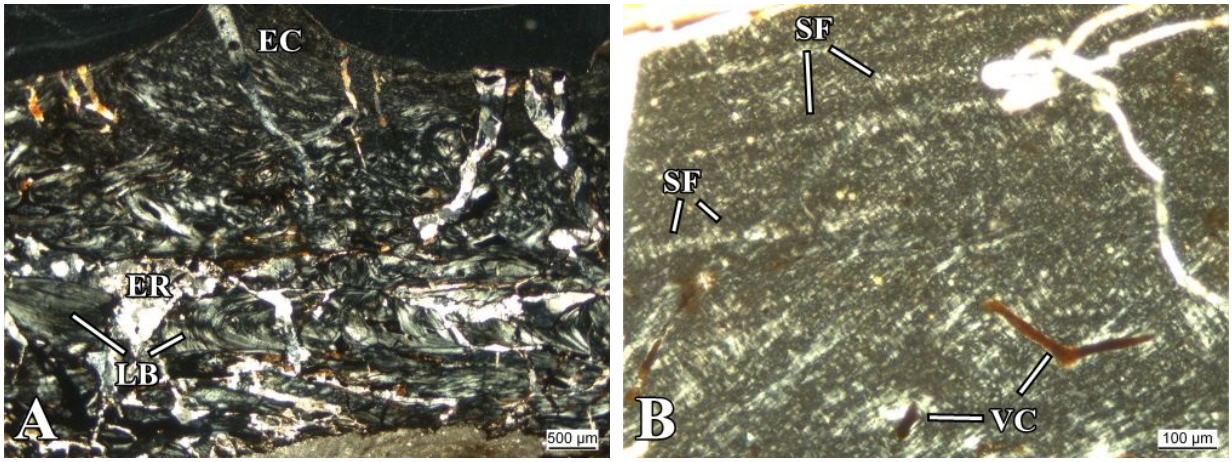

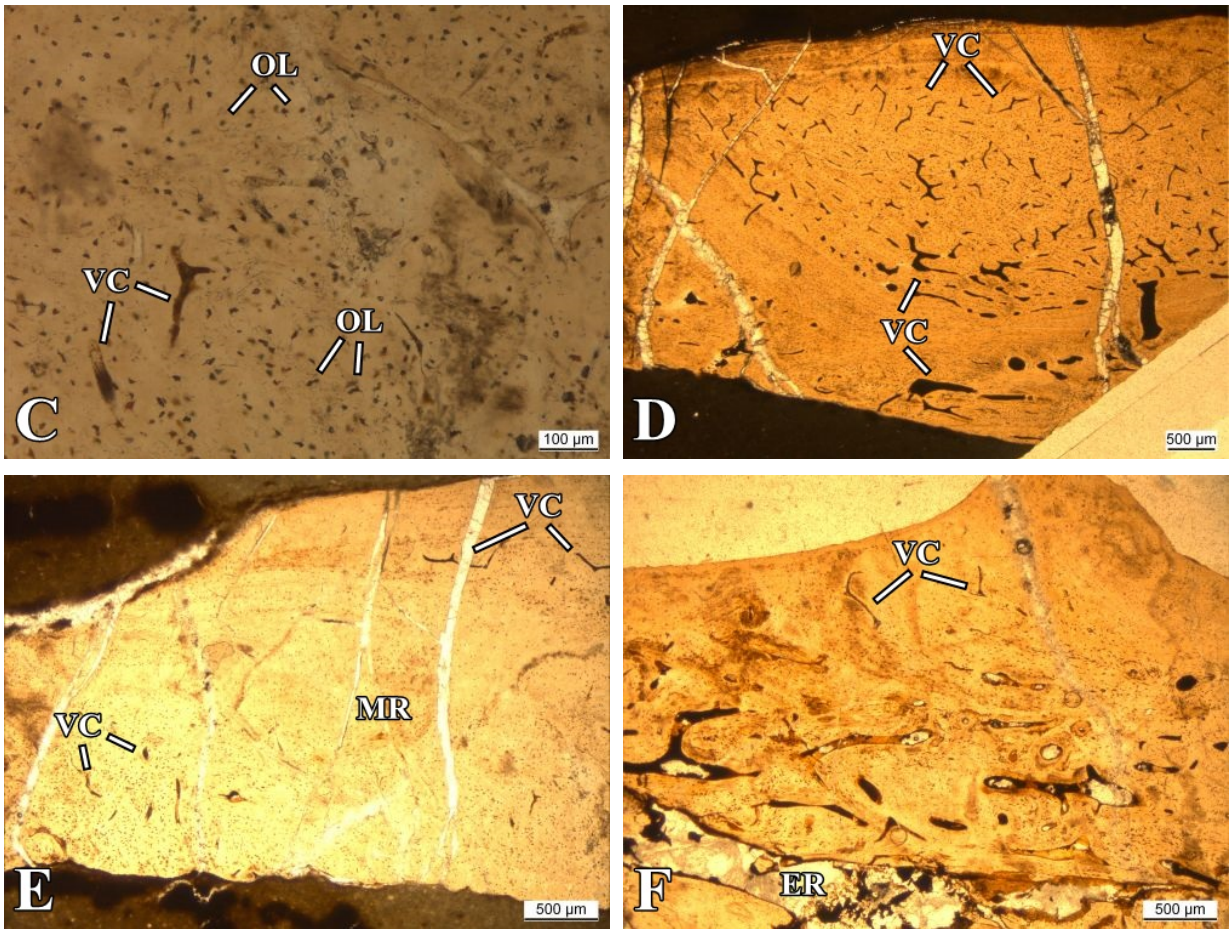

Fig. 24. The histological details of the squamosum 2 of *Metoposaurus krasiejowensis*. **(A)** Thick external cortex and highly remodeled middle region; image in CPL; **(B)** Dense bundles of thin Sharpey's fibers; image in CPL; **(C)** Rounded osteocyte lacunae; image in PPL; **(D-E)** Compact middle region with high and low degree of vascularization; images in PPL; **(F)** Poor vascularized external cortex and highly remodeled entire part of middle region; image in PPL. Abbreviations: EC = External cortex, ER = Erosion cavities, LB = Lamellar bone, SF = Sharpey's fibers, VC = Simple vascular canals, OL = Osteocyte lacunae, MR = Middle region, PPL= plane polarized light, CPL= cross polarized light.

Postparietal

The sample was made from the middle part of postparietal (Fig. 25). The external surface covers the ornament, about 1.5 mm high, builds up from steep ridges and polygonal pits. The sectional bone thickness is about 10 mm, and the ratio E:M:I is 1:3.1:0.2.

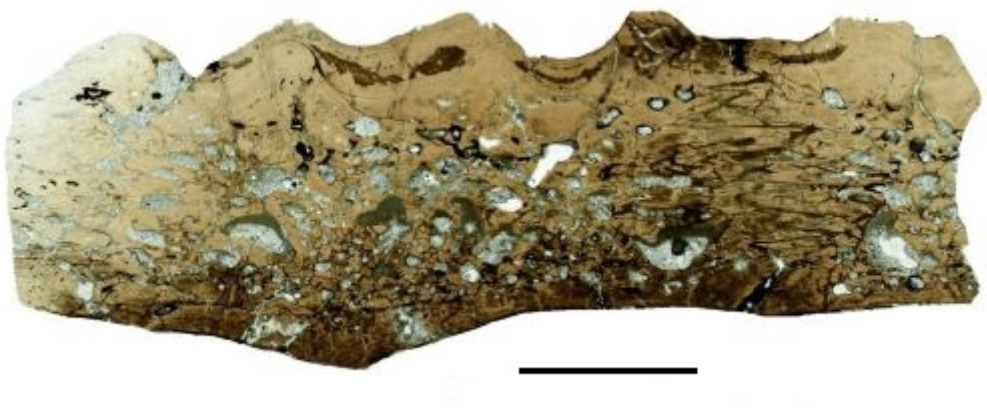

Fig. 25. Histological sections of the postparietal. Scale bar equals 5 mm.

External cortex - The external cortex of variable thickness consists of parallel-fibred bone. Its thickness is maximal in the ridges, about 2000 µm, while in the sculptural valleys is thinner having about 650 µm (Fig. 26A). The elongated simple vascular canals are present mainly in the grooves. The sculptural ridges are almost avascular. The small primary osteons, about 70 µm in diameter, appear very rarely. The thick collagen fibers form Interwoven Structural Fibers (IFS). They are usually short, but they occur on the entire width of the external cortex. The well mineralized Sharpey's fibers, with diameters about 20 µm, are numerous within the high ridges (Fig. 26B). The Sharpey's fibers occur also along the lateral edges of the cranial suture. The osteocyte lacunae with branched canaliculi are numerous in the entire external cortex. Within the sculptural ridges, the cyclical growth marks are visible as a sequence of layers of lamellar bone and layers with accumulation of ISF (Fig. 26C, D).

Middle region - The extensive and highly eroded middle region consists of the coarse cancellous and well vascularized bone. The irregular erosion cavities are varies in sizes, with some up to 800 µm in diameter (Fig. 26E). Their edges are partially surrounded by approximately 120 µm thin layers of the lamellar bone. The elongated simple vascular canals are rare. The secondary osteons, with diameters ranging from 50 µm to 200 µm, are more numerous (Fig. 26F). The osteocyte lacunae, about 20 µm in diameter and with branched

canaliculi occur numerously in the middle region and within the lamellar bone which surround the osteons and the erosion cavities.

Internal cortex - The internal cortex consists of parallel-fibred bone of constant thickness approximately 200 µm. The simple vascular canals are small and they occur in the whole internal cortex. The primary and secondary osteons cannot be observed. The elongated osteocyte lacunae with preserved canaliculi appear in similar quantities as in the external cortex. The Sharpey's fibers are not visible. The growth marks are visible as an alternation of lamellar layers and three resting lines.

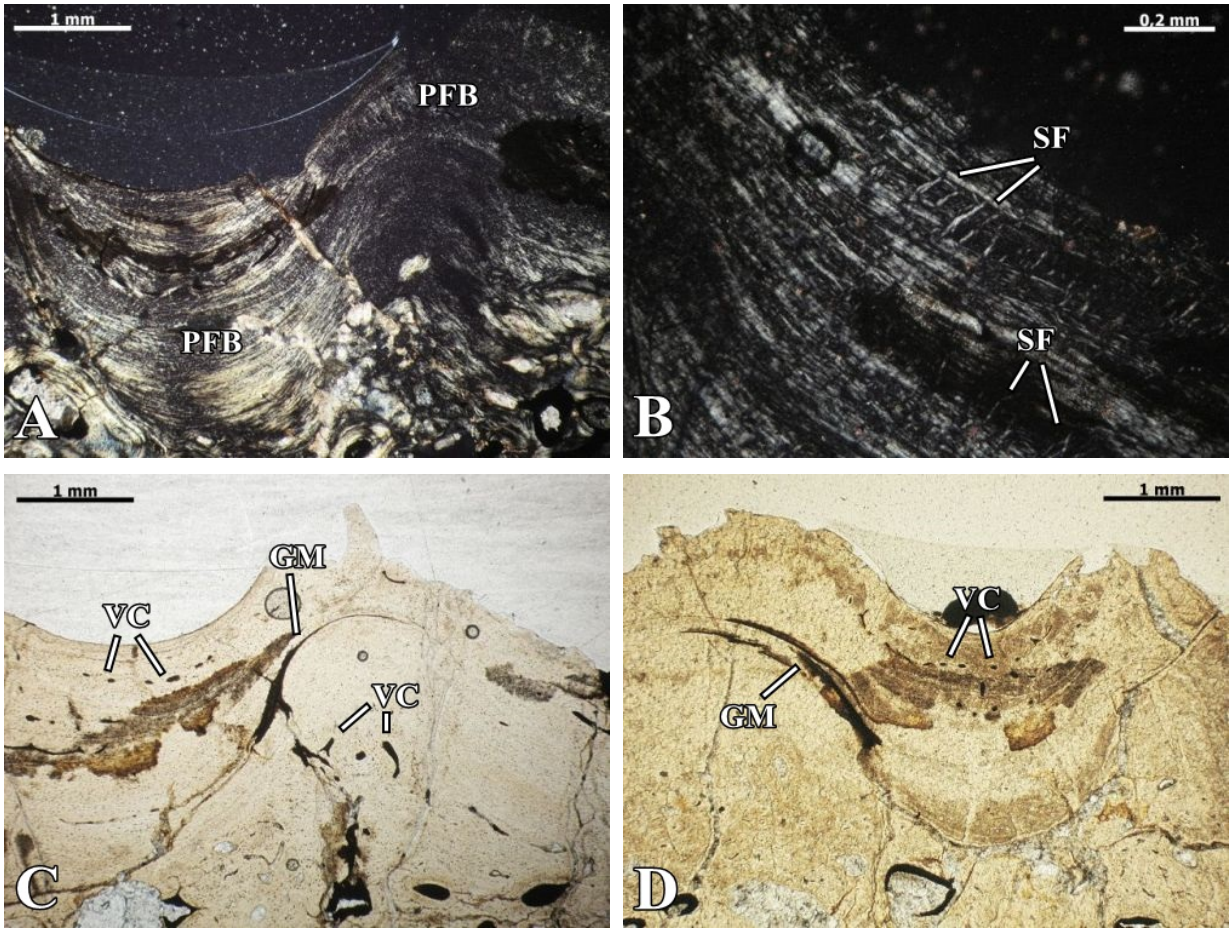

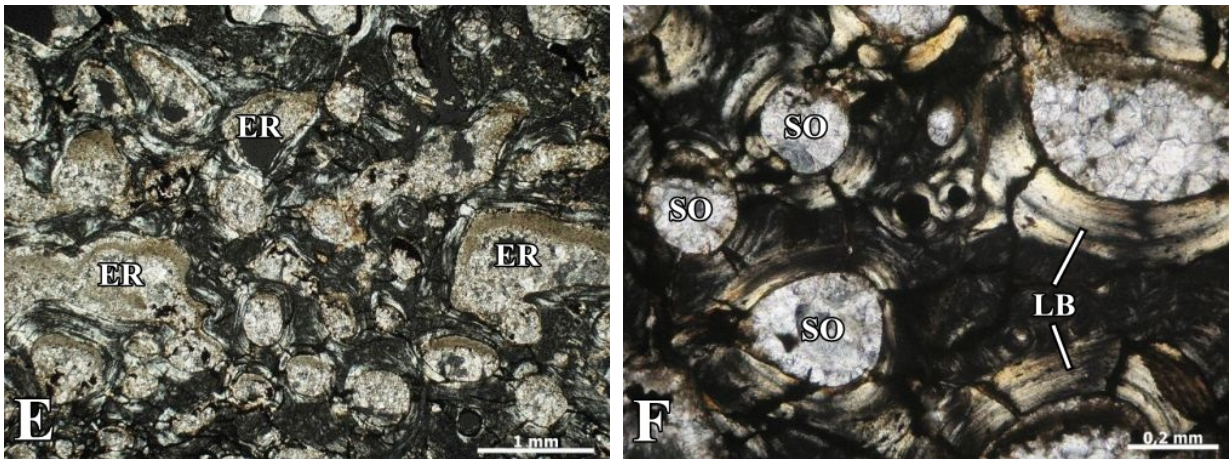

Fig. 26. The histological details of the postparietal of *Metoposaurus krasiejowensis*. **(A)** Thick layer of parallel-fibred bone in the area of sculptural vallyes and ridges; image in CPL; **(B)** Dense clumps of well mineralized Sharpey's fibers; image in CPL; **(C-D)** Distinct growth marks structure and vascular canals within the ornamented ridges; images in PPL; **(E)** Heavy eroded middle region; image in CPL; **(F)** Numerous and large secondary osteons in the central parts of middle region; image in CPL. Abbreviations: PFB = Parallel-fibred bone, SF = Sharpey's fibers, VC = Simple vascular canals, GM = Growth marks structure, ER = Erosion cavities, SO = secondary osteons, LB = Lamellar bone, PPL = plane polarized light, CPL = cross polarized light.

Tabular

The histological sample was prepared from the right tabular, from about the middle part of this bone (Fig. 27). The external surface of tabular bears the polygonal sculpture consists of high, about 1 mm ridges and wide pits. The bone thickness ranges from 10 mm to 12 mm, and the ratio E:M:I is 1:6.5:0.8.

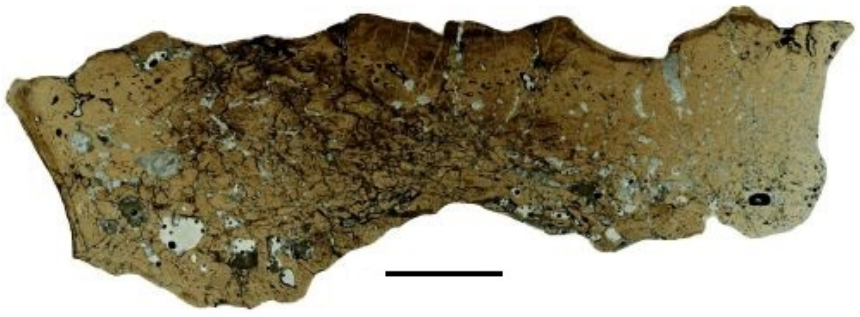

Fig. 27. Histological section of the right tabular. Scale bar equals 5 mm.

External cortex - The about 1000 μm thick well vascularized external cortex consists of parallel-fibred bone (Fig. 28A). The numerous and irregular in shape simple vascular canals mainly occur in the central and deeper parts of external cortex. The simple vascular canals, about 350 μm in length, are the most numerous within the sculptural ridges, while in the valleys their length does not exceed 150 μm (Fig. 28B). They are arranged in rows, along to superficial edge of the bone. The primary osteons are small, about 50 μm in diameter, and they occur in the central parts of the external cortex and in the border with the middle region. The numerous and well mineralized Sharpey's fibers, with a diameter about 20 μm, occur in the upper and deeper parts of the cortex (Fig. 28C). The distinct collagen fibers create a thick Interwoven Structural Fibers (IFS). Within the sculptural ridges, the cyclical growth marks, manifested as a sequence of thin resting lines and the layer of parallel-fibred bone are present (Fig. 28D). In some places the alternation of valleys and ridges is preserved. The osteocyte lacunae with branched canaliculi and rounded in shape occur numerously within the bone matrix.

Middle region - The middle region consists of coarse cancellous bone. The very large erosion cavities, with a diameter up to 1500 μm, occur only in the deeper parts of the middle region, partially in the border with the internal cortex. Their edges are fragmentary surrounded by a thin layer of the lamellar bone. The most part of the middle region is highly remodeled; however the porosity of this bone is low (Fig. 28E). The secondary osteons, with a diameter about 120 μm, are more numerous. The slightly elongated osteocyte lacunae, about 10 μm in length, and with branched canaliculi are common in the middle region.

Internal cortex - The internal cortex of constant thickness, about 1000 μm, consists of parallel-fibred bone. The irregularly in shapes, simple vascular canals, about 100 μm in length, are present in large amounts (Fig. 28F). In some areas they are arranged in several rows at angle of about 40^0 to the internal cortex. The secondary osteons rarely appear, and in

some places they penetrate into the internal cortex from the middle region. The numerous Sharpey's fibers are packed in bundles. The elongated osteocyte lacunae, about 10 µm in length and with branched canaliculi are numerous.

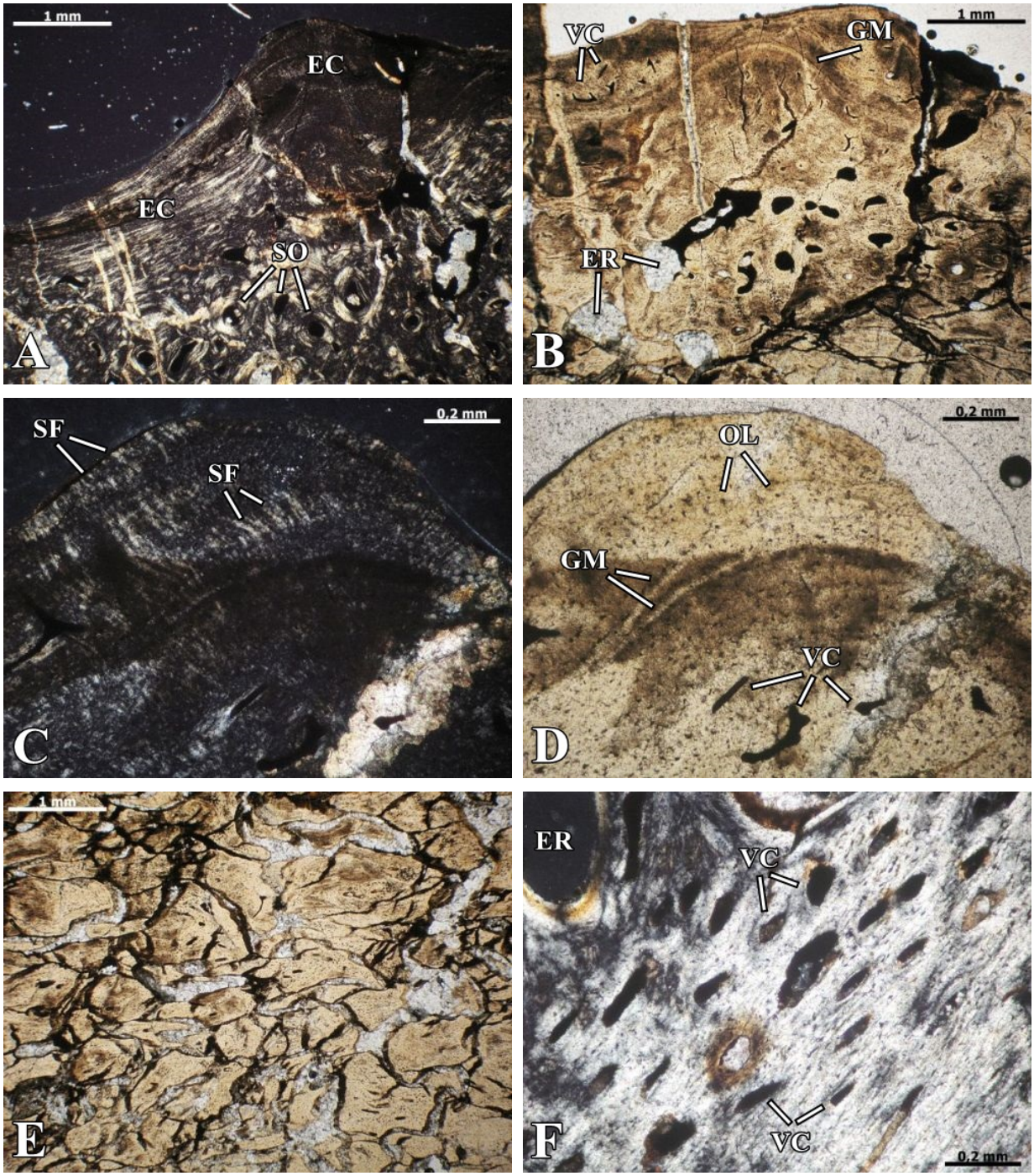

Fig. 28. The histological details of the tabular of *Metoposaurus krasiejowensis*. **(A-B)** External cortex and middle region; images in CPL (A) and PPL (B); **(C)** Numerous and packed in dense bundles Sharpey's fibers visible in the external cortex; image in CPL; **(D)** Growth marks structure in the area of sculptural ridges; image

in PPL; **(E)** Heavy eroded middle region; image in PPL; **(F)** Numerous vascular canals in the parallel-fibred bone of internal cortex; image in CPL. Abbreviations: EC = External cortex, SO = secondary osteons, ER = Erosion cavities, VC = Vascular canals, SF = Sharpey's fibers, GM = Growth marks structure, OL = Osteocyte lacunae, PPL = plane polarized light, CPL = cross polarized light.

Quadratojugal

The histological sample was prepared from the middle part of the left quadratojugal. The external surface of the bone possesses distinct sculpture, which consists of about 1 mm high ridges and the deep grooves (Fig. 29). The average thickness of quadratojugal is 5 mm, and the ratio E:M:I is 1:2.9:0.6.

Fig. 29. Histological section of the left quadratojugal. Scale bar equals 5 mm.

External cortex - The external cortex consists of parallel-fibred bone of a variable thickness. The thickest bone, even exceeding 1000 μm, is in the area of the sculptural grooves (Fig. 30A). Various in sizes and shape simple vascular canals are numerous, especially within the ridges (Fig. 30B). The small primary osteons are rare. The well mineralized Sharpey's fibers can be observed within the sculptural ridges and in the ridges (Fig. 30C). The cyclical growth marks, manifested as a sequence of thin resting lines and layers of parallel-fibred bone, are present within the sculptural ridges. In some places the alternation of valleys and

ridges is preserved. The osteocyte lacunae, about 10 μm in diameter and with branched canaliculi are numerous.

Middle region - The large and well vascularized middle region consists of cancellous bone. The large erosion cavities, about 1500 μm in diameter, occur in the central part of the middle region. The small and irregular simple vascular canals are not as numerous as in the external cortex. The secondary osteons varying in sizes appear in the larger amount. The largest of them reached almost 200 μm in diameter. The small secondary osteons, with a diameter about 40 μm, form the Haversian tissue in some parts of the middle region (Fig. 30D, E). The mostly rounded osteocyte lacunae with long, branched canaliculi are numerous.

Internal cortex - The relatively thick, of about 700 μm, and well vascularized internal cortex consists of parallel-fibred bone. The irregular and highly elongated, up to 300 μm long, simple vascular canals are numerous. Sometimes they are arranged in several, regular rows, parallel to cortex fibers (Fig. 30F). The secondary osteons of the average size appear in a much lower amount. The Sharpey's fibers are not visible. The rounded osteocyte lacunae with preserved canaliculi are very numerous.

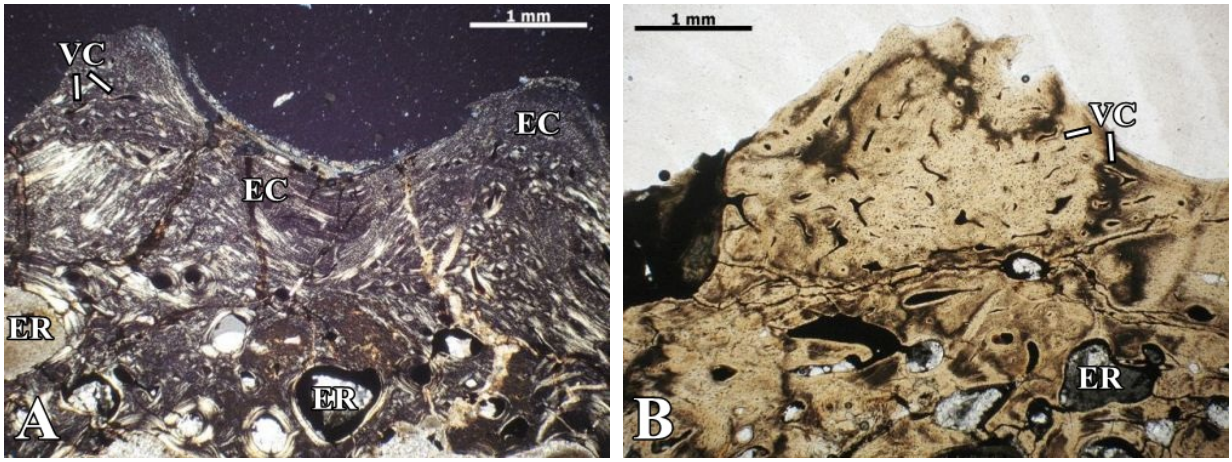

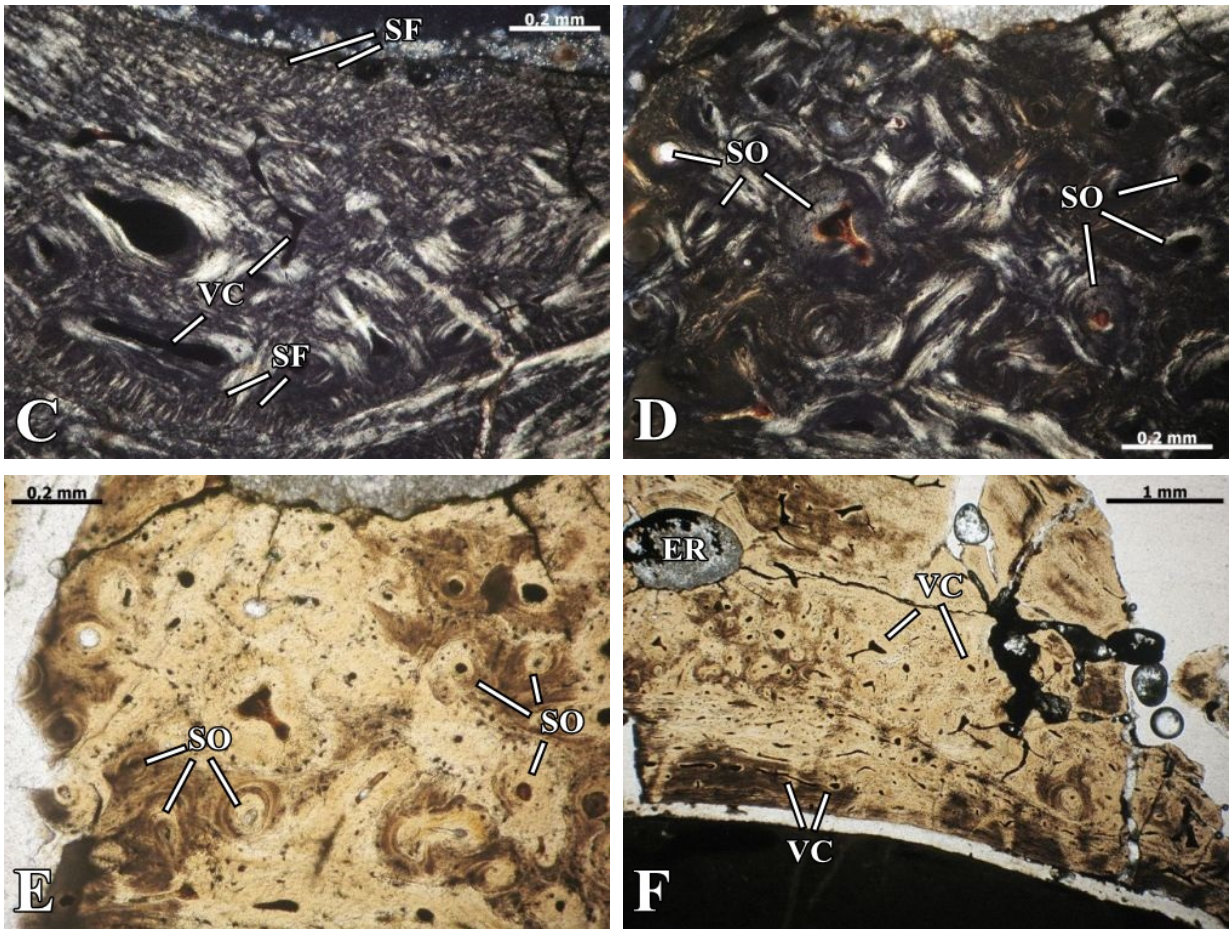

Fig. 30. The histological details of the quadratojugal of *Metoposaurus krasiejowensis*. **(A)** External cortex and middle region; image in CPL; **(B)** Numerous vascular canals in the area of sculptural ridges; image in PPL; **(C)** Well mineralized bundles of Sharpey's fibers in external cortex; image in CPL; **(D-E)** Incipient Haversian tissue; images in CPL (D) and PPL (E); **(F)** Well vascularized part of internal cortex; image in PPL. Abbreviations: EC = External cortex, ER = Erosion cavities, VC = Simple vascular canals, SF = Sharpey's fibers, SO = secondary osteons, PPL = plane polarized light, CPL = cross polarized light.

Histology of the dermal bones of palate

Vomer

The thin section examined histologically was prepared from the left part of vomer (Fig. 31). The external surface of the bone bears a small, about 150 µm in high circum-vomerine teeth. The sectional bone thickness varies from 3 mm to 6 mm, and the ratio E:M:I is 1:2.8:0.7.

Fig. 31. Histological section of the vomer. Scale bar equals 5 mm.

External cortex - The well vascularized external cortex of a maximal thickness about 450 µm, consists of parallel-fibred bone (Fig. 32A). The secondary osteons with diameters of 70 µm are numerous. The simple vascular canals appear in a lower amount. ~~The~~ Sharpey's fibers are very rare. The elliptical osteocyte lacunae of approximately 20 µm in length are arranged with their long axis parallel to the collagen fibers.

Middle region - The large and highly eroded middle region consists of cancellous bone. The erosion cavities reach the largest size among all of the dermal bone examined (Fig. 32B, C). They are even 3000 µm in length and are partially surrounded by a thin layer of the lamellar bone. The secondary osteons, of about 70 µm in diameter, occur mainly in the subsurface and in the deeper parts of the middle region. The rounded osteocyte lacunae are numerous and possess branching canaliculi.

Internal cortex - The internal cortex of a constant thickness of approximately 650 µm, consists of parallel-fibred bone. The very large secondary osteons, about 70 µm in diameter, are numerous and in some areas are arranged in orderly rows (Fig. 32D & 32E). The simple vascular canals are not visible. The well mineralized Sharpey's fibers occur in the subsurface parts of the internal cortex and are oriented at an angle of 45^0 to the bone surface (Fig. 32F). The rounded osteocyte lacunae with a diameter of about 10 µm and with branched canaliculi are very numerous.

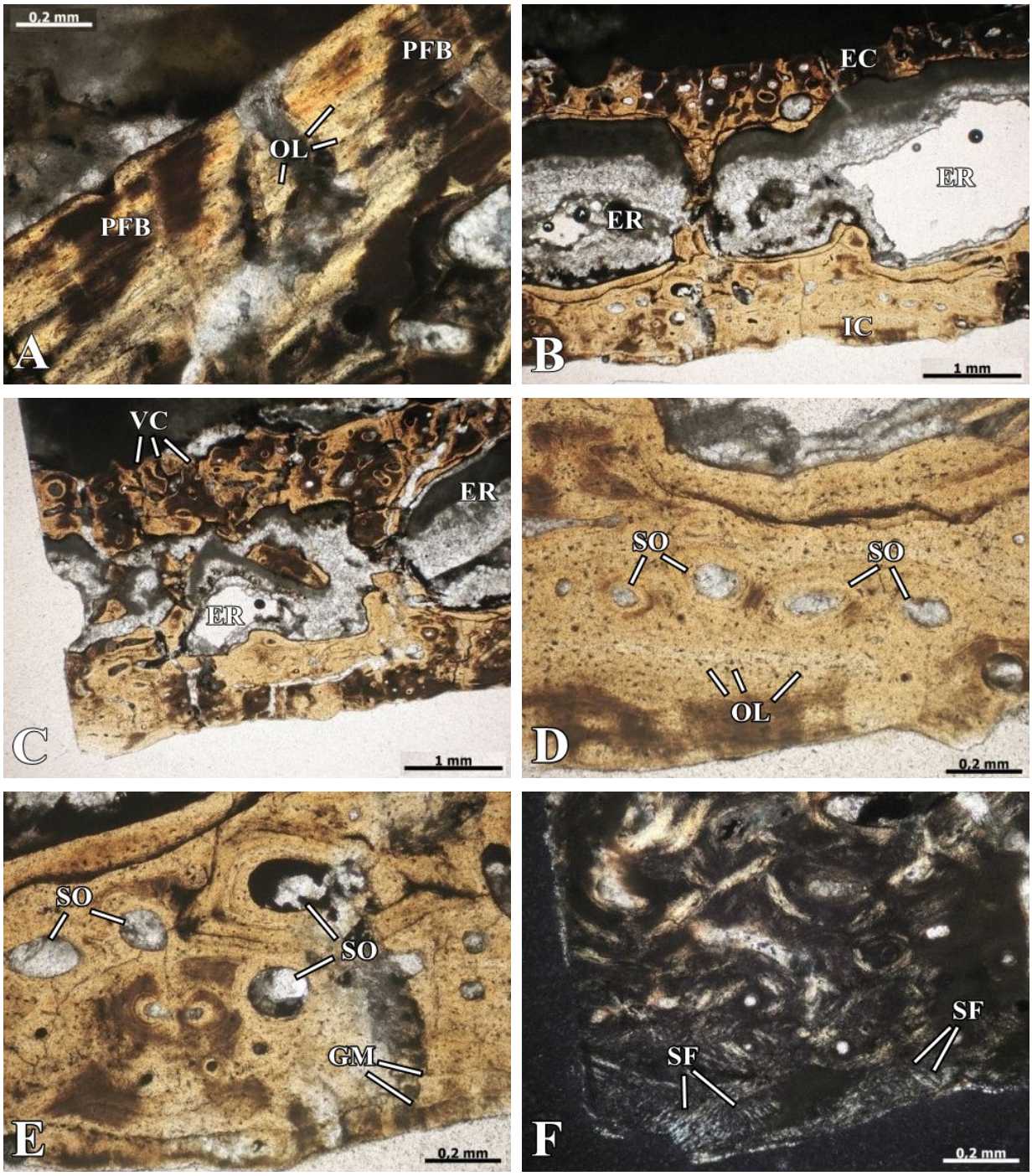

Fig. 32. The histological details of the vomer of *Metoposaurus krasiejowensis*. **(A)** External cortex in cross polarized light; **(B-C)** Large erosion cavities within the middle region; images in PPL; **(D-E)** Internal cortex with well develop vascular network and with distinct growth marks structures; images in PPL; **(F)** Numerous Sharpey's fibers in the upper part of internal cortex; image in CPL. Abbreviations: SF = Sharpey's fibers, PO = Primary osteons, SO = secondary osteons, GM = Growth marks structure, ER = Erosion cavities, VC = Simple vascular canals, IC = Internal cortex, PFB = Parallel-fibred bone, OL = Osteocyte lacunae, PPL = plane polarized light, CPL = cross polarized light.

Parasphenoid

The thin section was made from the posterior part of *processus cultriformis* (Fig. 33). The bone has the clearly ornamented external surface (located ventrally). The sectional bone thickness ranges from 2 mm to 5 mm, and the ratio E:M:I is 1:5:1.5.

Fig. 33. Histological section of the parasphenoid. Scale bar equals 5 mm.

External cortex - The external cortex consists of parallel-fibred bone. It possesses a constant thickness, of an average of 900 µm. In the deeper parts of the external cortex, the highly elongated simple vascular canals are arranged in several rows parallel to the cortex surface (Fig. 34A). The secondary osteons appear in a very small amount. The Sharpey's fibers are not visible. The elongated osteocyte lacunae, 10 µm in diameters, are very numerous and have branched canaliculi.

Middle region - The coarse cancellous middle region is well vascularized. The numerous erosion cavities have various sizes, ranging from 300 µm to over 2500 µm in length (Fig. 34A & 34B). Their lateral edges are partially surrounded by thin layers of the lamellar bone. The middle region possess well-developed vascular network. The secondary osteons, with diameters ranging from 80 µm to nearly 200 µm, appear in a large amount, and they are lined with thick, up to 100 µm, layer of the lamellar bone (Fig. 34C). The simple vascular canals are not visible within the middle region. The osteocyte lacunae with a diameter 10 µm, and with branched canaliculi are numerous (Fig. 34D).

Internal cortex - The relatively thin and moderate vascularized internal cortex consists of parallel-fibred bone. The irregular in shape, small simple vascular canals and secondary osteons, about 60 µm in diameter, are not numerous. The Sharpey's fibers are absent. The numerous, rounded and elongated osteocyte lacunae possess branched canaliculi. The alternation of two thick well vascularized and two avascular layers is visible, represent the zones and annuli, respectively.

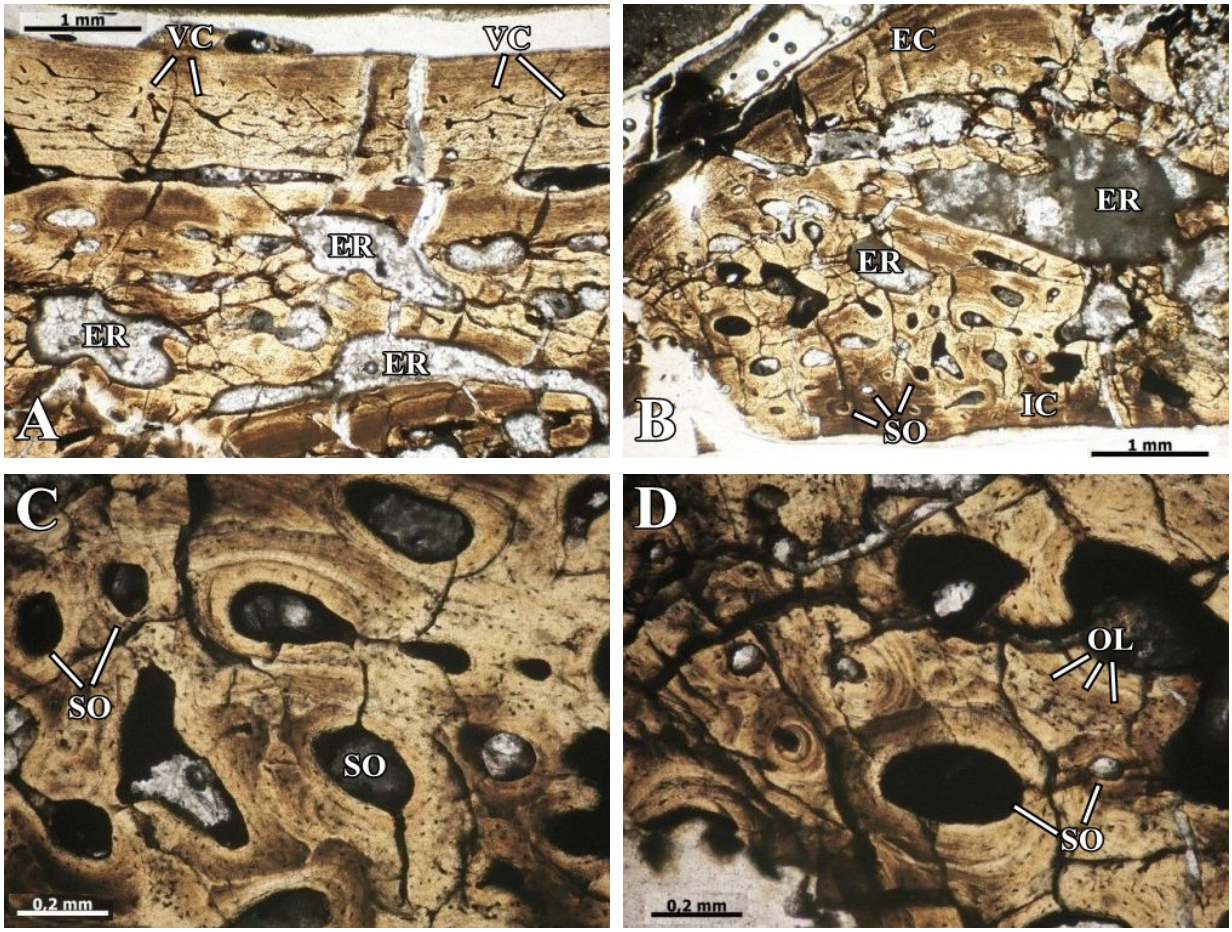

Fig. 34. The histological details of the parasphenoid of *Metoposaurus krasiejowensis*. **(A)** Cross section of the parasphenoid with clearly visible well vascularized external cortex and remodeled middle region; image in PPL; **(B)** Heavy eroded middle region; image in PPL; **(C-D)** Large and numerous secondary osteons in middle region; images in PPL. Abbreviations: EC = External cortex, SO = secondary osteons, ER = Erosion cavities, VC = Simple vascular canals, IC = Internal cortex, OL = Osteocyte lacunae, PPL = plane polarized light, CPL = cross polarized light.

Pterygoid

The histological section was prepared from the posterior part of the palatine branch, of the right pterygoid, in a place where the bone is thicker and contacts with the parasphenoid (Fig. 35). The external part of pterygoid is poorly preserved, but the preserved areas show a lack of the ornamentation. The average bone thickness is approximately 8 mm, and the ratio E:M:I is 1:5:1.

Fig. 35. Histological section of the right pterygoid. Scale bar equals 5 mm.

External cortex - The well vascularized external cortex, about 550 µm thick, consists of parallel-fibred bone. The numerous and elongated simple vascular canals are arranged parallel to the external cortex. The small secondary osteons, with a diameter about 60 µm, appear in smaller amounts. The Sharpey's fibers are not observed. The numerous osteocyte lacunae are variable in shapes.

Middle region - The coarse cancellous middle region is highly eroded. The irregularly shaped erosion cavities are very large. Their size varies from 500 µm to over 3500 µm, and their edges are surrounded by thick, about 200 µm, layer of the lamellar bone (Fig. 36A, B). The nutritional canals, 180 µm in diameter, occur in the middle region. Because the middle region is highly eroded, so the simple vascular canals and osteons are not visible. The secondary osteons, with a diameter about 100 µm, occur only in the subsurface parts and on

the border with the internal cortex. The osteocyte lacunae, about 20 µm in diameter, are very numerous.

Internal cortex - The partially preserved internal cortex consists of parallel-fibred bone. Its thickness is about 550 µm. The simple vascular canals are absent and the small secondary osteons, with diameters of 70 µm, occur very rarely. The Sharpey's fibers are not visible. However, the elliptically osteocyte lacunae are numerous and they are parallel to the internal cortex.

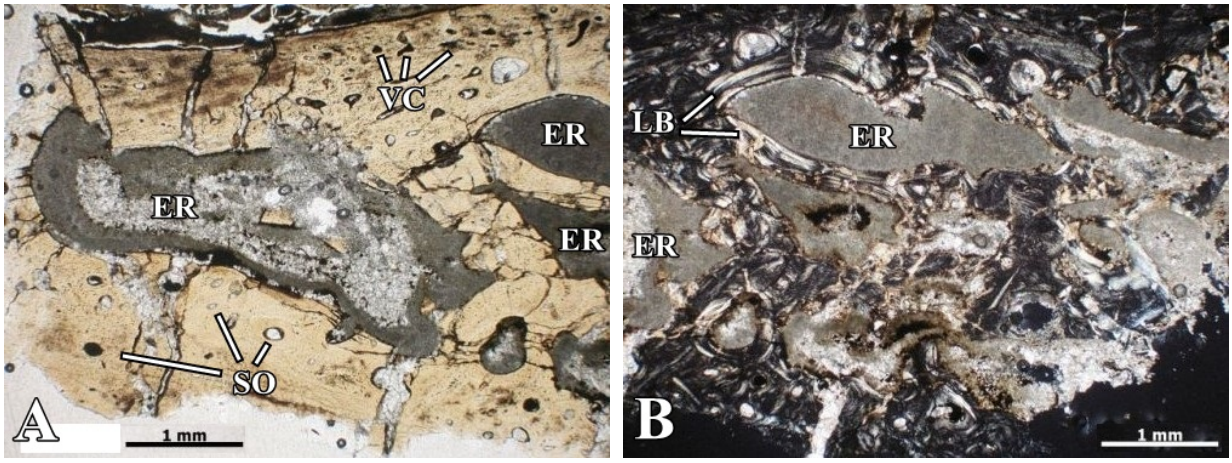

Fig. 36. The histological details of the pterygoid of *Metoposaurus krasiejowensis*. **(A-B)** Cross section from the pterygoid in PPL (A) and CPL (B) with distinct large and irregular erosion cavities. Abbreviations: SO = secondary osteons, ER = Erosion cavities, VC = Simple vascular canals, LB = Lamellar bone, PPL = plane polarized light, CPL = cross polarized light.

Quadrate

The left quadrate was sectioned transversally in the central part of the bone (Fig. 37). The diameter of the quadrate is about 20 mm.

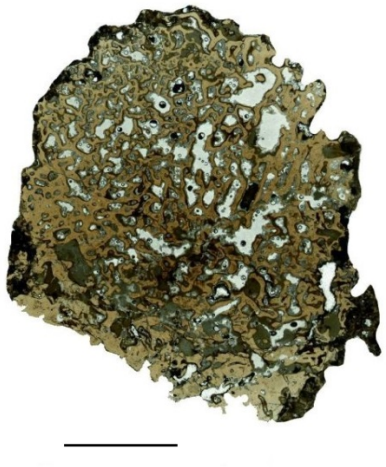

Fig. 37. Histological section of the left quadrate. Scale bar equals 5 mm.

The partially preserved and well vascularized cortex consists of parallel-fibred bone. Its thickness is 200 µm. The simple vascular canals occur sporadically, but the secondary osteons, with diameters ranging from 60 µm to 170 µm, are more numerous (Fig. 38A). The lamellar bone inside the secondary osteons is relatively thick, up to 60 µm. The Sharpey's fibers are very short and they occur only in the subsurface parts of the cortex. The elongated osteocyte lacunae mainly are present within the lamellar bone. They not possess canaliculi. The growth marks are not visible.

The central part of the bone is trabecular with irregular and variable in thickness and length bone trabeculae. The trabecular thickness is approximately 150 µm. The most numerous trabeculae are in the central parts of the bone, less frequent, shorter and thicker, on the border with cortex (Fig. 38B, C). On the border with cortex the secondary osteons, with a diameter of about 100 µm, are observed. The elongated osteocyte lacunae to about 20 µm, in the subsurface parts of the cancellous bone are rare, while in the deeper parts of the middle region their number rapidly increasing. In the central part of middle region, the relatively large accumulations of calcified cartilage remains are visible (Fig. 38D).

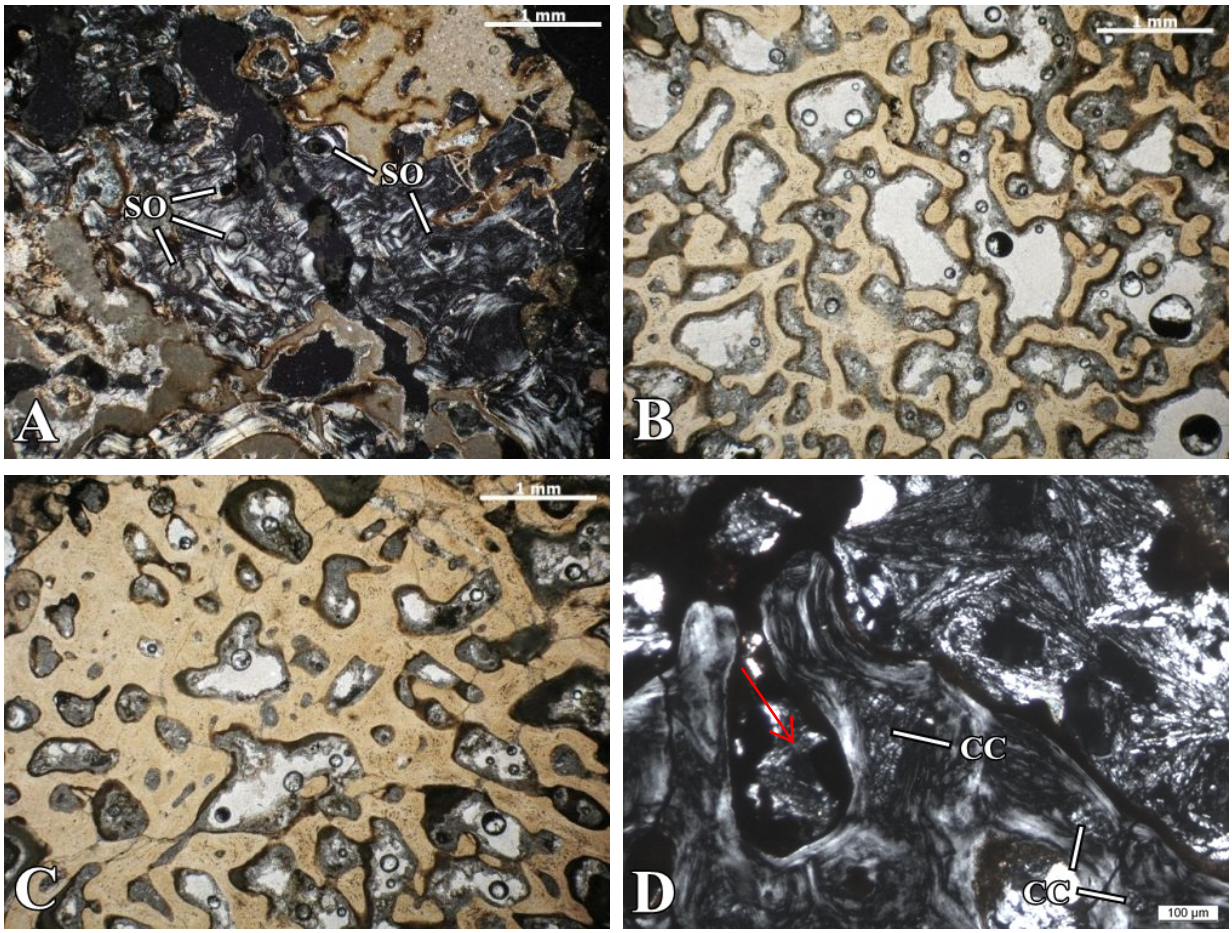

Fig. 38. The histological details of the quadrate of *Metoposaurus krasiejowensis*. **(A)** External surface of quadrate; image in CPL; **(B-C)** Trabecular middle region; images in PPL; **(D)** Middle region with distinct remains of calcified cartilage; image in CPL. Abbreviations: SO = secondary osteons, CC = Calcified cartilage, PPL = plane polarized light, CPL = cross polarized light.

Exoccipital

The thin section was prepared from the right exoccipital. The bone was cut approximately in their central part (Fig. 39). The diameter of the bone is about 20 mm.

Fig. 39. Histological section of the right exoccipital. Scale bar equals 5 mm.

The cortex, with a thickness of more than 2000 µm, consists of parallel-fibred bone. The entire cortex is relatively well vascularized. The simple vascular canals occur rarely, secondary osteons are relatively numerous. The single rounded erosion cavities, with diameters of about 900 µm are visible. The well mineralized, very numerous and packed in densely bundles Sharpey's fibers are present (Fig. 40A, B). They occur in the entire cortex, and the diameter of some bundles can reach up to 50 µm. The rounded osteocyte lacunae are numerous in the cortex. The growth marks are absent.

The central part of the bone consists of an irregular network of bony trabeculae, with large pore spaces between them. The number and length of trabeculae increase in the central area of bone. The thickness of the trabeculae is small in these areas, to about 200 µm (Fig. 40C, D). In the subsurface parts of middle region, the trabeculae thickness can ~~rise~~ almost double. The elongated osteocyte lacunae, with a diameter of about 10 µm, are very numerous and irregularly arranged. In the medial parts of the bone, where the trabeculae are the least developed, the numerous accumulations of calcified cartilage remains can be observed (Fig. 40E, F).

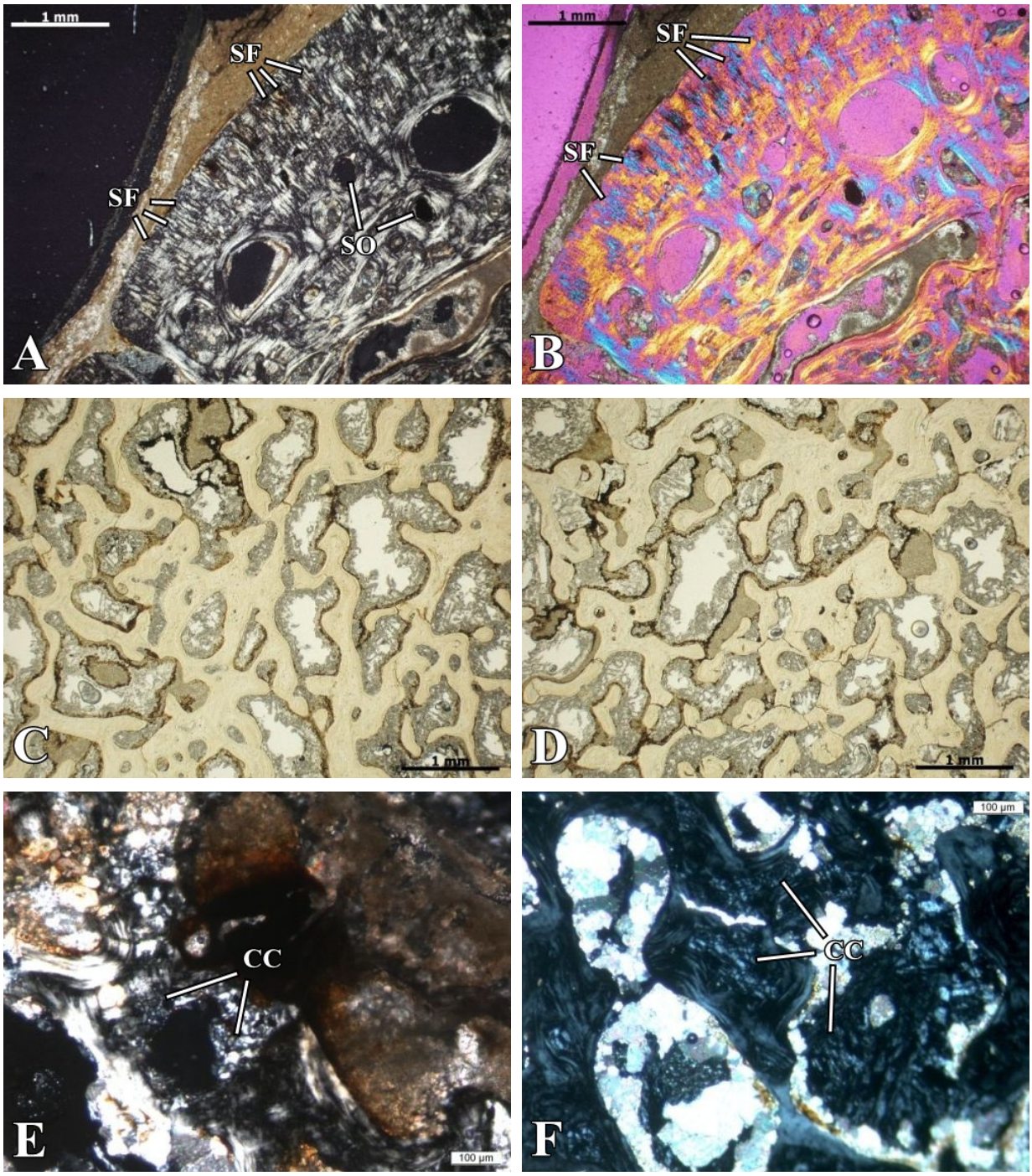

Fig. 40. The histological details of the exoccipital of *Metoposaurus krasiejowensis*. **(A-B)** External surface of exoccipital, with distinct thick and numerous Sharpey's fibers; images in CPL (A) and in ¼ Lambda filter (B); **(C-D)** Middle region with dense network of bony trabeculae; images in PPL; **(E-F)** Numerous relicts of calcified cartilage in the middle region; images in CPL. Abbreviations: SF = Sharpey's fibers, SO = secondary osteons, CC = Calcified cartilage, PPL = plane polarized light, CPL = cross polarized light.